UNIVERSITY OF Southampton

University of Southampton Research Repository
ePrints Soton

http://eprints.soton.ac.uk

UNIVERSITY OF SOUTHAMPTON

FACULTY OF NATURAL AND ENVIRONMENTAL SCIENCES

School of Ocean and Earth Sciences

Cell size, coccosphere geometry and growth in modern and fossil coccolithophores

by

Rosie Melanie Sheward

Submitted in partial fulfilment for the degree of Doctor of Philosophy

April 2016

UNIVERSITY OF SOUTHAMPTON

<u>ABSTRACT</u>

FACULTY OF NATURAL AND ENVIRONMENTAL SCIENCES

SCHOOL OF OCEAN AND EARTH SCIENCE

Doctor of Philosophy

Cell size, coccosphere geometry and growth in modern and fossil coccolithophores

Rosie Melanie Sheward

Coccolithophores are a key phytoplankton group that exhibit remarkable diversity in their biology, ecology, and in the highly distinctive morphological architecture of their calcite exoskeletons (coccospheres). Their extensive fossil record is testament to the crucial role that they play in the biogeochemical cycling of carbon through the production and export of inorganic coccoliths and organic matter. This fossil record provides an excellent archive of their biotic responses to environmental variability over thousands to millions of years that can be used to investigate the possible sensitivity of coccolithophores to potential changes in future climate. In this thesis, I explore how the fossil record of coccospheres can be utilized to investigate coccolithophore growth and physiology, providing a new cellular-level perspective on how we understand their interactions with global climate. This work focuses particularly on coccolithophores during the Paleogene, ~66 to ~23 million years ago, that was characterized by initially warm, high CO_2 'greenhouse' conditions that progressively cooled, involving substantial restructuring of marine systems. By imaging and measuring thousands of individual coccospheres, I have extensively documented the fundamentals of coccosphere architecture, including coccosphere size and shape and its relationship to coccolith size, number of coccoliths and their arrangement around each cell. This unprecedented dataset reveals the remarkable level of diversity in the architecture of Paleogene coccospheres for the first time, including multiple extinct species that had not previously been observed in this original form. Understanding what this dataset of coccosphere 'geometry' can tell us has necessitated the parallel exploration of modern coccolithophore biomineralisation and physiology. My culturing experiments on multiple modern species reveal that cell size and the number of coccoliths per cell is strongly regulated by cellular physiology, specifically responding to a decoupling between cellular division and calcification ability as populations transition between exponential and non-exponential phases of growth. Drawing direct comparisons between the coccosphere geometry of modern and fossil coccolithophores enables a proxy for growth phase to be developed that allows cellular physiology in the fossil record to be directly investigated. This is a potentially powerful new tool for understanding biotic-abiotic interactions in geological time. Furthermore, taxon-specific cellular geometry information provides us with a unique means to begin to reconstruct community-level cellular size structure and, crucially, its associated biovolume. These first reconstructions of community cell size structure across the transition from the Early Eocene greenhouse to the Early Oligocene icehouse demonstrate a massive shift in community biovolume distribution towards larger cells. This radically different-looking community must, in part, reflect the ability of the environment to support the demands of larger cells. Taken in conjunction with inferred changes in nutrient availability by the Late Eocene, this shift in population size structure was likely accompanied by an increase in community biomass, with potentially important implications for carbon export and size-specific grazing. Overall, my research illustrates that coccosphere geometry is a valuable tool for investigating fossil coccolithophore assemblages as populations of individual cells that are recording daily physiological responses to their immediate environment that ultimately determines the response of species and communities to environmental change.

Contents

List of tables

List of figures

List of Appendices

DECLARATION OF AUTHORSHIP

I, **Rosie Melanie Sheward**, declare that this thesis entitled **Cell size, coccosphere geometry and growth in modern and fossil coccolithophores** and the work presented in it are my own and has been generated by me as the result of my own original research.

I confirm that:

1. This work was done wholly or mainly while in candidature for a research degree at this University;

2. Where any part of this thesis has previously been submitted for a degree or any other qualification at this University or any other institution, this has been clearly stated;

3. Where I have consulted the published work of others, this is always clearly attributed;

4. Where I have quoted from the work of others, the source is always given. With the exception of such quotations, this thesis is entirely my own work;

5. I have acknowledged all main sources of help;

6. Where the thesis is based on work done by myself jointly with others, I have made clear exactly what was done by others and what I have contributed myself;

7. None of this work has been published before submission

Signed: ....

Date: ...... 12th May 2016 ....

Acknowledgements

I am indebted to Sam Gibbs for introducing me to the beautiful world of coccolithophores. From my very first email expressing interest in her work, she has been a constant source of inspiration and enthusiasm, helping to develop my ideas and run with them in new and exciting directions. I have benefitted more than I can express from her mentoring and support and I look forward to many more years of coccolithophore research in the future because of her guidance. I would like to thank Alex Poulton for venturing into palaeo with equal amounts of enthusiasm and pragmatism at the right time for an oceanography graduate to begin a PhD project on fossils. I always leave our weekly meetings with so many more questions than when I entered and have enjoyed many hours of musings about the unknowns about coccolithophores. I hope that in the future I can play my part in shaking up some of your paradigms. Thank you to Paul Wilson for your support from the outset and for the opportunity to commence a career in research.

Enormous thanks must go to Paul Bown for his enthusiastic and inspiring involvement in coccosphere research. I have benefited greatly from guidance about coccolithophore taxonomy, discussions around evolving results, thought provoking feedback on the work in this thesis, and of course for generously sourcing the most exquisite fossil material for me to use in this research. Many thanks to Ian Probert of the Roscoff Culture Collection for supplying the cultures used in this study. I am grateful to Leah LeVay for generously providing the original data from her study for use in Chapter 4. Jeremy Young has generously provided field samples from the Arctic for microscopy work. To Ian Harding, I am grateful for your formal role as my panel chair, but I am particularly grateful to you for all of the demonstrating opportunities that you have offered to me so that at times I can play the part of a 'real' geologist – hard hat and all. This work has benefitted greatly from discussions with many including Tom Dunkley Jones, Tom Ezard, Marcus Badger, Kirsty Edgar, Gavin Foster and Steve Bohaty. I gratefully acknowledge funding from the University of Southampton and NERC.

I am hugely grateful to many people at NOC that for their support, encouragement and friendship. Special thanks to Chris for your endless expertise on all things lab and culturing related, as well as constant willingness to help with Matlab and generally sit and discuss ideas and concepts. Sarah left big boots to fill and has been hugely helpful in

helping me to find my feet with microscopy and when I started. Lena has been there from the very beginning and I am so glad that we went through our PhDs together. Jason has been incredibly supportive and always happy to listen and offer advice. Lucie and Kyle are almost as enthusiastic about coccolithophores as I am, making for a hugely enjoyable office. Also thank you both for sacrificing your time to proof-read Chapters. And thank you to Helen for looking out for me and Dave, Di and Fran for being there for the first half of this journey.

I have been fortunate to have had the opportunity to participate in several summer schools and conferences during this PhD. I have had some wonderful experiences and met some amazing Early career scientists to whom I am grateful for their insights, enthusiasm and for introducing me to so many different areas of research.

Lastly, but by no means least, thank you to my family for always believing in me and providing the endless support and encouragement I needed to get here.

Definitions and Abbreviations

Ø	coccosphere diameter
Θ	cell diameter
Θ_{95}	95th percentile of cell size
Θ_5	5th percentile of cell size
b	the sum of all physiological factors affecting carbon fixation
b'	the sum of all physiological factors affecting carbon fixation, revised to reflect volume to surface area relative to *Emiliania huxleyi*
C_L	coccolith length (long-axis measurement)
C_N	number of coccoliths per cell
C_W	coccolith width (short axis measurement)
C_{SA}	coccolith surface area
C	carbon
CO_2	carbon dioxide
$CO_{2(aq)}$	aqueous carbon dioxide
pCO_2	partial pressure of atmospheric carbon dioxide
^{13}C	carbon-13 isotope
DNA	deoxyribonucleic acid
DSDP	Deep Sea Drilling Project
EECO	Early Eocene climatic optimum
ε_f	isotopic fractionation during carbon fixation
ε_p	isotopic fractionation of carbon during photosynthesis
$\varepsilon_{p37:2}$	isotopic fractionation of carbon in alkenones, long-chain ketones with 37 carbons
k_s	coccolith shape factor
K/20	type of seawater 'recipe' for culturing
LM	light microscope

Ma	millions of years
mbsf	meters below sea floor
Mg/Ca	magnesium to calcium ratio
μ	growth rate
N	nitrate
NP	Paleogene nannoplankton zone
ODP	Ocean Drilling Program
P	phosphate
PETM	Paleocene-Eocene thermal maximum
PIC	particulate inorganic carbon
POC	particulate organic carbon
ppm	parts per million
RCC	Roscoff Culture Collection
RNA	ribonucleic acid
SA:V	surface area to volume ratio
SEM	scanning electron microscope
Sr/Ca	strontium to calcium ratio
V	volume
V:SA	volume to surface area ratio

Chapter 1:
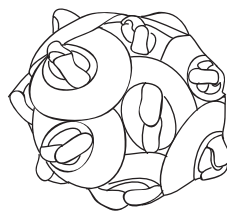
Introduction

1.1   Coccolithophores and environmental change

Coccolithophores are an abundant and ubiquitous group of single-celled phytoplankton. Their most distinguishing characteristic is the intricate calcite plates (coccoliths) that they produce to form an exoskeleton called a coccosphere that covers the organic cell (Figure 1.1). Coccoliths come in a multitude of geometric architectures that are distinct to each species and their varied arrangement around the cell produces a striking diversity of coccosphere shapes and sizes (Figure 1.2). The production of coccoliths makes coccolithophores a major pelagic calcite producer (alongside foraminifera and other calcified organisms such as pteropods; Berelson et al., 2007) and their coccolith remains form a considerable component of carbonate export to the deep ocean (Broecker and Clark, 2009). Coccolithophores are therefore an important component of both the biological carbon pump and the carbonate pump that transports particulate organic and inorganic carbon from the surface to the deep ocean (Ziveri et al., 2007).

Coccolithophores have become a focal group for researchers investigating how populations of marine phytoplankton may respond to changes in global climate. It is currently expected that increasing concentrations of carbon dioxide (CO_2) in the atmosphere will alter many fundamental physical and chemical properties of the ocean including seawater chemistry (including pH and saturation state), temperature, light, water column stratification, and macro- and micro- nutrient availability (Doney et al., 2012). Coccolithophores and other phytoplankton groups are likely to be highly sensitive to any degree of environmental variability as their growth, fitness and biogeographic distribution is dependent on these parameters. It is widely thought that the rate at which multiple environmental parameters are changing simultaneously could detrimentally impact the physiology of plankton, resulting in changes to many elements of marine ecosystems including shifts in species biogeography, loss of diversity through extinctions, physiological impairment and phenological shifts (Edwards and Richardson, 2004; Hays et al., 2005; Brierley and Kingsford, 2009; Hoegh-Guldberg and Bruno, 2010; Doney et al., 2012). In addition, there has been particular concern that calcifying organisms such as coccolithophores will be adversely affected by the changes in carbonate chemistry of seawater that are anticipated to result from increasing atmospheric CO_2 (Riebesell et al., 2000; Bach et al., 2015). It is therefore vital to understand the potential sensitivity of

a. coccosphere   **b.** coccoliths   **c.** coccolith morphology of life-stages

coccolith

central area

distal shield view

tube cyle (central column)

proximal shield view

heterococcoliths

holococcoliths

1μm
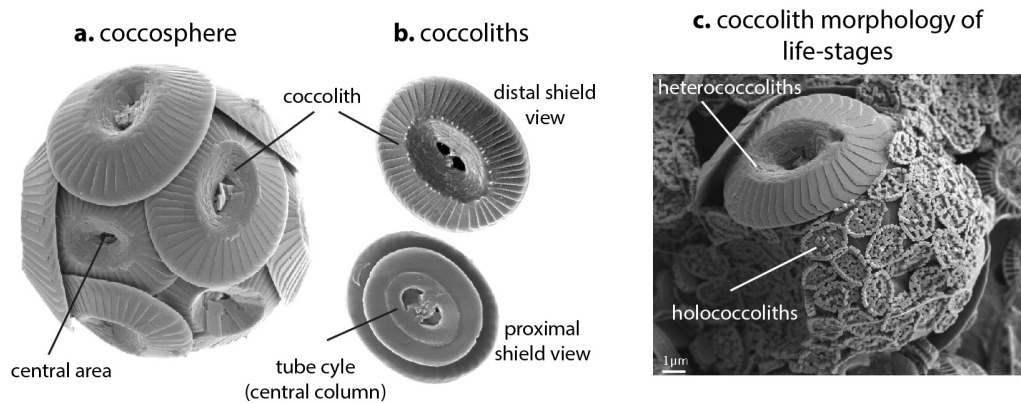
Figure 1.1: Coccolithophore terminology that is used throughout this thesis. Images are from Nannotax 3 (Young et al., 2014).

different phytoplankton groups, including coccolithophores, to environmental variability and the possible capacity that they may have for acclimation or adaptation (Lohbeck et al., 2012; Boyd et al., 2015).

Our current understanding of the response of coccolithophores to changes in temperature, light, nutrients and carbonate chemistry is largely based on short-term (<1 year) culturing experiments. The results of these experiments reveal that the physiological response of coccolithophores to changes in environmental parameters are complex and highly variable between species, genetic strains, and specific environmental parameters used (e.g., Langer et al., 2009). Additionally, some longer duration experiments have shown that coccolithophores can adapt to initially detrimental environmental conditions over hundreds of generations (Jin et al., 2013; Lohbeck et al., 2014; Schlüter et al., 2014). It is therefore not easy to interpret the interactions of coccolithophore physiology with the environment.

1.2   Fossil coccospheres as important palaeobiological archives

The fossil record is a unique archive of the net biotic response of coccolithophores to past environmental conditions that can provide a much-needed perspective on the responses of species, populations and entire communities to complex environmental interactions over longer timescales. Fossils of coccolithophores can be found as far back as the Late Triassic, ~225 Ma, and they provide an extensive and stratigraphically continuous record of their evolutionary history (Bown et al., 2004) that is widely used in palaeoceanographic and
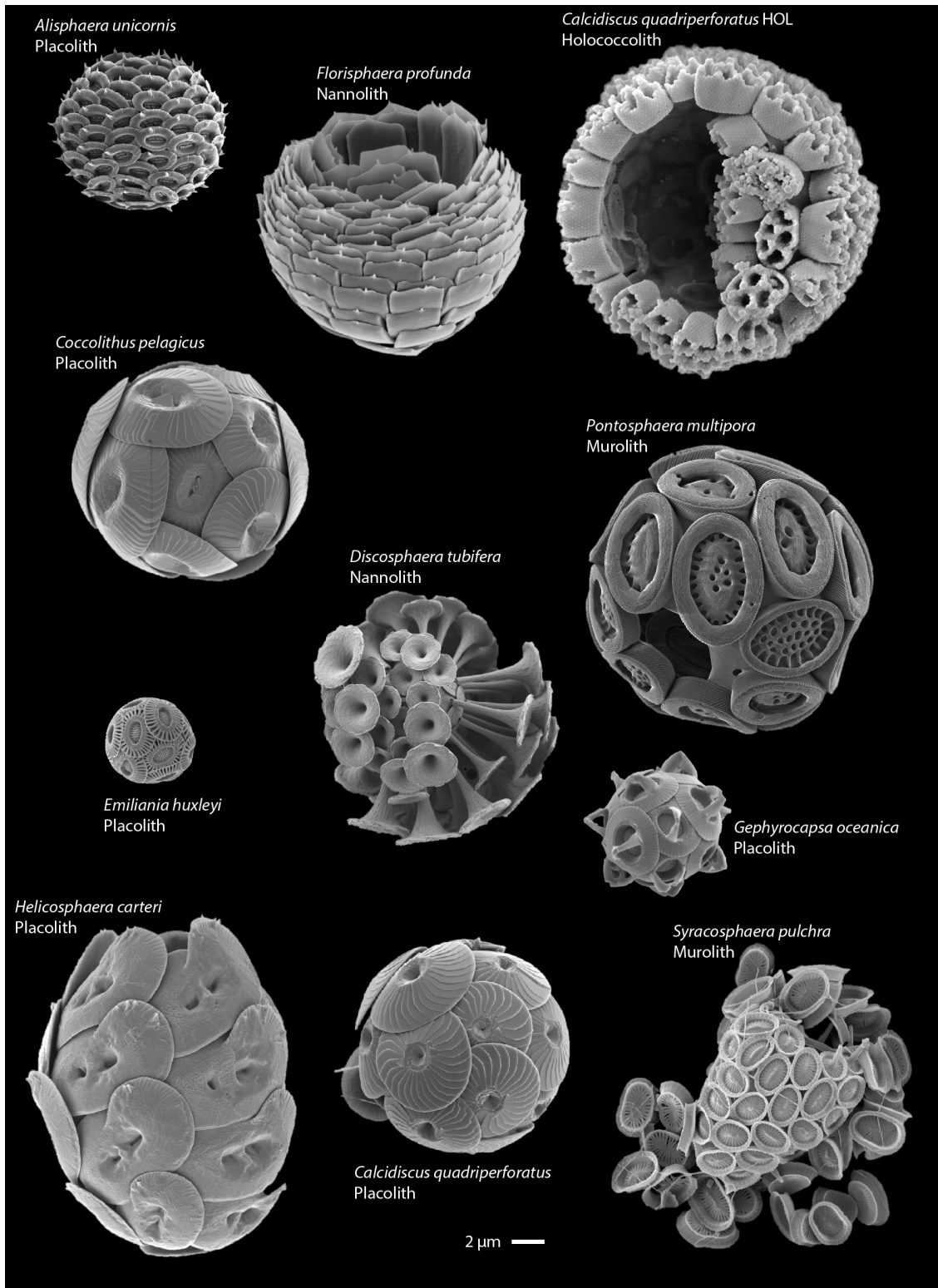
Figure 1.2: Examples of the diversity of coccosphere size, shape, coccolith morphology, coccolith arrangement around the cell and number of coccoliths per cell in some modern coccolithophores. All images are to the same scale to illustrate the variability in size (scale bar equals 2 μm). Images are from Nannotax 3 (Young et al., 2014).

palaeoclimatic studies. The vast majority of this fossil record consists of individual coccoliths that can be used to study spatial and temporal patterns in diversity, evolution, biogeography and ecological preferences, as well as proving to be useful indicators of palaeoceanographic conditions (e.g., Beaufort and Heussner, 2001; Bown, 2005b; Gibbs et al., 2006b; Stoll et al., 2007). However, the fossil record of coccoliths alone is missing a substantial amount of cellular-level information that can only be determined reliably from the original coccosphere. Fortunately, although they can be difficult to find, fossils of intact coccospheres are also found preserved in the fossil record. These fossil coccospheres provide fundamental information about the original size and shape of the cell and the specific arrangement of coccoliths that form the exoskeleton. These are important biological characteristics that can help to distinguish between species, particularly where coccolith morphology is similar (Saez et al., 2003), suggest a functional morphology that implies the preferred ecology of species (Young, 1994), and, for example, capture growth information (Gibbs et al., 2013). Fossil coccospheres therefore capture an unparalleled perspective of the growth of individual cells within a fossil population that importantly can be directly compared to modern coccolithophore species. The integration of data from fossil and modern specimens is a powerful tool to access previously unobtainable evidence of growth, cellular division and calcification in geological time, as highlighted by Gibbs et al. (2013). Studying both fossil and modern coccospheres is therefore an approach through which we can advance our understanding of the physiological sensitivity of coccolithophores to environmental change and assess their adaptive potential.

1.3   Cell size as an important trait of phytoplankton physiology

While my thesis is concerned with all aspects of coccosphere architecture (cell size and shape, coccolith size, and coccolith number and arrangement around the cell), as an introduction I focus here on reviewing controls on cell size. This is the most basic of cellular parameters that, thus far, we have had very little information on for fossil coccolithophores. Cell size is a fundamental 'master trait' of cellular physiology with virtually every aspect of cellular physiology in phytoplankton either directly or indirectly regulated by cell size (Chisholm, 1992). In the following, I review the key aspects of phytoplankton physiology that are connected with cell size to provide a starting context for the study of coccospheres in both modern and fossil populations. A number of these aspects are revisited in subsequent science Chapters.

1.3.1 Cell size, allometry, metabolic rate and growth

Allometry is the study of the dependence of physiological traits and rates on body size, specifically cell size and cell volume in phytoplankton (Gould, 1966; Tang, 1995; Beardall et al., 2009). The concept of allometry in part arises from the tendency of smaller organisms to have higher mass-specific metabolic rates - the rate at which an organism acquires energy and essential materials from the environment and converts that energy into products required for maintenance, growth and reproduction. Relationships between cell volume, V, and physiological trait or metabolic rate, T, can therefore often be described in the form:

$$T = cV^{\alpha} \qquad \qquad \text{Eqn. 1.1}$$

where c is a constant and α is a scaling exponent that, in phytoplankton, often deviates from the value of -0.25 (mass-normalised) predicted by the metabolic theory of ecology (Tang, 1995; Finkel and Irwin, 2000; Brown et al., 2004; Mei et al., 2011). In phytoplankton, metabolic processes include carbon assimilation (through photosynthesis), nutrient acquisition rates and rates of cell division (Huete-Ortega et al., 2012). The size-normalised surface area of the cell is very important for metabolic rate as it affects the relative abundance of membrane transporters that 'import' and 'export' growth-essential molecules across the cell membrane, such as the transport of macro- and micronutrients (Beardall et al., 2009). As cell size increases, the average distance within the cell across which materials must be transported also increases (Banavar et al., 2002). Decreasing surface area to volume ratio with increasing cell size therefore makes diffusion an increasingly insufficient mechanism by which materials can be transported through the cell to maintain cell functioning and may affect the growth rate that the cell can maintain (Beardall et al., 2009). The interaction of cell size with metabolic rate is usually assumed to result in faster growth rates of smaller cells relative to larger cells under the same conditions (Marañón et al., 2013), although this is likely to be an oversimplified perspective.

1.3.2 Cell size, nutrients and gaseous exchange

The cell surface area to volume ratio is a major determining factor in the rate at which nutrient uptake occurs and aqueous gases such as $CO_{2(aq)}$ are diffused into the cell, as described above. Cell size additionally determines the quantity and composition of intercellular macromolecules (including proteins, carbohydrates and enzymes) that define

the cellular concentrations of carbon, nitrogen, phosphorous, silica, iron and other elements that is termed cellular elemental stoichiometry (Geider and La Roche, 2002) and dictates the minimum nutrient requirements of the cell to sustain growth. The mean ratio of carbon to nitrogen to phosphorous in marine phytoplankton is 106 C : 16 N : 1 P, referred to as the Redfield ratio (Redfield, 1934). Cellular carbon content scales proportionally with cell volume (Menden-Deuer and Lessard, 2000), such that a larger cell will have an increased carbon content and, as such, more nitrate and phosphate relative to smaller cells. Larger cells therefore have a higher overall nutrient requirement to sustain basic cell functioning and are less efficient at transporting nutrients and carbon into the cell compared to smaller cells. Currently, the lack of comprehensive cellular stoichiometry data for coccolithophores makes it difficult to suggest whether this group, or specific species within this group, deviates away from Redfield stoichiometry. However, some evidence suggests that C:N may be higher than Redfield and N:P lower than Redfield in *Emiliania huxleyi* and *Gephyrocapsa oceanica* (Ho et al., 2003; Jin et al., 2013). Stoichiometry may also vary between coccolithophore species of different sizes, with cell size changes within species, or with changes in physiology resulting from varying environmental parameters (e.g., Rickaby et al., 2010; Langer et al., 2013).

The effect of cell size on nutrient demand and uptake rates may explain why biogeographic patterns in phytoplankton community size structure occur, as it theoretically determines that smaller cells should have a competitive advantage over larger cells when nutrient availability is restricted. As such, oligotrophic (low nutrient) regions are typically characterised by communities of smaller phytoplankton cells relative to regions of high nutrient availability (eutrophic) and environmental instability (such as upwelling areas) where larger cells can dominate (Falkowski, 1998).

1.3.3   Cell size and light

Light absorption of the cell per unit chlorophyll *a* decreases as cell volume increases (for a fixed pigment concentration) due to self-shading. This is known as the 'package effect' (Beardall et al., 2009). Under light-limited conditions, larger phytoplankton cells are therefore unlikely to be able to use the available photons as efficiently as smaller phytoplankton cells (Finkel, 2001; Key et al., 2010). As such, smaller cells are likely to be more abundant under reduced light conditions or in regions of very strong vertical mixing as they are more able to maintain photosynthetic rates compared to larger cells.

1.3.4   Cell size and physiological trade-offs

Cell size is clearly intricately linked with the cellular demand for CO_2, nutrients and light that varies proportionally with cell volume and the rate at which these essential 'materials' can be exchanged between the cell and the surrounding microenvironment, which is proportional to cell surface area. When all of these physiological interactions with cell size are considered collectively, it becomes clear that a necessary balance must be reached between physiological demands and particular environmental variables. For example, larger cells prefer higher light levels to reduce the impact of self-shading, however these conditions are more typical of stratified regions of the ocean that do not necessarily provide the higher nutrient availability necessary to meet the increased demands of larger cells. Additionally, at a community-level, size-selective zooplankton grazing (e.g., Bergquist et al., 1985) will provide a top-down control on species abundance. As such, the size structure of species and communities is a complex interplay of size-specific cellular demands and rates, environmental conditions and grazing pressures.

1.3.5   Cell size and physiology – in the fossil record?

Fossil coccospheres preserve the original exoskeletal structure of the organic cell and therefore provide us with the means to measure cell size in the fossil record. Using fossil coccospheres we can therefore consider aspects of cell physiology such as cellular carbon, nitrate and phosphate that require knowledge of 'true' cell size. Cell size can also be used from the perspective of species and species interactions within communities to consider changes in cell size as potentially direct physiological outcomes to variability in environmental parameters such as nutrients and light. These themes will be addressed throughout this thesis alongside other aspects of coccosphere geometry including coccolith number per cell that also appear to reflect aspects of cellular physiology (Gibbs et al., 2013).

1.4   The hunt for fossil coccospheres

Whilst intact fossil coccospheres have the potential to transform our understanding of cellular to community-level physiological responses of coccolithophores to environmental change in the past, they are not commonly found in sediments. Examination of a surface water coccolithophore community in contrast with a fossil assemblage (Figure 1.3) shows
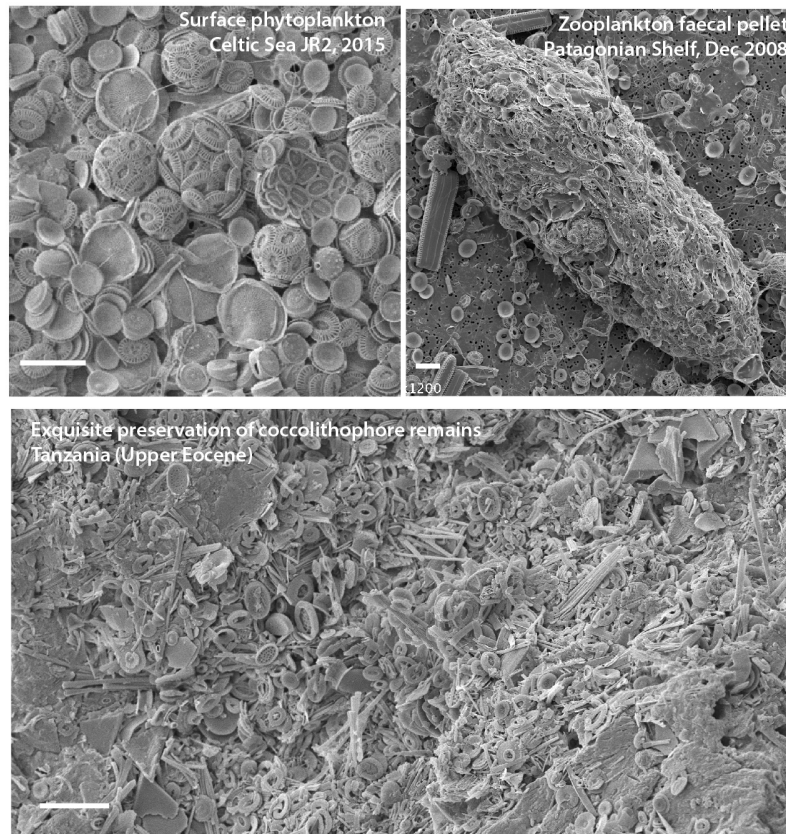
Figure 1.3: Examples of coccolithophore remains in the surface ocean (top left; photo: K. Mayers), in a zooplankton faecal pellet (top right; photo: A. Poulton) and in exquisitely preserved rock surface samples (bottom; photo: P. Bown). Scale bar = 5 μm

that the calcitic parts of coccolithophores and nannoplankton are susceptible to taphonomic losses at varying stages in the process of sedimentation (Young et al., 2005). There is a particular bias against the preservation of coccoliths that are small and/or fragile, where only ~20% of coccoliths <3 μm have a Holocene fossil record (Young et al., 2005). There is an even more significant bias against the preservation of intact fossil coccospheres, which are observed only occasionally in sediments (Covington, 1985; Mai, 1999).

There are many processes that can cause the disarticulation of a coccosphere into its component coccoliths between cell death and sedimentation. Firstly, the type of coccosphere construction governs the structural integrity of the coccosphere once the cell has died and any organic membranes have decayed. In this respect, coccospheres can be considered in two groups – coccolithophore species with coccolith types that sit side-by-side on the cell surface forming structurally fragile coccospheres (murolith, nannolith, holococcolith types) and the structurally more robust placolith-forming coccolithophores that produce coccoliths of two plates joined by a central tube (Figure 1.1), enabling each

coccolith to interlock and overlap with its neighbouring coccoliths. Species with placolith-type coccoliths therefore have a greater capacity to retain their coccosphere shape on cell death, which is less likely in non-placolith taxa. Secondly, recycling processes in the euphotic zone and during export through the water column can break up the coccosphere, including bacterial or viral cell lysis (Wilson et al., 2002) and mechanical disarticulation and chemical dissolution during ingestion by zooplankton (Harris, 1994; Langer et al., 2007). Plankton trap data suggests that coccosphere loss in the upper water column can be substantial (greater than 95%) and is regionally and seasonally variable (Ziveri et al., 2000; Smith, 2014), as well as biased against less robust species, as discussed above. Should the coccosphere reach the sea-floor intact, we can also expect coccospheres to be broken apart by bioturbation activity, by chemical dissolution and carbonate diagenesis, or by compaction pressures.

Generally, coccospheres have most commonly been encountered in sediments that have an overall exceptional quality of calcareous nannofossil preservation, arguably earning them Konservat-Lagerstätte status (Bown et al., 2008). These sediments are characterised by unprecedented diversity and the exquisite preservation of small (<3 μm) coccoliths, holococcolith taxa, and delicate and fragile morphological details that are more typically chemically or mechanically lost from specimens. These characteristics are exemplified by Cretaceous and Paleogene sediments of Tanzania (Bown, 2005a; Bown et al., 2009; Dunkley Jones et al., 2009), and subsequently by Paleogene (predominantly Late Paleocene – Early Eocene) sediments from the New Jersey Shelf, including Bass River and Wilson Lake, and the Lodo section of California (Gibbs et al., 2006a; Gibbs et al., 2006b; Gibbs et al., 2010). The depositional environments and lithologies of these sites with remarkable levels of preservation have a number of characteristics in common that minimise the various taphonomic processes that may lead to coccosphere disarticulation. Initially, higher primary productivity increases the quantity of coccospheres that have the potential to reach the seafloor. It also leads to higher productivity of grazers, which can be advantageous for coccosphere preservation because the sinking speeds of zooplankton faecal pellets are likely to exceed the sinking speeds of individual coccospheres (Honjo, 1976). This means that there is less time for bacterial digestion of the material in the water column and it reaches the sediment surface more rapidly. Images of zooplankton faecal pellets show that abundant coccospheres have the potential to be transported to the sediment in this way (Figure 1.3). Continental shelf palaeo-environments are an ideal example of sustained

higher productivity regions. Their closer proximity to terrestrially-derived sediments, higher productivity and shallower water depths means that sedimentation rates are typically high and biologically-derived material is rapidly buried.

At this stage, physical and chemical taphonomic processes that could potentially lead to coccosphere disarticulation can be limited in several ways. Sediments that are rich in impermeable clays but low in organic carbon content are particularly good for the preservation of calcite, which is sensitive to dissolution, carbonate diagenesis and overgrowth. Finally, low sediment oxygen concentrations may also increase coccosphere preservation potential by deterring intense bioturbation activity that churns up the sediment.

Within this thesis, I complement previous calcareous nannoplankton studies and coccosphere research from Tanzania, Bass River, Wilson Lake, and Lodo, seeking coccospheres from as many of these sediments containing 'exceptionally' preserved nannofossil assemblages as possible.

1.5   Thesis outline

The primary aim of this thesis is to investigate how the coccospheres of coccolithophores can be a used as a record of their physiological response to environmental variability. To achieve this, I consider modern coccolithophores alongside fossil coccospheres observed in sediments that contain exquisitely preserved calcareous nannofossil material. As these sediments are mostly of Paleogene age ($\sim$66 to 23 million years ago), my research is focused on this period particularly. The Paleogene is frequently described as having had a 'greenhouse' climate state with high atmospheric CO_2 (1000 - 2000 ppm) and globally warm temperatures (e.g., Zachos et al., 2008). During the Eocene, decreasing atmospheric CO_2 concentrations (Beerling and Royer, 2011) and evolving continental configuration instigated long-term global cooling towards the initiation of Southern Hemisphere glaciations around the Eocene-Oligocene boundary, 33 - 34 million years ago (Inglis et al., 2015). This greenhouse to icehouse transition was presumably associated with major environmental changes in the marine system, as seen in significant changes in coccolith assemblages (e.g., Dunkley Jones et al., 2008; Schneider et al., 2011). These fossil coccospheres therefore capture how coccolithophores have responded and adapted to the environmental conditions of a past warm, high CO_2 world and its transition towards a new

icehouse climate state. My research has necessarily involved the investigation of both living coccolithophores and fossil coccospheres, as we so far have very little understanding of the processes that govern not only size and architecture in fossil coccolithophore species, but also, perhaps surprisingly, in living coccolithophores as well. To achieve the overarching aim of this thesis I have therefore considered the following questions:

1. **What is the observed diversity in coccosphere geometry in Paleogene coccolithophores?**

   In **Chapter 2** I explore the range of cell and coccosphere size in Paleogene fossil coccospheres and its relationship with coccolith length and the number of coccoliths per cell. I uncover interesting new observations on the ranges of coccosphere geometries in a diversity of species, many of which have never been observed as intact coccospheres before, and the range in coccosphere geometry observed within individual species. To highlight the wider potential applications of this coccosphere dataset, I additionally explore approaches to cell-size adjustment in alkenone-based pCO$_2$ reconstructions.

2. **What are the fundamental controls on coccosphere geometry?**

   In **Chapter 3** I investigate how coccosphere geometry is regulated by physiology, specifically growth phase, in four important modern coccolithophore species that have long fossil records. I show that the cell size and number of coccoliths across families can be used as a proxy for growth phase in fossil coccolithophore populations.

3. **What is the biotic response of coccolithophores to climate changes during the Paleogene?**

   In **Chapter 4**, the extensive dataset of coccosphere geometry in different genera is used to reconstruct the cell size structure of coccolithophore communities at multiple sites between the Early Eocene and Early Oligocene. Community cell size and biovolume structure shows trends through the Eocene that are driven by the cell size evolution of species with respect to changing background nutrient conditions as the 'greenhouse' state of the Early Eocene transitioned into the new 'icehouse' state of the Early Oligocene.

Chapter 2:
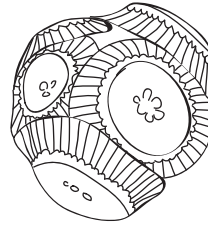
Coccospheres of the Paleogene greenhouse

Rosie M. Sheward, Samantha J. Gibbs, Paul R. Bown, Alex J. Poulton, Sarah A. O'Dea, David Higgins, Heather Jones, Geoff Thiemann

Abstract

Coccolithophores have a distinctive mineralized cell covering of multiple calcite plates (coccoliths) that exhibit a striking diversity of morphologies and cellular architectures across modern species. The geological record is a rich source of fossilized individual coccoliths but fully intact coccospheres are less commonly found. For many now-extinct species, we subsequently know very little about the species-specific characteristics of cell size and how it varies with coccolith size and shape, as well as the number of coccoliths and their arrangement around the cell. Here, I illustrate the range of coccosphere architecture and specific coccosphere geometry that is observed in fossil coccospheres of Paleogene age, ~66 to 23 million years ago. In many of these species, the complete coccosphere has not been previously observed. Relationships between coccosphere size, coccolith length and number of coccoliths per cell are diverse across the more than 40 species encountered, with some species exhibiting distinctive cells of many, smaller coccoliths and others characterized by cells of fewer, larger coccoliths. These taxa diverge substantially from the overall trend of larger cells covered by larger coccoliths. In addition to these novel palaeobiological observations, quantitative systematic relationships in coccosphere geometry within species and genera have the potential to be highly useful for other areas of palaeoclimatic research. As an example, I reconsider the approach to cell size adjustment in the alkenone pCO$_2$ proxy using new coccosphere geometry data from the presumed ancient alkenone-producer *Reticulofenestra*. Size-corrected pCO$_2$ differs by 200 to 1000 ppm during the Pliocene and Eocene respectively depending on the approach used. In light of the considerable range in pCO$_2$ concentrations that result from different approaches, the method of cell size adjustment in the alkenone pCO$_2$ proxy should be revisited to explore whether it could better reflect the degree of cell size information that can now be retrieved from the fossil record.

2.1   Introduction

The fossil record of coccolithophores within past marine geological successions is extensive and abundant, extending back ~225 million years (Ma; Bown et al., 2004). However, this fossil record almost exclusively consists of individual fossil coccoliths rather than the intact calcite cell covering (coccosphere) that is extremely susceptible to disarticulation by taphonomic processes after cell death. Modern coccolithophores, of which there are more than 200 species, demonstrate a substantial variability in cell size, shape, coccolith architecture and cellular geometry between species and genera (Young et al., 2003), some of which are illustrated in Figure 1.2. However, for the majority of now-extinct coccolithophore species we have limited knowledge of the architecture of intact coccospheres or even just the basic parameter of cell size. This is in stark contrast to other mineralised plankton groups such as foraminifera, diatoms, and radiolaria, where the entire 'skeleton' is commonly preserved intact within marine sediments.

Recently, intact fossil coccospheres have been observed in the fossil record (Gibbs et al., 2013; Bown et al., 2014) that offer valuable insights into palaeobiology and palaeoecology. This Chapter builds on this work, describing and quantifying the coccosphere construction and morphology of different fossil species, including details such as cell size and shape, the number of coccoliths each cell has, and whether multiple different coccolith types are found on the same cell. Information about the complete exoskeleton, the coccosphere, of different species is particularly important for a number of reasons. Firstly, temporal trends in body size are often studied in palaeontology as a record of micro- and macroevolution, for example due to bias towards small species after mass extinction events (Wade and Twitchett, 2009) and the general radiation of body size that often occurs with continuing speciation events (Stanley, 1973; Norris, 1991). Cell size is additionally a trait that is fundamentally linked to physiology and ecology in phytoplankton (see **Chapter 1** for overview and Finkel et al., 2010 and references therein). Recently, coccosphere geometry has been directly linked to cellular growth and division (Gibbs et al., 2013; **Chapter 3**). Cell size in coccolithophores and other plankton groups can therefore be used as a record of micro- and macroevolutionary responses to environmental variability that directly affects the physiology of populations and their biogeography.

In addition to the important palaeobiological information that intact fossil coccospheres provide, certain palaeoenvironmental proxies that analyse the geochemistry

of coccolith calcite or coccolithophore organic matter use calculations that are dependent on cell size assumptions. This arises from the influence that cell size and growth rates have on intracellular processes that have been shown experimentally to affect the partitioning of elements and isotopes involved in organic carbon and coccolith production (e.g., Ziveri et al., 2003). For example, cell size and/or growth rates are expected to strongly influence the organic alkenone biomarker proxy used for reconstructions of past atmospheric CO_2 concentrations and sea-surface temperatures (Pagani, 2002; Henderiks and Pagani, 2007; Brassell, 2014), the use of Sr/Ca and Mg/Ca in coccolith calcite as palaeo-productivity and palaeotemperature indicators respectively (Stoll and Schrag, 2000; Stoll et al., 2001; Rickaby et al., 2002; Stoll et al., 2002a; Stoll et al., 2002b; Rickaby et al., 2007), and the stable isotopes of carbon and oxygen obtained from coccolith calcite (Ziveri et al., 2003; Bolton et al., 2012; Bolton and Stoll, 2013; Rickaby et al., 2010).

Here, I document the coccosphere architecture and geometry (size, coccolith length and number of coccoliths from each coccosphere) of intact fossilised coccospheres that were living during the 'greenhouse' world of the Paleogene, ~66 to ~23 Ma. The observation and measurement of so many fossil coccospheres has been made possible by exploiting multiple geological successions with exquisite calcareous nannofossil preservation (Bown et al., 2008; Pearson and Burgess, 2008; Dunkley Jones et al., 2009; Bown et al., 2014) that contain far greater numbers of fossil coccospheres than ever previously observed. The processes by which coccospheres are more or less likely to be preserved in the fossil record are discussed in **Chapter 1**. The resulting dataset of coccosphere geometry from this ongoing research is of unprecedented detail, consisting of more than 4000 individual coccospheres, and provides novel insights into coccolithophore palaeobiology that will be of additional benefit to palaeoclimate studies using coccolithophore-derived geochemical proxies. To illustrate this, I used the new dataset presented here to explore the implications of different approaches to cell size adjustment used in the alkenone-based pCO$_2$ proxy.
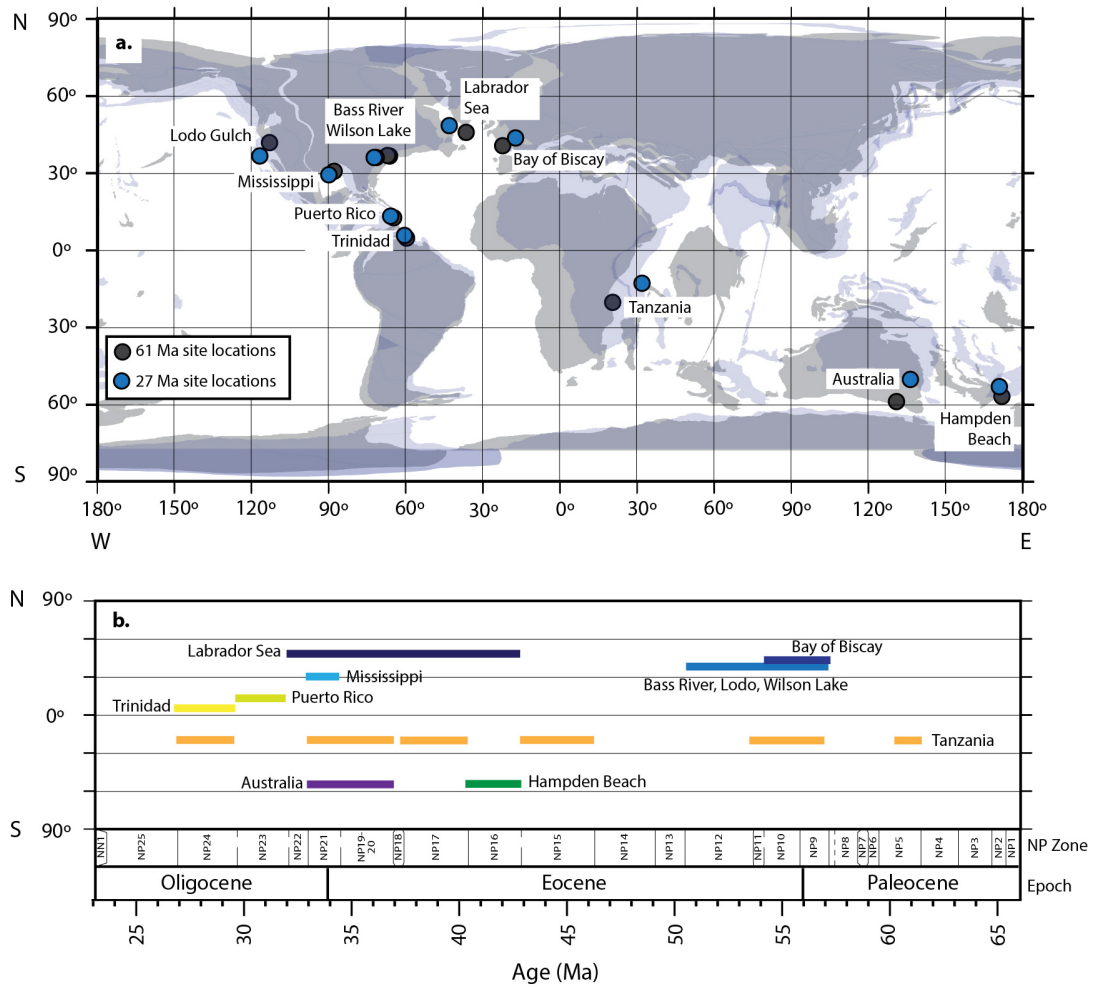
Figure 2.1: Sites used in this study. **a.** Palaeo-locations at ~61 Ma (Mid Paleocene) are shown as grey circles relative to the grey tectonic reconstruction and the palaeo-location of these sites at ~27 Ma (Late Oligocene) are shown as the blue circles relative to the blue tectonic reconstruction. Site locations have been reconstructed for the relevant time intervals based on the tectonic plates relevant to the modern latitude and longitude of the sites (http://www.odsn.de) and have been used to estimate site palaeolatitude, shown in Table 2.1. **b.** The nannoplankton zone (Martini, 1971) coverage of samples used from sites of different latitudes.

2.2   Materials and methods

2.2.1   Site descriptions

Material for this study was initially examined from sites that are interpreted to have a depositional environment that is advantageous for coccosphere preservation based on lithology and general quality of preservation (**Chapter 1**). Coccosphere data was collected from 11 localities at multiple latitudes and from different ocean basins (Figure 2.1a; Table

Site	Core ref.	Ocean[a]	Palaeolatitude[b]	Sample coverage[c]	Sample no.[d]	References
Labrador Sea	ODP Leg 105 Site 647A	ATL	~47 °N	NP16 to NP20-19	n=19	Srivastava et al. (1987)
Bay of Biscay	DSDP Leg 48 Site 401	ATL	~40 – 43 °N	NP9, NP10	n=12	Montadert et al. (1979)
Lodo Gulch		PAC	~37 – 42 °N	NP9, NP10, NP12	n=9	John et al. (2008)
Bass River	ODP Leg 147X	ATL	~37 °N	NP9 to NP11	n=38	Miller et al. (1998)
Wilson Lake	USGS Survey Site	ATL	~37 °N	NP10	n=11	Miller et al. (1998)
Mississippi		ATL	~30 °N	NP20-19	n=1	
Puerto Rico		ATL	~12 °N	NP23	n=3	Wade (2007)
Trinidad		ATL	~4 – 6 °N	NP24	n=1	Pearson and Wade (2009)
Tanzania	Tanzania Drilling Project	IND	~12 – 22 °S	NP5, NP9 to NP11 NP15, NP17, NP21 NP24	n=20	Pearson et al. (2004); Bown and Jones (2006); Nicholas et al. (2006); Pearson et al. (2006); Jimènez Berrocoso et al. (2012)
Australia		SO	~50 – 58 °S	NP20-19	n=1	Kamp et al. (1990)
New Zealand	Hampden Beach	SO	~ 52 – 57 °S	NP16	n=3	Burgess et al. (2008); Morgans (2009)

Table 2.1: Overview of sites and samples used in this study.

[a]Ocean basins – ATL – Atlantic Ocean, PAC – Pacific Ocean, IND – Indian Ocean, SO – Southern Ocean

[b]Palaeolatitudes are estimated from tectonic plate reconstruction maps at each of the specified intervals (Ocean Drilling Stratigraphic Network, odsn.de).

[c]The biostratigraphic marker species used in Martini (1971) are detailed in Appendix Table A2.2.

[d]Details of individual samples examined can be found in Appendix Table A.2.1.

2.1; Appendix Table A2.1), targeting samples with the highest coccosphere occurrence at each location. Tanzania (Tanzania Drilling Project) and Labrador Sea (ODP 647A) sites provided the samples with the greatest stratigraphic coverage (Figure 2.1b). Samples were assigned to the biostratigraphic Paleogene zonation scheme of Martini (1971) based on the composition of the sample assemblage and the presence or absence of marker taxa (Appendix Table A2.2). Combining data across sites generated a good distribution of samples (Figure 2.1b) beginning ~61 Ma in the Mid Paleocene (Paleogene calcareous nannoplankton zone NP5) to ~23 Ma during the Mid-Late Oligocene (NP24). Labrador Sea site ODP 647A provided calcareous nannoplankton from a high latitude assemblage (~47°N palaeolatitude) and a deep-ocean setting. Mid-latitude sites included the Bay of Biscay (DSDP site 401), Lodo Gulch (California), and Bass River (ODP site 174AX) and Wilson Lake (New Jersey) in the Northern Hemisphere. Southern Hemisphere mid-latitude material was obtained for Australia and Hampden Beach, New Zealand. Low-latitude sites in the Atlantic Ocean and Indian Ocean include Mississippi, Trinidad, Puerto Rico and Tanzania. Sites were mostly continental shelf settings with relatively high sedimentation rates and clay-rich lithologies, greatly improving preservation potential. The exception to this is deep-sea site Labrador Sea ODP 647A that has lower sedimentation rates but is rich in clays sourced from Greenland and North America (Srivastava et al., 1987).

2.2.2 Coccosphere geometry measurements

Standard smear slides (following Bown and Young, 1998) were produced for each sample. During preparation we endeavoured to manipulate the material as little as possible to reduce any potential mechanical disarticulation of coccospheres. Samples were examined under cross-polarised light microscopy (Olympus BX51 microscope with DP71 colour camera) and viewed at x1000 magnification using a x100 oil-immersion objective (Olympus UIS2 UPlanApo N). Slides were surveyed along continuous transects and each coccosphere encountered was recorded and identified to species level where possible following the taxonomy detailed in Bown (2005a) and the number of coccoliths comprising the coccosphere (C_N) counted. After imaging a coccolith-focused and a cross-section focused view of the coccosphere, measurements of coccolith length (C_L), coccosphere diameter (Ø), and cell diameter (Θ) were taken using Olympus Cell^D software (v3.4; Gibbs et al., 2013; Figure 2.2).
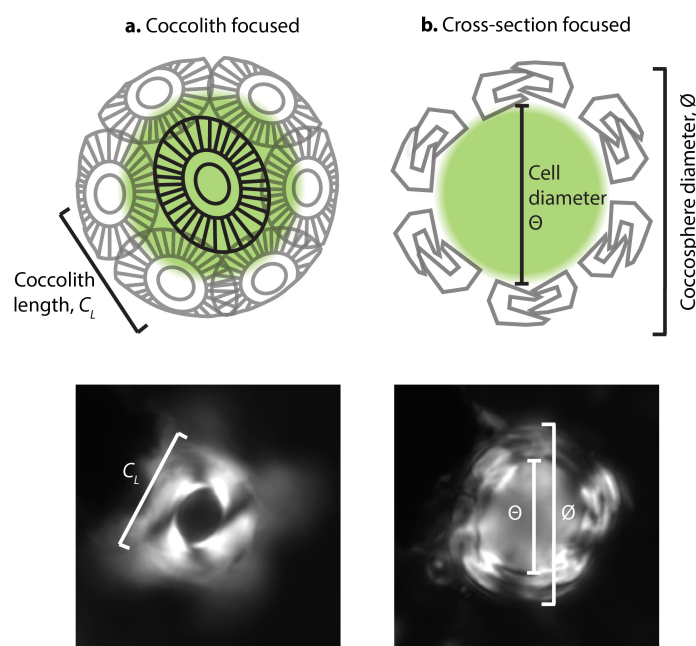
Figure 2.2: Illustration of the coccosphere geometry terminology used and the size measurements made on each individual coccosphere. Following taxonomic identification and counting the number of coccoliths per cell (C_N), images are taken of **a.** an in-focus, representative coccolith on either the top or bottom surface of the coccosphere from which coccolith length (C_L) is measured, and **b.** a cross-sectional view from which the coccosphere diameter (Ø) and internal coccosphere diameter, representing cell diameter (Θ), are measured.

2.3   Results

2.3.1   Coccosphere observations

A total of 4388 individual coccospheres were observed during this study, spanning 8 families, 15 genera and more than 40 Paleogene species (Taxonomic Appendix). Example coccospheres for many of these species are illustrated in Figures 2.3 to 2.5. The most common genera observed were *Coccolithus* (1770 coccospheres), *Toweius* (1376 coccospheres), *Reticulofenestra* (606 coccospheres), and *Cyclicargolithus* (203 coccospheres). These four genera were also typically the most common in the assemblages studied (frequently multiple coccoliths per field of view). Considerable numbers of coccospheres have also been collected for other Paleogene taxa such as *Biscutum* (n = 22), *Braarudosphaera* (n = 18), *Chiasmolithus* (n = 26), *Clausicoccus* (n = 40), *Cruciplacolithus* (n = 117), *Kilwalithus* (n = 68), and *Markalius* (n = 71). Additionally, rare to uncommon coccospheres of *Goniolithus*, *Umbilicosphaera*, *Campylosphaera*, *Biantholithus*, and *Crypotococcolithus* were also observed.

Toweius

■ 2 μm
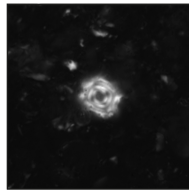
Toweius callosus
NP5 Tanzania
TDP 27 7/1 46-48 cm
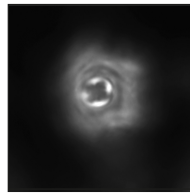
Toweius eminens
NP9 Bass River
BR 88
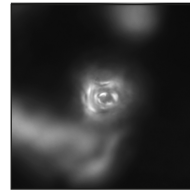
Toweius occultatus
NP12 Lodo
LO-03-21
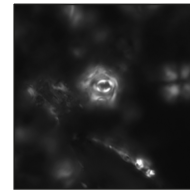
Toweius occultatus
NP12 Lodo
LO-03-21
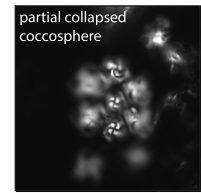
Toweius gammation
NP12 Lodo
LO-03-21
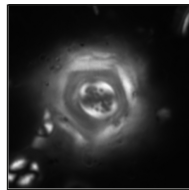
Toweius serotinus
NP10 Bass River
BR 42
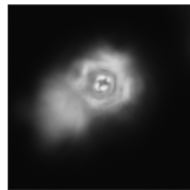
Toweius pertusus
NP10 Bay of Biscay
401 14/1 4 cm
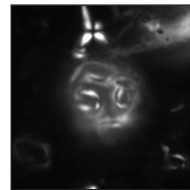
Toweius pertusus
NP11 Bass River
BR 10
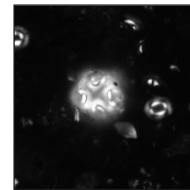
Toweius pertusus
NP9 South Dover Bridge
SDB N12417
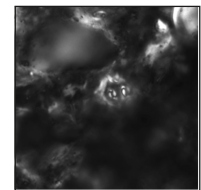
Toweius pertusus
NP5 Tanzania
TDP 27 7/1 46-48 cm

Cyclicargolithus
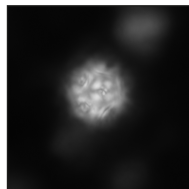
Cyclicargolithus luminis
NP9 Bass River
BR 103
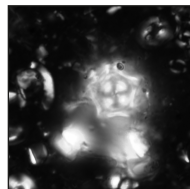
Cyclicargolithus luminis
NP16 Labrador Sea
647A 49-1 137-139 cm
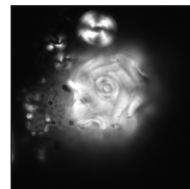
Cyclicargolithus floridanus
NP23 Puerto Rico
PR 139/17
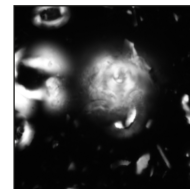
Cyclicargolithus floridanus
NP20-19 Labrador Sea
647A 34-1 104 cm
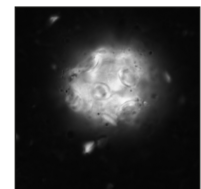
Cyclicargolithus floridanus
NP24 Tanzania
TDP RAS 99-42

Reticulofenestra
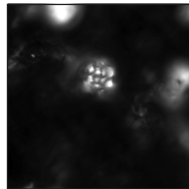
Reticulofenestra minuta
NP23 Puerto Rico
PR 139/9
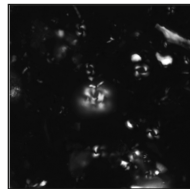
Reticulofenestra minuta
NP20-19 Australia
COLN 51
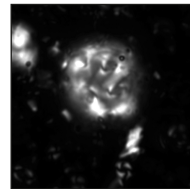
Reticulofenestra dictyoda
NP20-19 Mississippi
Miss BSWID BW 1.12
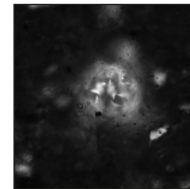
Reticulofenestra dictyoda
NP17 Tanzania
TDP LIN 99-17
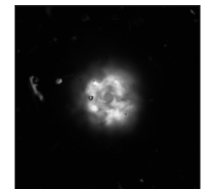
Reticulofenestra dictyoda
NP15 Tanzania
TDP MPC 25/1 62 cm
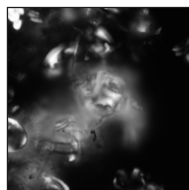
Reticulofenestra davesii
NP20-19 Labrador Sea
647A 32-3 13 cm
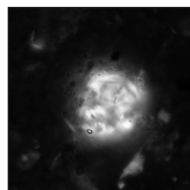
Reticulofenestra bisecta
NP17 Tanzania
TDP LIN 99-17
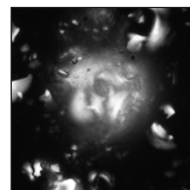
Reticulofenestra lockeri
NP20-19 Labrador Sea
647A 34-1 104 cm
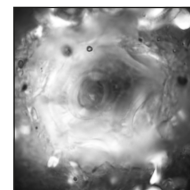
Reticulofenestra hillae
NP20-19 Labrador Sea
647A 34-1 104 cm
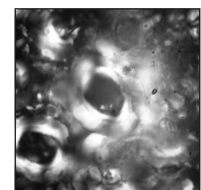
Reticulofenestra umbilicus
NP16 Labrador Sea
647A 49-3 45-47 cm

Figure 2.3: LM images of fossil coccospheres in the families Prinsiaceae and Noelaerhabdaeceae. Species name, NP zone, site and sample reference are given for each specimen.

Coccolithus

— 2 µm
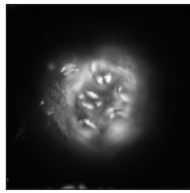
Coccolithus pelagicus
NP20-19 Labrador Sea
647A 32-3 13 cm
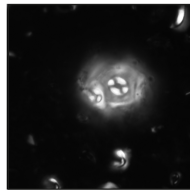
Coccolithus pelagicus
NP11 Bass River
BR 12
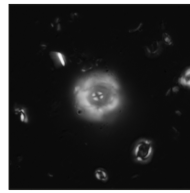
Coccolithus pelagicus
NP10 Bay of Biscay
401 14/1 4 cm
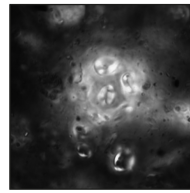
Coccolithus pelagicus
NP10 Bass River
BR 57
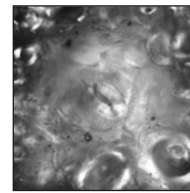
Coccolithus pelagicus
NP16 Labrador Sea
647A 49-5 108-110 cm
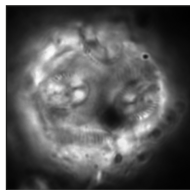
Coccolithus pelagicus
NP12 Tanzania
TDP 12 9/1 20-21 cm
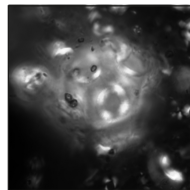
Coccolithus latus
NP16 New Zealand
HB 205
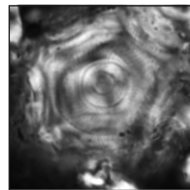
Coccolithus formosus
NP20-19 Mississippi
Miss BSWID BW1.12
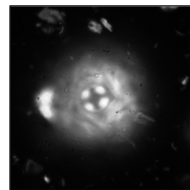
Coccolithus formosus
NP20-19 Mississippi
Miss BSWID BW1.12
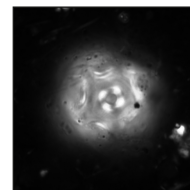
Coccolithus formosus
NP15 Tanzania
TDP 6 9/1 85-86 cm

Chiasmolithus
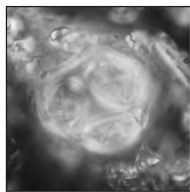
Chiasmolithus bidens
NP10 Bay of Biscay
401 14/3 20 cm
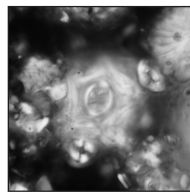
Chiasmolithus solitus
NP9 Bay of Biscay
401 14/3 99 cm
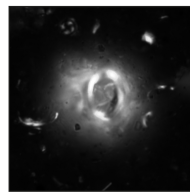
Chiasmolithus solitus
NP9 Bass River
BR 100
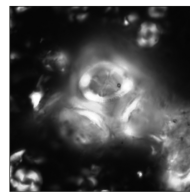
Chiasmolithus solitus
NP16 Labrador Sea
647A 49-5 108-110 cm
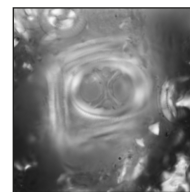
Chiasmolithus oamaruensis
NP20-19 Australia
COLN 51

Clausicoccus
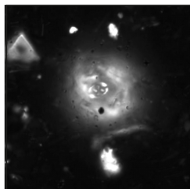
Chiasmolithus nitidus
NP23 Tanzania
TDP 2 9/1 85-86 cm
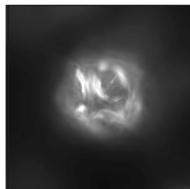
Chiasmolithus eoaltus
NP16 New Zealand
HB 205
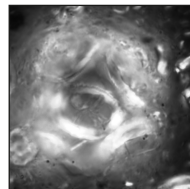
Chiasmolithus expansus
NP17 Labrador Sea
647A 46-4 85-87 cm
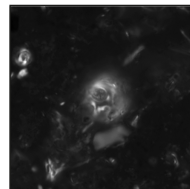
Clausicoccosu subdistichus
NP12 Lodo
LO-03-21
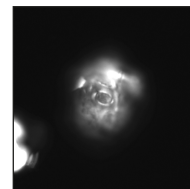
Clausicoccus fenestratus
NP20-19 Labrador Sea
647A 32-3 13 cm

Campylosphaera
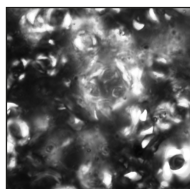
Clausicoccus subdistichus
NP16 Labrador Sea
647A 51-1 7-9 cm
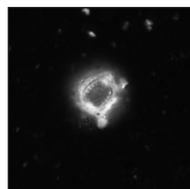
Clausicoccus vanheckiae
NP20-19 Tanzania
TDP 12 26/2 62 cm
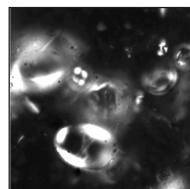
C. eroskayi
NP10 Bass River
BR 30
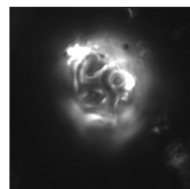
Campylosphaera dela
NP9 Tanzania
TDP 14 6/1 42 cm
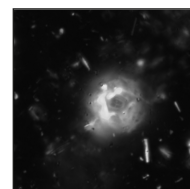
Campylosphaera dela
NP11 Tanzania
TDP 3 12/1 62-63 cm

Figure 2.4: LM images of fossil coccospheres in the family Coccolithaceae. Species name, NP zone, site and sample reference are given for each specimen.

Cruciplacolithus

— 2 μm
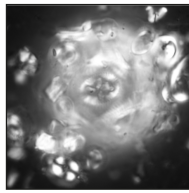
Cruciplacololithus edwardsii
NP10 Bay of Biscay
401 14/3 50 cm
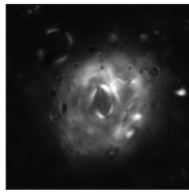
Cruciplacolithus primus
NP10 Bass River
BR 42
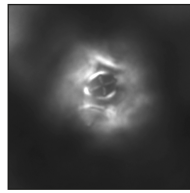
Cruciplacolithus primus
NP10 Bass River
BR 42
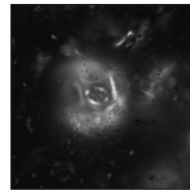
Cruciplacolithus frequens
NP10 Bass River
BR 57
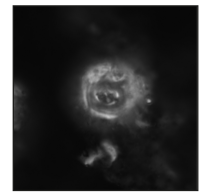
C. asymmetricus
NP15 Tanzania
TDP 6 9/1 85-86 cm
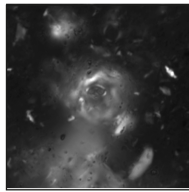
Kilwalithus

Cruciplacolithus latipons
NP12 Tanzania
TDP 12 9/1 20-21 cm
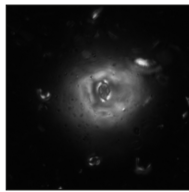
Cruciplacoltihus latipons
NP10 Bass River
BR 30
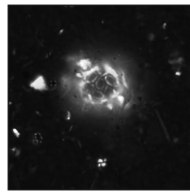
Kilwalithus cribum
NP15 Tanzania
TDP 6 9/1 85-86 cm
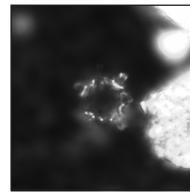
Kilwalithus cribum
NP15 Tanzania
TDP 6 9/1 85-86 cm
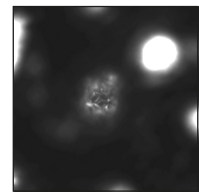
Kilwalithus cribum
NP15 Tanzania
TDP 6 9/1 85-86 cm

Umbilicosphaera
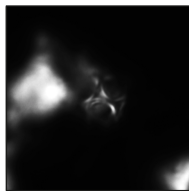
Goniolithus

Umbilicosphaera bramletti
NP12 Lodo
LO-03-14
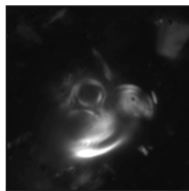
Umbilicosphaera bramletti
NP10 Bass River
LO-03-32
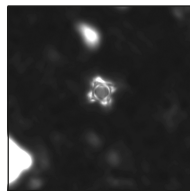
Umbilicosphaera bramletti
NP9 Bass River
BR 100
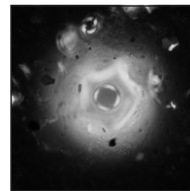
U. protoannulus
NP9 Bass River
BR 103
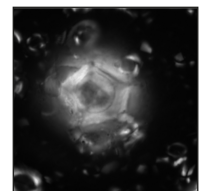
G. fluckigeri
NP16 Labrador Sea
647A 49-3 45-47 cm

Braarudosphaera
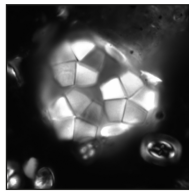
Biantholithus

B. bigelowi
NP12 Lodo
LO-03-14
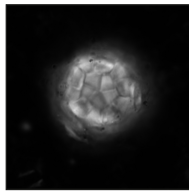
B. bigelowi
NP10 Tanzania
TDP 8 1/1 30 cm
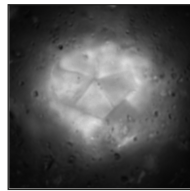
B. bigelowi
NP9 Tanzania
TDP 14 8/3 67-69 cm
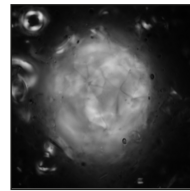
Biantholithus astralis
NP9 Bass River
BR 85
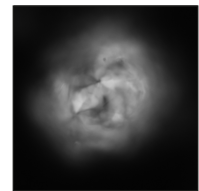
Biantholithus astralis
NP9 Bass River
BR 82

Biscutum   *Helicosphaera*   *Markalius*   *Cryptococcolithus*
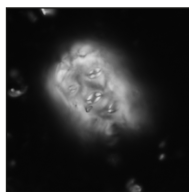
Biscutum braloweri
NP9 Bass River
BR 82
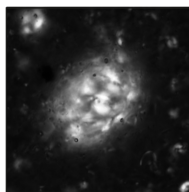
Helicosphaera sp.
Miocene Malta
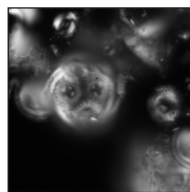
Markalius inversus
NP20-19 Labrador Sea
647A 32-3 13 cm
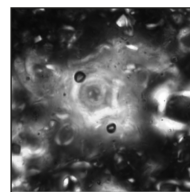
Markalius inversus
NP18 Labrador Sea
647A 46-3 8-10 cm
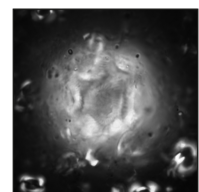
C. mediaperforatus
NP16 Labrador Sea
647A 49-2 64-66 cm

Figure 2.5: LM images of fossil coccospheres in the family Calcidiscaceae and other species. Species name, NP zone, site and sample reference are given for each specimen.

Prior to this study and Gibbs et al. (2013), the only other study to present measurements of coccolith and cell size data was by Henderiks (2008), comprising of a total of 152 coccospheres from only three taxa, *Coccolithus*, *Reticulofenestra* and *Cyclicargolithus*. Many of the taxa documented here are therefore being imaged and measured in the form of intact coccospheres for the first time, for example *Markalius*, *Cyclicargolithus luminis*, *Kilwalithus*, and several species of *Chiasmolithus, Cruciplacolithus, Clausicoccus* and *Campylosphaera.*

Except for *Braarudosphaera* and *Goniolithus,* all of the coccospheres observed and measured were heterococcolith placolith species, meaning coccoliths that consist of two shields connected by a central tube (Figure 1.1). This is not unsurprising, as this coccolith morphology allows adjacent coccoliths to overlap and interlock, forming structurally robust coccospheres. Species producing other coccolith morphologies that sit side-by-side on the cell surface (e.g., murolith, planolith or in holococcolith phase) are more susceptible to disarticulation, which significantly decreases their preservation potential. The pentagonal coccolith shape of *Braarudosphaera* and *Goniolithus* (Figure 2.5) forms highly regimented dodecahedral coccospheres of tightly abutting coccoliths that may help to increase the preservation potential of these non-placolith taxa.

Spherical coccosphere geometries are by far the most common shape, as is also the case for extant species. However, other fossil coccosphere shapes have been observed including the prolate spheroid coccospheres of Miocene *Helicosphaera* (Figure 2.5) that are consistent with the coccosphere shape of modern *Helicosphaera* (**Chapter 3**) and the ovoid to ellipsoidal shape of *Biscutum braloweri* (Figure 2.5). Cuboid coccosphere shapes have additionally been commonly observed in several species including *Umbilicosphaera bramletti* (Figure 2.5), which is almost exclusively cuboid in shape, as well as in *Chiasmolithus bidens*, *Toweius pertusus* and *Reticulofenestra dictyoda* that more typically have spherical coccospheres with a larger number of coccoliths per cell. Remarks on many of the coccosphere architectures identified during this study have been published in Bown et al. (2014).

2.3.2   Coccosphere geometry

To quantify the specific geometry of each fossil coccosphere observed, the coccosphere and cell size, coccolith length and number of coccoliths per cell were measured. An overall correlation between coccosphere size (Ø) and coccolith length (C_l) is generally a persistent feature of coccosphere geometry, with larger coccospheres typically associated with larger
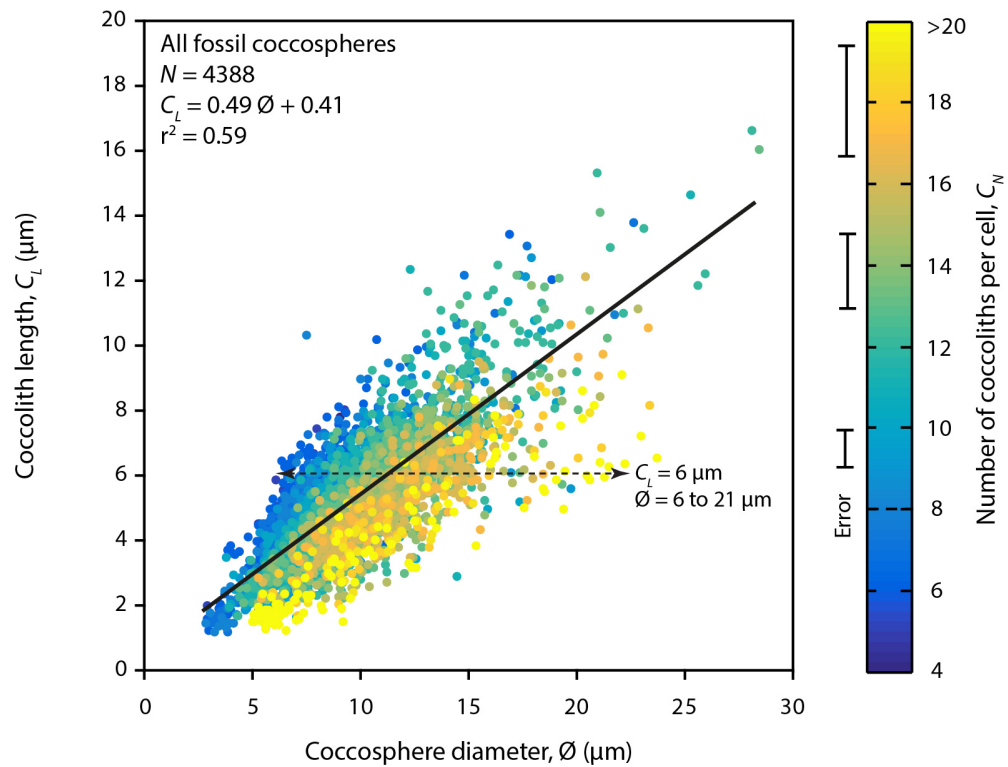
Figure 2.6: The relationship between coccosphere diameter (Ø), and coccolith length (C_L) is also related to number of coccoliths per cell (C_N; colourbar). Model II major axis regression model result (black line) shows the linear relationship between Ø and C_L. Reproducibility of C_N counts decreases as C_N increases (shown by error bars). The horizontal dotted lines shows that a specific coccolith length can be associated with a range of coccosphere diameters, in this example, coccoliths of length 6 µm are observed on coccospheres between ~6 and 21 µm in diameter.

coccoliths (Figure 2.6) as previously reported by Henderiks (2008) and Gibbs et al. (2013).

Coccosphere size shows an order of magnitude range in diameter, from 2.7 µm to 28.4 µm (Figure 2.6). The range of coccolith lengths observed on fossil coccospheres (1.1 µm to 16.6 µm) is consistent with the range of coccolith lengths typically observed across loose coccoliths in assemblages of Paleogene age (<3 µm to >14 µm). However, few coccospheres with coccolith lengths >9 µm are observed (Figure 2.6), even though the same sample may contain larger coccoliths of the same genus. Coccosphere geometry data for modern *Coccolithus*, *Calcidiscus* and *Helicosphaera* also suggests that coccospheres >20 µm in diameter with coccoliths >9 µm are very common within culture populations in the modern descendants of these genera (Appendix Figure A2.3; **Chapter 3**). This could perhaps suggest that larger coccospheres with larger coccoliths occur less frequently within field communities, that the coccosphere geometry of modern descendant species within some genera has evolved and/or that there is a taphonomic bias against the preservation of
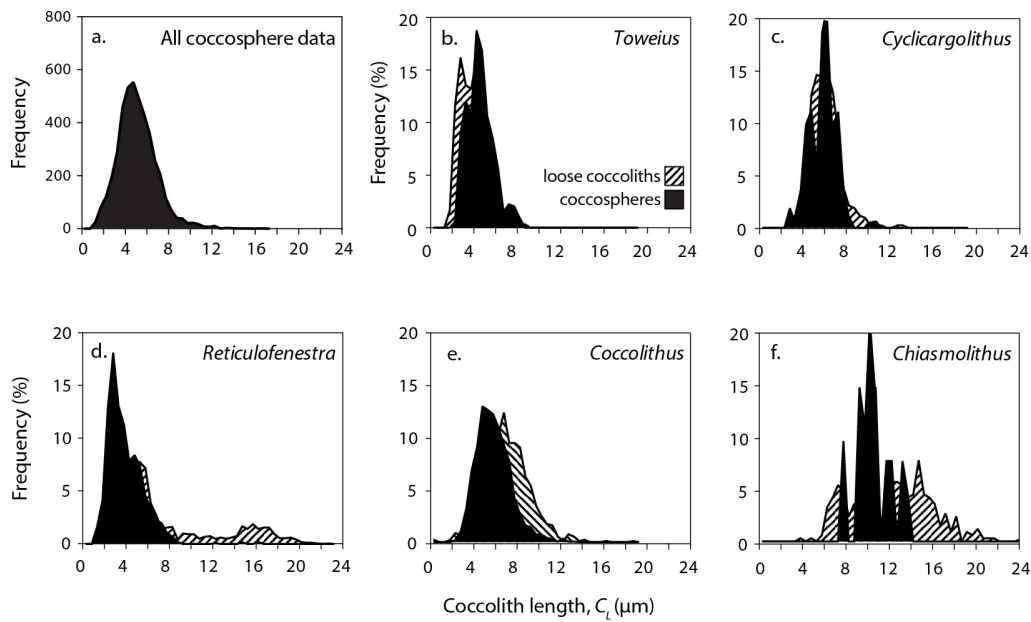
Figure 2.7: Comparison of the frequency of coccolith lengths occurring on fossil coccospheres (black) relative to the size distribution of loose coccoliths (shaded) in a sub-set of samples. **a.** The frequency distribution of coccolith length across all fossil coccospheres (n=4388). The relative frequency of coccolith size from coccospheres and loose coccoliths in five common Paleogene genera, **b.** *Toweius*, **c.** *Cyclicargolithus*, **d.** *Reticulofenestra*, **e.** *Coccolithus*, **f.** *Chiasmolithus*.

larger coccospheres with larger coccoliths. However, comparing the frequency distribution of coccolith lengths measured from coccospheres of *Coccolithus*, *Toweius*, *Reticulofenestra* and *Cyclicargolithus* with the C_L distribution measured on loose fossil coccoliths of the same genera clearly shows that this C_L size bias is not consistent across taxa (Figure 2.7). For example, the general shape of the loose C_L distribution is well reflected by C_L measured from coccospheres in *Toweius* and *Cyclicargolithus,* whereas C_L from coccospheres are skewed towards smaller sizes in *Coccolithus* and *Reticulofenestra*. In *Reticulofenestra* and *Chiasmolithus*, the small abundance of very large coccoliths (10 to 20 μm and 14 to 22 μm coccoliths respectively) observed within loose coccolith material only occur as the occasional coccosphere. Future investigations into the relative differences in species composition, relative abundance and coccosphere geometry of coccolithophore communities in the modern surface ocean compared to sediment core top samples would provide further insight into the potential taxonomic or size biases that might affect the preservation of coccospheres in the fossil record.

The notable scatter in the relationship between Ø and C_L (Figure 2.6) is systematically associated with a large range in number of coccoliths per cell (C_N). For example, a 6 μm coccolith could be associated with a ~6 μm coccosphere of 5 coccoliths up to a 21 μm cell with >20 coccoliths. The minimum observed C_N needed to cover a cell is 4-7 coccoliths whilst the maximum number observed on a single *Kilwalithus* cell is ~52 (Figure 2.5). Because many of these species have not been observed or systematically measured as coccospheres before, this study is revealing a previously unappreciated range of coccoliths per cell in fossil coccolithophores that is more comparable to the range in C_N observed on modern placolith coccospheres, which range up to ~60 coccoliths per cell in genera such as *Syracosphaera* and up to several hundred coccoliths per cell in the genus *Alisphaera* when C_N is estimated from SEM images (Appendix Table A2.4; Figure 1.2 and Figure 2.8b; Nannotax3, Young et al., 2014). C_N and Ø are therefore variables that can become strikingly decoupled from C_L in some groups, characterised by smaller cells with fewer, large coccoliths or larger cells with many, smaller coccoliths.

2.3.3 Genus- and species-level coccosphere geometry

Genus specific differences in coccosphere geometry (Figure 2.8; Figure 2.9a) can be highlighted by calculating the difference between observed coccosphere size and the coccosphere size that would be calculated from coccolith length using the linear regression equation $C_L = 0.49$ Ø $+ 0.41$ derived from the complete coccosphere dataset shown in Figure 2.6. Positive values of observed Ø minus calculated Ø (Figure 2.9a) indicate that C_L is likely to underestimate true cell size because the taxa is characterised by a coccosphere geometry of more, smaller coccoliths relative to its coccosphere size. Conversely, a negative value indicates that C_L overestimates true cell size. Although there is variability in the C_L and Ø size range within all genera, Figure 2.9 shows that C_L is a poor predictor of observed coccosphere size in *Biscutum, Kilwalithus, Clausicoccus* and *Campylosphaera*, where observed Ø is larger than suggested by C_L as cells are associated with a higher C_N (Figure 2.9b). *Biantholithus, Chiasmolithus, Umbilicosphaera* and *Toweius* are characterised by fewer, larger coccoliths relative to their coccosphere size, as observed Ø is smaller than suggested by C_L.

Proposed phylogenetic lineages (Figure 2.8; Bown et al., 2014) do not provide an obvious pattern of coccosphere geometry characteristics. Species within the genus *Cruciplacolithus* for example are often characterised by coccospheres of more, smaller coccoliths (Figure 2.8a, 2.9) however coccospheres of *Chiasmolithus*, which is proposed to

Number of coccoliths per cell, C_N

a. Paleogene genera and species

Paleogene family phylogeny

Isochrysidales:
- △ Noelaerhabdaceae
- ⬡ Prinsiaceae
- ⊗ Biscutaceae

Coccolithales:
- ○ Coccolithaceae
- □ Calcidiscaceae

Zygodiscales:
- ◇ Helicosphaeraceae
- ◁ Pontosphaeraceae

Syracosphaerales:
- ✶ Rhabdosphaeraceae
- ✕ Syracosphaeraceae
- ✳ Calciosolinaceae

- ⬦ Markalius
- ⊗ Biantholithus

Coccolith families *inc. sed.*:
- ☆ Umbellosphaeraceae
- + Alisphaeraceae

b. Extant species by family

Modern family phylogeny

Coccolith length, C_L (μm)

Coccosphere diameter, Ø (μm)

Figure 2.8 (opposite): The mean Ø and C_L of genera and species are shown with the colour of the data point representing the mean C_N. **a.** Paleogene genera and some species from this study. **b.** For comparison, the coccosphere geometry of selected modern species are also shown, calculated for *Coccolithus pelagicus*, *Coccolithus braarudii*, *Calcidiscus leptoporus*, *Calcidiscus quadriperforatus* and *Helicosphaera carteri* from culture experiments (Chapter 3) and for other modern species estimated from SEM images on Nannotax3 (Young et al., 2014). Data symbols denote the family and proposed phylogenetic relationships to which each species/genus belongs, based on Bown et al. (2004) and Nannotax3 (Young et al., 2014), with K/Pg the Cretaceous-Paleogene boundary. The number in brackets following some modern species denotes the approximated number of coccoliths per cell (C_N), where C_N is greater than 20, as indicated by the colour bar. Coccosphere geometry measurements for these extant species can be found in Table A2.4. Taxa that plot to the right of the linear regression have, on average, larger coccospheres than would be suggested from coccolith length and a greater number of coccoliths per cell. Taxa that plot to the left of the linear regression are typically smaller cells than C_L would suggest with fewer coccoliths per cell.

have evolved from *Cruciplacolithus* (Bralower and Parrow, 1996), are more typically comprised of fewer larger coccoliths (Figure 2.8a, 2.9). In contrast, the closely related genera *Reticulofenestra* and *Cycliargolithus* show a broadly similar relationship between C_L, Ø and C_N that is notably different from *Toweius* (Figure 2.9, 2.10) from which they are presumed to have evolved (Young et al., 1992). In modern coccolithophores, coccospheres with high (>30) C_N are mostly restricted to the highly-morphologically diverse *Syracosphaera* genus (C_N = ~30 – 85) and species within the families Rhabdosphaeraceae, Alisphaeraceae (C_N = ~100 – 300) and Calciosoleniaceae (Figure 2.8b). These high-C_N families within the order Syracosphaerales evolved within a distinct evolutionary lineage (Figure 2.8; Bown et al. 2004) and their Paleogene ancestors typically exhibited small (<3-5 μm) coccoliths with murolith or planolith morphologies (i.e., not interlocking placolith-type coccoliths) that reduce the preservation potential of intact coccospheres.

The abundant number of coccospheres collected of *Coccolithus*, *Toweius*, *Reticulofenestra* and *Cyclicargolithus* provides ample data with which to investigate genus- and species-specific coccosphere geometry (Figure 2.10). *Cyclicargolithus* has the smallest range in Ø (7 to 19 μm) and C_L (3 to 11 μm) and *Toweius* has the smallest range in C_N, with only four coccospheres exceeding 12 coccoliths per cell. The relationship between Ø and C_L is relatively similar in *Coccolithus* (C_L = 0.53 Ø + 0.14), *Reticulofenestra* (C_L = 0.53 Ø + 0.33) and *Cyclicargolithus* (C_L = 0.49 Ø + 0.29). In contrast, the relationship between Ø and C_L in *Toweius* is considerably steeper, with coccoliths associated with smaller coccospheres on average than observed in *Coccolithus*, *Reticulofenestra* or *Cyclicargolithus* (Figure 2.10i).

Some of the variability in coccosphere geometry seen within these genera can be attributed to the mixing of multiple species that exhibit differences in specific coccosphere
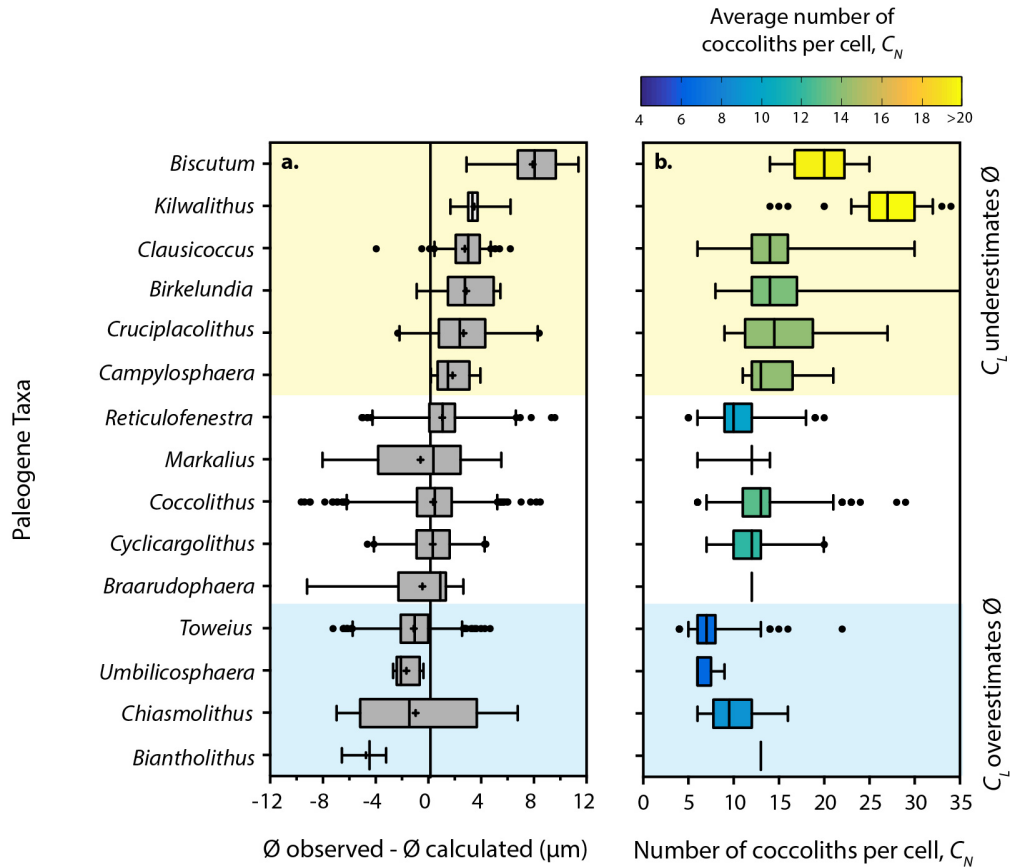
Figure 2.9: Residual plot of coccosphere data for each genus relative to number of coccoliths per cell, C_N. **a.** Residuals of the Model II major axis regression relationship between coccosphere diameter (Ø) and coccolith length (C_L) shown in Figure 2.6, where $C_L = 0.49Ø + 0.41$ and the residual of each data point is calculated as (measured Ø - calculated Ø). Each genus is represented as a box and whisker plot, with the box and whiskers representing the 25th-75th and the 5-95th percentiles of the data respectively. The mean of the data is additionally shown as +. Positive residuals plot below the line of best fit in Figure 2.6 and show genera where measured Ø is larger than would be predicted by C_L. Negative residuals plot above the line and show genera where measured Ø is larger than would be predicted by C_L. **b.** Box and whisker plots of number of C_N for each genus. Genera where coccolith length overestimates coccosphere diameter (positive residuals) are typically coccospheres of many, small coccoliths, whereas genera where coccolith length overestimates coccosphere diameter (negative residuals) have fewer coccoliths per cell.

geometry (Figure 2.10). This certainly appears to be the case for *Reticulofenestra*. However, it is interesting to note that *Toweius*, whilst having the narrowest range in C_L, Ø and C_N, is species diverse whilst C_L, Ø and C_N in *Coccolithus* shows an incredibly broad range considering it is a virtually monospecific dataset. As such, coccosphere geometry also shows a high degree of within-species variability in Ø and C_N, which has recently been shown to be a function of growth phase in modern *Coccolithus* populations (Gibbs et al., 2013) and in modern *Calcidiscus* and *Helicosphaera* (**Chapter 3**). Different populations of the same species experiencing different environmental or ecological conditions also show

Number of coccoliths per cell, C_N

4 6 8 10 12 14 16 18 >20

a.
Coccolithus
$N = 1770$
$C_L = 0.53Ø - 0.14$
$r^2 = 0.55$

c.
Toweius
$N = 1376$
$C_L = 0.66Ø - 0.25$
$r^2 = 0.50$

e.
Cyclicargolithus
$N = 203$
$C_L = 0.49Ø + 0.29$
$r^2 = 0.50$

g.
Reticulofenestra
$N = 606$
$C_L = 0.53Ø - 0.33$
$r^2 = 0.72$

i.
Relationship between
Ø and C_L in each genus

Toweius
Coccolithus
Reticulofenestra
Cyclicargolithus

b.
C. pelagicus *C. latus*
C. formosus *C. pauxillus*

d.
T. pertusus *T. serotinus*
T. rotundus *T. eminens*
T. occultatus *T. callosus*

f.
C. floridanus
C. luminis

h.
R. dictyoda *R. hillae*
R. minuta *R. bisecta*
R. umbilicus *R. davesii*

j.
Ø and C_L relationships
Henderiks (2008)

Coccolithus
Ø = 1.10 + 1.53 C_L
Reticulofenestra
Ø = 1.02 + 1.42 C_L
Cyclicargolithus
Ø = 1.44 + 1.46 C_L

Coccolith length, C_L (µm)

Coccosphere diameter, Ø (µm)

Figure 2.10 (opposite): Coccosphere diameter (Ø), coccolith length (C_L) and number of coccoliths per cell (C_N) for four key Paleogene genera. **a., b.** *Coccolithus* coccospheres. **c., d.** *Toweius* coccospheres. **e., f.** *Cyclicargolithus* coccospheres. **g., h.** *Reticulofenestra* coccospheres. The top image of each pair shows how C_N varies with Ø and C_L while the bottom image shows a breakdown of the species within each genus. Model II major axis regression model results (black line) show the relationship between Ø and C_L. The linear regression of each genus, **i.,** is compared to **j.** the linear regression of Henderiks (2008).

subtle variability in coccosphere geometry that leads to a range of Ø, C_N and C_L in field and fossil populations (Gibbs et al., 2013). Furthermore, coccospheres from a wide range of geological time intervals have also been integrated so there is also likely to be a degree of temporal size variability within each species. Within-species variability in coccosphere geometry therefore integrates genetic, growth, ecological and evolutionary signals that results in the range of coccosphere geometry relationships seen for each genus.

2.4 Discussion

2.4.1 Structural and physiological constraints on coccosphere geometry

Coccosphere size, number and arrangement of coccoliths around each coccolithophore are highly diverse in our fossil observations and in modern species (Figure 1.2, 2.8b). What constrains the minimum and maximum coccosphere geometry? In the following, I consider how the architectural construction of coccospheres can pose a limit on the minimum number of coccoliths per cell. Generally, observed C_N is greater than 4 across all the species observed (Figure 2.9b), with taxa such as *Chiasmolithus* and *Umbilicosphaera* characterised by a C_N close to this value (5 to 8). Additionally, the minimum C_N observed within species is associated with cells that have recently undergone cell division (**Chapter 3**). I then consider how coccosphere geometry may be constrained by the C_N and C_L of a species relative to its cell volume to ensure that the rate of coccolith and therefore calcite production keeps pace with growth rate.

2.4.1.1 Structural constraints on minimum number of coccoliths per cell

Is there a hypothetical minimum C_N for each taxa that is related to potential structural limitations of forming a coccosphere? By making the assumption that the cell surface area must be covered by coccoliths and that coccolith length cannot exceed cell diameter (as coccoliths are formed within the cell) the C_N threshold below which coccolith length would exceed cell diameter can be calculated. Coccolith surface area (C_{SA}) must first be calculated
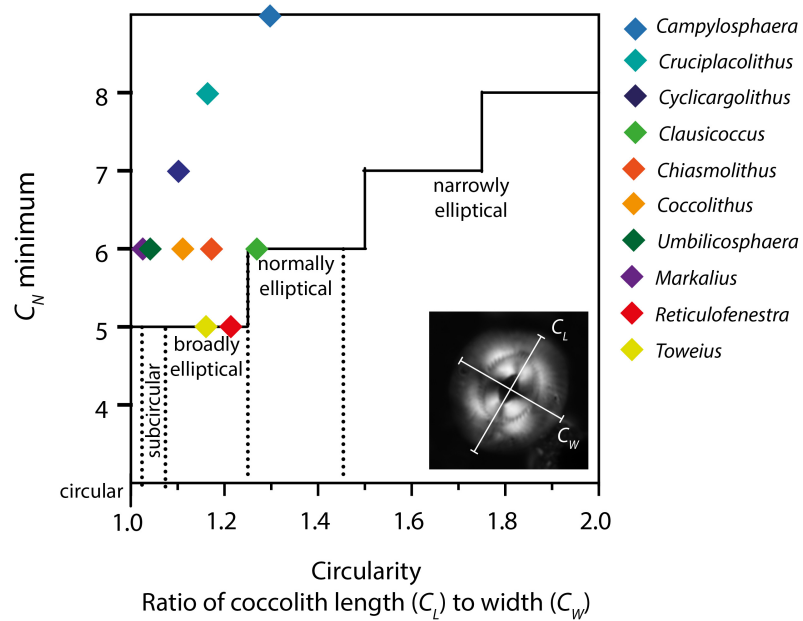
Figure 2.11: Structural constraints on the minimum number of coccoliths per cell (C_N) in coccolithophore taxa is proportional to the circularity of the coccolith outline (the ratio of coccolith length to width). This derives from the fundamental constraint that maximum coccolith length cannot exceed cell diameter and that decreasing circularity (increase in $C_L : C_W$) means that more coccoliths of a fixed size are able to cover the cell surface area. The minimum observed C_N in different taxa is shown for comparison.

from coccolith length, C_L, and width, C_W, where $C_{SA} = \pi \, (C_L/2) \, (C_W/2)$. Cell surface area is calculated by multiplying C_{SA} by C_N. By incrementally decreasing C_N whilst keeping C_L and C_W constant, the value of C_N below which C_L exceeds cell diameter is identified as the minimum possible C_N. Through this method, the determining factor of minimum C_N is identified as the ratio between C_L and C_W, i.e., how circular the coccolith shape is (Figure 2.11). This is because the surface area of circular coccoliths is greater than that of elliptical coccoliths of the same length, therefore fewer are needed to cover the cell surface area. Although many placolith taxa overlap adjacent coccoliths, any degree of overlapping would enable increased numbers of coccoliths to cover the cell surface area, therefore the hypothetical minimum C_N is calculated by assuming no overlap.

The structural minimum C_N on a coccosphere is ~5 coccoliths per cell for species with circular coccoliths and increases to a minimum C_N of 8 for species with strongly elliptical coccoliths (Figure 2.11). Plotting the minimum observed C_N for a number of

genera against the $C_L : C_W$ ratio measured from their coccoliths shows that all of our fossil observations are either at or greater than the calculated minimum C_N (Figure 2.11). Genera with an observed minimum C_N that is higher than the calculated minimum are likely to be those taxa with greater degrees of overlapping between adjacent coccoliths, which is inline with our observations. These include *Campylosphaera*, *Cruciplacolithus* and *Cyclicargolithus*. Where minimum observed C_N matches calculated C_N, as for *Toweius* and *Reticulofenestra*, this does not necessarily mean that there is no overlap between coccoliths in these taxa. Rather, the increased curvature of the cell relative to the coccolith length at the minimum C_N will increase the angle between adjacent coccoliths and is likely to reduce the capacity of coccoliths to overlap to their full extent.

2.4.1.2   Physiological constraints on number of coccoliths per cell

Physiology can potentially place a fundamental constraint on the maximum C_N of a cell based on how quickly new coccoliths can be formed relative to the time per division (growth rate). The minimum number of coccoliths per cell (species-specific) must be approximately doubled between cell divisions in order for two daughter cells to have a complete cell covering of coccoliths after division. For example, the modern species *Coccolithus pelagicus* has an average of 14 coccoliths per ~16 μm cell, ranging from a minimum of 7 to a maximum of 23 based on culturing studies (**Chapter 3**; Sheward et al., 2014). *C. pelagicus* must subsequently produce a minimum of 7 new coccoliths between each cell division cycle to ensure that the two new daughter cells have a complete cell covering. Under a theoretical rapid field growth rate of 0.7 d^{-1} (approximately 24 hours between divisions), each cell must produce one coccolith every one to two hours (assuming 12 - 16 hours of daylight within each 24 hour division cycle during which calcification is assumed to occur; Müller et al., 2008). *Calcidiscus leptoporus* (minimum C_N = 10 - 14, average Ø = 14 μm; **Chapter 3**), a species with a larger minimum C_N but comparable coccosphere size, would need to produce coccoliths more quickly in the same time between cell divisions (more than one coccolith every hour during the 12-16 hours of daylight between cell divisions). Therefore, as minimum C_N increases, cells must either produce coccoliths more quickly or grow at lower growth rates to increase the time between divisions.

As cell size increases, the surface area that must be covered with calcite increases whilst the rate at which the cell can deliver sufficient calcium and carbonate ions to the coccolith vesicle decreases with surface area to volume ratio. Species with larger

coccospheres and/or higher C_N relative to other species of a similar size may not be able to maintain high growth rates even if conditions for growth are favourable because they cannot support coccolith (calcite) production that is rapid enough to match the time between cell divisions at a higher growth rate.

In the modern ocean, many of the taxa with very high C_N, e.g., *Syracosphaera* (Figure 2.8b), are typically assumed to show the highest abundances in more stratified, oligotrophic regions of the ocean (Ziveri et al., 2004) where growth rates are likely to be lower on average. However, high abundances of *Syracosphaera bannockii* and assemblage dominance (~87%) analogous of a bloom scenario have also been observed in the temperate North Atlantic during April (Daniels et al., 2014), suggestive of high net growth rates. The biogeography and ecology of modern high-C_N species within the Syracosphaerales and Alisphaeraceae is very poorly documented and *Syracosphaera pulchra* is the only species studied in culture (Geisen et al., 2002; Young et al., 2003; Fiorini et al., 2011). As such, it is not yet possible to identify from biogeographic patterns whether high-C_N species are more common in regions of lower productivity, where an inability to achieve high growth rates and maintain calcite production might not lead to outcompetition. If further investigation indentifies that modern high-C_N species are most characteristic of particular biogeographies such as eutrophic or oligotrophic, the number of coccoliths per cell could become a valuable indicator of the ecological preferences of extinct species in the fossil record that could provide further evidence of environmental variability and its impact on phytoplankton communities in the past.

2.4.2 Revisiting the cell size adjustment of the alkenone $p\text{CO}_2$ proxy

Past CO_2 concentrations can be reconstructed from the stable isotopes of carbon within long-chain alkenone lipids produced by certain algae and preserved in marine sediments (e.g., Pagani, 2002; Pagani et al., 2005). Alkenone lipids are thought to be metabolic storage molecules (Epstein et al., 2001), although their precise biological purpose is not clear. Modern alkenone production is dominated by the coccolithophore species *Emiliania huxleyi* and *Gephyrocapsa oceanica* of the family Noelaerhabdaceae (Marlowe et al., 1984; Conte et al., 1995; Volkman et al., 1995). As these species evolved relatively recently (Late Pleistocene and Pliocene respectively; Thierstein et al., 1977; Raffi et al., 2006), alkenone production deeper in the Cenozoic is thought to have been associated with other genera within the

Noelaerhabdaceae family, notably *Reticulofenestra* and *Cyclicargolithus* (Marlowe et al., 1990; Brassell, 2014).

The carbon isotope signature in alkenones is not identical to that of the surrounding seawater $CO_{2(aq)}$ due to the fractionation of carbon during photosynthesis. The degree of carbon isotope fractionation is related to growth rate and the size of the cell, specifically surface area that regulates rates of gaseous diffusion into and out of the cell (Popp et al., 1998) and volume, to which the carbon content of the cell is proportional (Menden-Deuer and Lessard, 2000). Variability in the cell size of alkenone-producers through time therefore exerts a primary control on the carbon isotope signal recorded in alkenones. Adjustments for cell size have been made in recent studies using a linear coccolith length to cell size relationship derived by Henderiks and Pagani (2007) from fossil *Reticulofenestra* coccospheres (n=55) of Late Eocene to Miocene age. The substantial number of coccosphere geometry measurements obtained for Paleocene to Oligocene *Reticulofenestra* during this study enables a re-evaluation of this method of cell size adjustment.

Recent studies (Henderiks and Pagani, 2007; Henderiks and Pagani, 2008; Seki et al., 2010; Badger et al., 2013; Davis et al., 2013; Zhang et al., 2013) adjust pCO$_2$ for cell size by amending the 'b' term that represents the total physiological discrimination of carbon isotope fractionation including cell size and growth effects:

$$\left[CO_{2(aq)} \right] = \frac{b}{\varepsilon_f - \varepsilon_p} \qquad \text{Eqn. 2.1}$$

where ε_f is the isotope fractionation of carbon during carbon fixation (typically assumed to be 25 ‰; Bidigare et al., 1997) and ε_p is isotopic fractionation between dissolved inorganic carbon and organic matter that occurs during photosynthesis (Laws et al., 2002). Henderiks and Pagani (2007) convert the mean coccolith length (C_L) in a sample to cell diameters (Θ) based on their fossil *Reticulofenestra* coccosphere data as follows,

$$\Theta = 0.88\, C_L + 0.55 \qquad \text{Eqn. 2.2}$$

and subsequently calculate volume to surface area ratios (V:SA) from mean Θ. The b term in Equation 2.1 is then adjusted (b') to reflect the ratio of V:SA in fossil samples relative to the V:SA ratio in modern *E. huxleyi* (determined to be 0.9 ± 0.1 by Popp et al., 1998), as follows:

$$b' = b \times \left(\frac{V{:}SA_{fossil}}{V{:}SA_{E.hux}} \right) \qquad \text{Eqn. 2.3}$$

Here, we use two previously published pCO_2 records from the equatorial Atlantic region during the Pliocene (Seki et al., 2010) and the Paleogene between 20 and 40 Ma (Pagani et al., 2011) to investigate the pCO_2 concentration that results from two different approaches to cell size adjustment. Each new adjustment method will be compared to the pCO_2 record with no size adjustment and the pCO_2 record with the commonly used Henderiks and Pagani (2007) method (hereafter called HP07).

Approach 1: The new C_L to Θ equation derived from the substantial dataset of *Reticulofenestra* coccosphere geometry presented in this study calculates mean Θ from mean C_L within the sample, following the method of HP07 that has been used by most recent studies. This new C_L to Θ relationship has a steeper gradient and higher intercept than HP07:

$$\Theta = 1.04\, C_L + 1.42 \qquad\qquad \text{Eqn. 2.4}$$

Approach 2: Arguably, mean Θ calculated from mean C_L (as above) is not actually the most appropriate reflection of mean volume, which is the important parameter for size-specific differences in fractionation. The second approach therefore calculates Θ of the sample from the frequency distribution of cell volume, which better reflects the disproportionate allocation of biomass in smaller abundances of larger cells (assuming that alkenone (lipid) content increases proportionally with increasing cell volume). In this second approach, Θ is calculated using a novel methodology that reconstructs the biovolume distribution of a sample. The frequency distribution of coccolith length data from each sample (used in Approach 1 to calculate mean C_L) and the frequency distribution of C_N measured from fossil coccospheres of *Reticulofenestra* are then used to calculate the frequency of each cell size class specific to each sample. This method of reconstructing Θ using both C_L and C_N data and the relationship between Θ, C_L and C_N from fossil coccospheres is described in detail in **Chapter 4**. The relationship between Θ, C_L and C_N in fossil *Reticulofenestra* coccospheres is:

$$C_L = 1.283 \left(\frac{\Theta_{SA}}{C_N}\right)^{0.486} \qquad\qquad \text{Eqn. 2.5}$$

where Θ_{SA} is surface area of the cell, which is $4\pi r^2$. The Θ of any combination of C_L and C_N can be calculated using this equation. This approach results in a plot of biovolume against equivalent cell diameter, where the 'average' cell volume can be found at the cell size that bisects the upper and lower 50% of cell volume. This approach therefore doesn't use
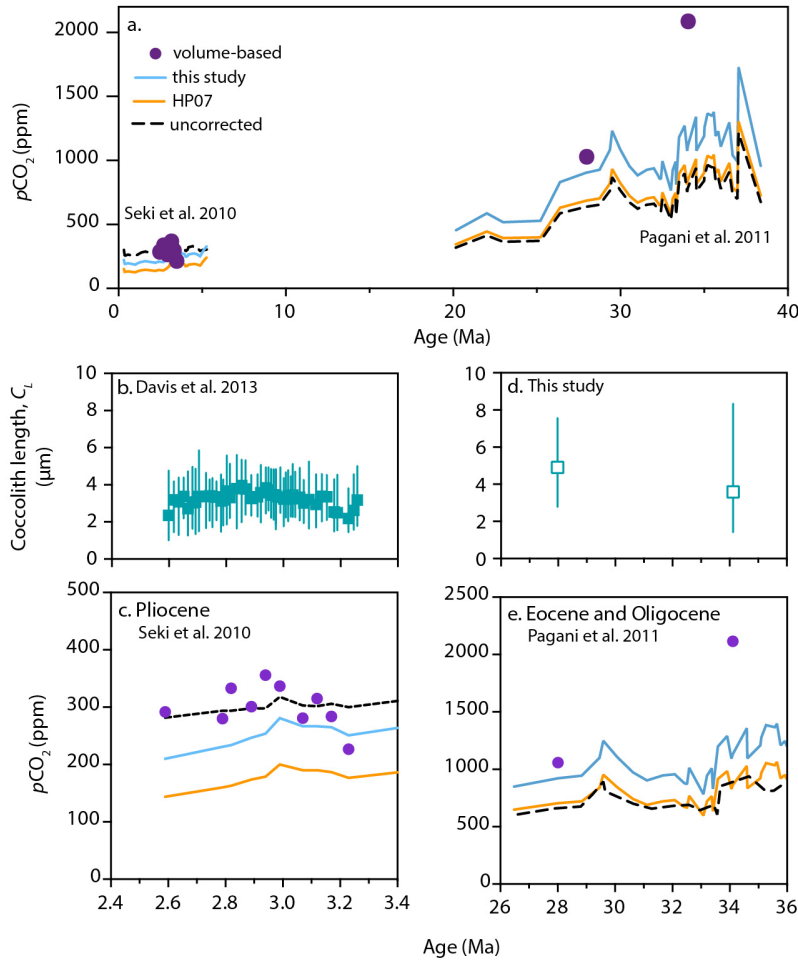
Figure 2.12: a. The pCO$_2$ record from alkenones (black dashed line, from Seki et al., 2010 and Pagani et al., 2011) is adjusted using the mean coccolith length (C_L) correction of Henderiks and Pagani (2007) (HP07; orange line), the mean C_L to cell size relationship determined from this study (blue line) and the mean cell size that is calculated from reconstructed population volume distribution (purple dots). **b.** The difference between pCO$_2$ calculated using HP07 compared to this study increases with increasing pCO$_2$.

cellular frequency to calculate average cell volume, as this would simply result in the same value as calculated from mean C_L and is biased towards smaller cells. Instead, this new approach takes into account the size-specific fractionation of each cell in the population as well as the biomass that each cell has contributed to the sample. The equivalent cell diameter of mean population cell volume is therefore used in the adjustment of pCO$_2$ calculations instead of mean C_L.

Figure 2.12a shows the record of pCO$_2$ that is produced using each cell size adjustment method. Using Approach 1 on Pliocene data (Figure 2.12b and c), the C_L to Θ adjustment of HP07 (Eqn. 2.2) and this study (Eqn. 2.4) reduces estimated pCO$_2$ by an

average of ~150 ppm and ~50 ppm respectively relative to the size-uncorrected data. Between 20 and ~33 Ma (Figure 2.12d and e), the HP07 adjustment increased the uncorrected data by 25-90 ppm, as b and b' were very similar (Eqn. 2.1 and 2.3). Our C_L to Θ adjustment increased $p\text{CO}_2$ by 135 to 520 ppm. As the cell sizes, and therefore volume to surface area ratios, calculated using our Equation 2.4 are always larger than those calculated using the relationship of HP07, the final $p\text{CO}_2$ calculation uses a larger b' term (Equation 2.1 and 2.3).

In Approach 2, average cell volume is used to adjust $p\text{CO}_2$ during the Pliocene interval between 2.4 and 3.4 Ma using the C_L data published in Davis et al. (2013) for the same site as the alkenone samples. The cell volume distribution at 28 Ma (Late Oligocene) and 34 Ma (Late Eocene) was calculated based on C_L data that were collected for this study from Trinidad and Mississippi respectively (Figure 2.1) as the original C_L dataset of Pagani et al. (2011) was not published with the manuscript. This C_L data is of a similar age and latitude and mean C_L is comparable to that used in the original calculations for those two alkenone samples. The cell volume distribution for the two Paleogene ages is therefore more speculative, but provides a relevant contrast to the cell size and cell volume structure of the Pliocene.

During the Pliocene, the average cell volume approach calculates $p\text{CO}_2$ concentrations that are ~50-100 ppm higher than adjusting to mean C_L based on Equation 2.4 (this study) and 50-170 ppm higher than adjusted to HP07 (Figures 2.12a and c). In the original study, Seki et al. (2010) found that the size-corrected record was lower than Pleistocene ice core $p\text{CO}_2$ records so they applied a secondary correction to adjust for this. The volume reconstruction method applied here broadly returns $p\text{CO}_2$ concentrations to pre-correction values, which may suggest that this approach produces a more appropriate size correction during this interval of low CO_2 and smaller cells. The average cell volume approach also increases $p\text{CO}_2$ by 150 to 350 ppm in the Late Oligocene (28 Ma) and by ~980 to 1260 ppm in the Late Eocene (34 Ma) relative to the C_L adjustment of this study and HP07 respectively (Figures 2.12a, e). Whilst these revised $p\text{CO}_2$ estimates may appear too high to be realistic compared to independently-derived CO_2 concentrations in the same interval (Beerling and Royer, 2011), the presence of a small number of significantly larger cells with high V:SA within the population (Figure 2.13) clearly has the potential to greatly increase $p\text{CO}_2$ concentrations.
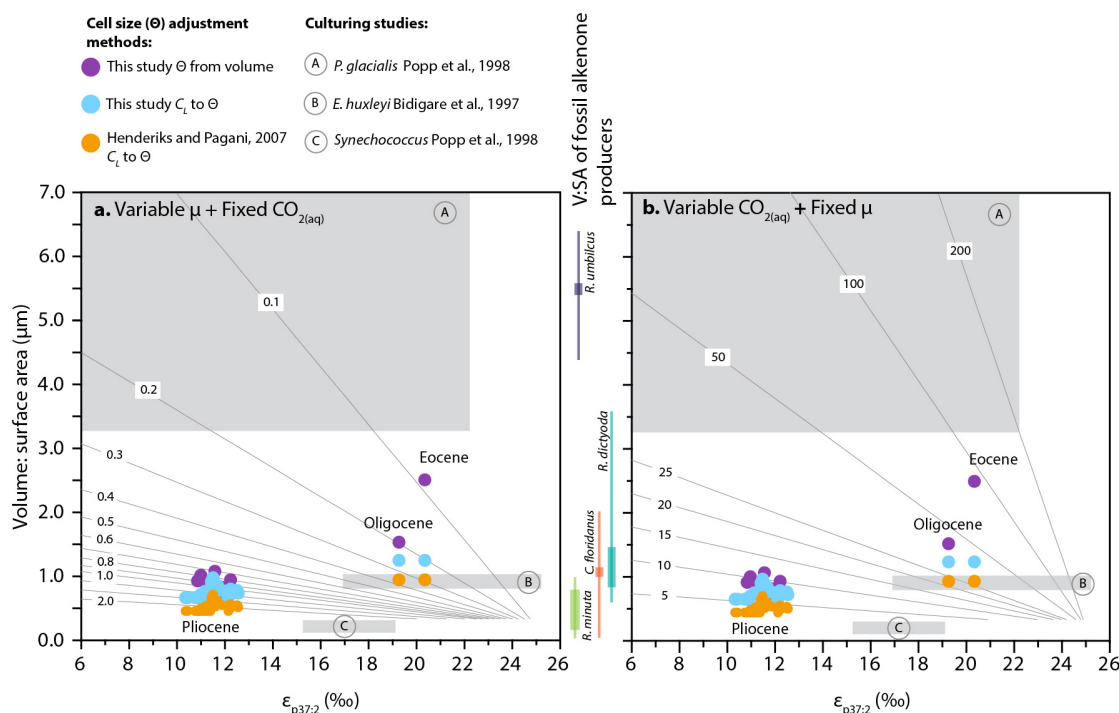
Figure 2.13: The relationship between the volume to surface area of the cell and the isotopic fractionation of carbon due to photosynthesis, $\varepsilon_{p37:2}$, is a function of growth rate, μ, and $CO_{2(aq)}$ assuming a constant value of 25 for the isotopic fractionation of carbon during carbon fixation ε_f (where μ and volume to surface area ratio are part of the b term in Equation 2.1). The same value of $\varepsilon_{p37:2}$ can therefore be associated **a.** with larger cells that have lower growth rates if $CO_{2(aq)}$ is assumed to remain constant at 10 μmol kg^{-1} or **b.** that larger cells must have a higher carbon demand and therefore represent higher $CO_{2(aq)}$ if growth rates are assumed to be constant (here at 0.82 d^{-1}). The volume to surface area ratios and $\varepsilon_{p37:2}$ values from the three size adjustment methods are shown based on the coccolith length to cell size equation of Henderiks and Pagani (2007) (HP07 – orange), the coccolith length to cell size equation derived from this study (blue) and the cell size that is calculated from the volume distribution of cells in the population from this study (purple). The grey boxes are the range of volume to surface area ratios and $\varepsilon_{p37:2}$ produced experimentally in cultures of the modern alkenone producers A. the Antarctic marine diatom *Porosira glacialis* (Popp et al., 1998), B. the coccolithophore *Emiliania huxleyi* (Bidigare et al., 1997), and C. the cyanobacteria *Synechococcus* (Popp et al., 1998). Also shown are the range of volume to surface area observed from coccospheres of the presumed Paleogene alkenone producers of the family Noelaerhabdaceae - *Reticulofenestra minuta, R. dictyoda, R. umbilicus* and *Cyclicargolithus floridanus.*

Importantly, the degree of pCO$_2$ adjustment based on the calculation of mean cell volume (Approach 2) is highly dependent on the specific distribution of C_L within the sample and is not directly proportional to C_L. Using mean C_L artificially biases the cell size adjustment towards smaller cells that discriminate more strongly against ^{13}C (larger $\boldsymbol{\varepsilon}_{p37:2}$; Figure 2.13), as they are likely to be more abundant in the population but contribute proportionally less to the total alkenones in the sample. As demonstrated here, the same value of $\boldsymbol{\varepsilon}_{p37:2}$ can be associated with different volume to surface area ratios (Figure 2.13).

However, the calculated value of $CO_{2(aq)}$ can remain constant if the change in V:SA is assumed to change with growth rate (Figure 2.13a) or it can change if growth rate is assumed to remain constant (Figure 2.13b). An increase in V:SA, such as evaluated for the Eocene and Oligocene, would indicate a higher cellular nutrient demand (**Chapter 1**) and may decrease average growth rates, as larger cells are typically thought to divide less rapidly relative to smaller cells (Marañón et al., 2013). However this would imply that pCO_2 remains fairly constant despite the change in cell size. The interacting effects of cell size and growth rate on the value of $\varepsilon_{p37:2}$ and $CO_{2(aq)}$ therefore complicates the interpretation of estimated pCO_2 that is derived by adjusting for cell size. However, the new approach presented here improves the quality of the cell size data that is used within the calculation of pCO_2. Regardless of the approach used, the current methods to adjust pCO_2 estimates for the size of alkenone-producers may not be the most effective method for accounting for the effect of size-specific fractionation.

2.5   Conclusions

The unprecedented number of Paleogene coccospheres in this study uncovers new observations on the diversity of size and coccosphere geometry – coccolith length, cell and coccosphere size, and number of coccoliths per cell – in a wide range of fossil coccolithophores. Whilst spherical coccospheres are by far the most common shape encountered, certain species exhibit ovoid to elliptical (*Helicosphaera*, *Biscutum*) and even cuboid coccospheres that are a characteristic feature of some taxa such as *Umbilicosphaera* but occur only in *Toweius* and *Chiasmolithus* in small cells that are presumably recently divided. There is a prominent range in all aspects of coccosphere geometry, including taxa characterised by up to 50 small coccoliths per coccosphere (e.g., *Kilwalithus*). Species with a particularly high or low number of coccoliths relative to their cell and coccolith size diverge conspicuously from the overall tendency for larger coccospheres to be covered with larger coccoliths and highlights that coccolith size is not always a useful indicator of cell size. Within-species coccosphere geometry remains loosely constrained owing to the mixing of populations with subtly different interactions between coccosphere size, coccolith length and the number of coccoliths, which can also vary with growth.

To demonstrate the potential usefulness of this dataset for broader palaeoceanographic research, we use the coccosphere data for *Reticulofenestra* to revisit the cell size adjustment of the alkenone pCO_2 proxy. Application of our relationship between

coccolith length and cell size increases $p\mathrm{CO}_2$ by ~200 ppm compared to the previously published method. We also find that the use of mean population volume structure calculated from coccolith size and using coccosphere data is potentially a more suitable reflection of the partitioning of alkenones from cells of different sizes. This questions whether current adjustments for cell size in the alkenone proxy are adequate given that a far greater degree of cell size information can now be incorporated into $p\mathrm{CO}_2$ calculations.

Chapter 3:
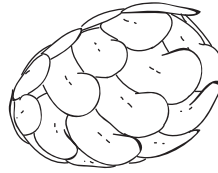
Growth phase and physiology regulates coccosphere size and architecture in four key modern coccolithophore species

As a manuscript in preparation:

Rosie M. Sheward, Alex J. Poulton, Samantha J. Gibbs, Chris J. Daniels, Paul R. Bown

Abstract

Cell size is known to be intimately associated with multiple aspects of cellular physiology, but our understanding of the potential links between physiology and other aspects of coccosphere geometry is limited as these parameters are not routinely measured in modern species. Without this information, we are missing a valuable means of interpreting the physiological processes that potentially underline the remarkable variability that we observe in the architecture and geometry of fossil coccospheres. However, Gibbs et al. (2013) recently demonstrated that coccosphere geometry in modern *Coccolithus* varies with different growth phases. As a result, *fossil* coccospheres have the potential to preserve valuable information on physiology in the geological record. Here, I further explore the interaction between cellular growth and the cell size, coccolith length and number of coccoliths per cell in cultures of *Coccolithus, Calcidiscus* and *Helicosphaera*, taxa that have a long fossil record. Cells experiencing exponential phase growth are typically smaller with fewer coccoliths per cell whereas cells experiencing growth-limiting nutrient depletion have increased coccosphere size and number of coccoliths per cell. Along with previously reported data from *Emiliania huxleyi*, the response of coccosphere geometry to shifts between growth phase is common to three different families, clearly demonstrating that this is a core physiological response in coccolithophores that is not restricted to specific family lineages. As such, it has the potential to be used as a proxy to identify changes in growth phase through time directly from fossil coccospheres, facilitating a defined link between the physiology of individuals and the response of species to environmental variability.

3.1 Introduction

Coccolithophores are a group of calcifying marine phytoplankton that first evolved ~225 million years ago (Ma). The remains of their biomineralised cell coverings contribute significantly to the export of biogenic calcite to deep-sea sediments (Broecker and Clark, 2009), forming a biogeographically and temporally extensive fossil record. Important palaeobiological information about the diversity (e.g., Bown et al., 2004; Bown et al., 2008) and relative abundance of different coccolithophore species is documented by these rich fossil remains, which are mostly in the form of individual calcite plates called coccoliths. From these fossils, the evolution, biogeography and ecology of past species can be inferred (e.g., Tremolada and Bralower, 2004; Ziveri et al., 2004; Gibbs et al., 2006b; Schneider et al., 2011) and they additionally record the biotic response of coccolithophore species and communities to palaeoceanographic and palaeoclimatic variability (e.g., Bollmann, 1997; Bown, 2005b; Bown and Pearson, 2009).

A valuable new insight into past coccolithophore communities is additionally provided by intact fossil coccospheres that have not disarticulated into their component coccoliths (Gibbs et al., 2013; Bown et al., 2014; O'Dea et al., 2014). Coccospheres have been observed in well-preserved marine sediments from which an extensive dataset has been compiled of the true cell size of individuals (**Chapter 2**) that are between 66 and 33 million years old, an interval known as the Paleogene. This dataset of fossil cell size with associated information on the size and number of coccoliths that cover the cell reveals snapshots of cell growth within the fossil record. Gibbs et al. (2013) first explored quantitative links between coccosphere geometry (coccosphere size, coccolith length and coccolith number) and population growth. Their laboratory experiments using modern *Coccolithus pelagicus*, *C. braarudii* and *Emiliania huxleyi* identified that the number of coccoliths per cell within a culture population was linked to the ability of the population to divide, i.e., the growth phase of the population. Within these experiments, cells that were in the phase of rapid cell division (exponential phase) were typically smaller with fewer coccoliths compared to cells that were in a phase of slowed to inhibited cell division (stationary phase). This initial evidence for a relationship between growth phase (rapid versus slowed growth) and coccosphere geometry was then used by Gibbs et al. (2013) as a framework to interpret their high-resolution record of coccosphere geometry for fossil taxa *Coccolithus* and

Toweius across an interval of rapid warming ~56 Ma called the Paleocene-Eocene Thermal Maximum.

However, the extensive dataset of fossil coccosphere geometry for more than 40 different Paleogene species presented in **Chapter 2** shows that cell size, coccolith length and the number of coccoliths per cell all vary considerably both between species and within species (Figures 2.6, 2.8, 2.10). Given this observed variability, can we reasonably hypothesise that the growth-geometry relationship reported by Gibbs et al. (2013) for two modern species is similar across coccolithophores in general? If this were the case, coccosphere geometry could prove to be highly useful as a proxy for growth phase, and hence the overall fitness of the population. A potential concern is that coccolithophores are well recognised for showing pronounced species-specific and even genetic strain-specific physiological responses to a variety of environmental manipulations such as carbonate chemistry and nutrient availability in culturing experiments (Langer et al., 2006; Langer et al., 2009; Krug et al., 2011). Therefore, in order to further develop the use of coccosphere geometry as an indicator (or even proxy) of growth phase in the fossil record it is necessary to have confidence that quantifiably distinct differences in coccosphere geometry during phases of rapid and slowed growth can be viewed as a 'universal' feature of coccolithophores rather than just a species-specific feature. To investigate this, coccosphere geometry data from other modern coccolithophore species experiencing different growth phases is therefore required.

In this study, experiments on three additional modern coccolithophore species – *Calcidiscus leptoporus*, *Calcidiscus quadriperforatus* and *Helicosphaera carteri* – aim to determine relationships (if any) between the phase of growth and coccosphere geometry across different coccolithophore families (*Calcidiscus* in the family Calcidiscaceae and *Helicosphaera* in the family Helicosphaeraceae). These are pertinent species to investigate as *C. leptoporus*, *C. quadriperforatus* and *H. carteri* have widespread modern and geological biogeographic occurrences and long evolutionary histories. *C. leptoporus, C. quadriperforatus* and *H. carteri* are important components of mid- to low-latitude coccolithophore communities, preferring warmer temperate to tropical waters (Ziveri et al., 2004). They are also three of the largest and most heavily calcified of the modern common species, along with *Coccolithus pelagicus* in the high latitudes and *Coccolithus braarudii* in the mid- to high-latitudes (Ziveri et al., 2004). As such, these species are important contributors to the export of inorganic carbon to the

deep ocean (Ziveri et al., 2007). These genera additionally have well-documented fossil records that extend back to the first occurrence of *Calcidiscus* ~57 Ma (Bown et al., 2007) and *Helicosphaera* ~54 Ma (Perch-Nielsen, 1985). Alongside *Coccolithus* they have been significant proportions of coccolithophore communities over much of the last ~55 Ma.

Helicosphaera and *Calcidiscus* additionally have distinct evolutionary and physiological differences that may highlight whether growth-geometry relationship are restricted to specific lineages rather than being a feature of coccolithophores generally. The two orders to which the families Helicosphaeraceae and Calcidiscaceae belong, along with Coccolithaceae (Zygodiscales and Coccolithales respectively), diverged very early in coccolithophore evolutionary history (during the Jurassic, ~150-200 Ma; de Vargas et al., 2007). As such, species within the Helicosphaeraceae have evolved in a distinct lineage to Coccolithaceae and Calcidiscaceae. *H. carteri* is also physiologically distinct from both *Coccolithus* and *Calcidiscus* species in that it 'swims' by means of a flagella. We might therefore expect that the *Calcidiscus* species will show fundamental similarities in coccosphere construction and features of coccosphere geometry with growth phase to those reported in *Coccolithus* by Gibbs et al. (2013). If these same characteristics are also observed in *Helicosphaera* it would be strong evidence that the regulation of coccosphere geometry by growth phase is highly unlikely to be restricted to specific family lineages. To our knowledge, the experiments undertaken for this study have produced the most extensive dataset of modern coccosphere geometry yet to be presented, comprising a total of more than 13,500 measurements of coccosphere and cell size, coccolith length and coccoliths per cell from more than 2,000 individual cells.

3.2 Methods

3.2.1 Experiment design

Monoclonal cultures (genetically identical cells) of South Atlantic Ocean *Calcidiscus quadriperforatus* strain RCC 1135, *Calcidiscus leptoporus* strain RCC 1130 and *Helicosphaera carteri* strain RCC 1323 were obtained from the Roscoff Culture Collection (RCC) and maintained at an incubation temperature of 19 °C at the National Oceanography Centre, Southampton (Appendix Table A3.1). Following standard procedure, cultures were acclimated to new experimental temperature and light conditions for a minimum of 2 weeks (>10 generations) prior to the start of each experiment. The light regime remained consistent

across all experiments at non-limiting irradiance levels of 75 - 90 µmol photons m^{-2} s^{-1} (equivalent to a daily photon flux of ~7 mol photons m^{-2} d^{-1}) with a 12 hour light, 12 hour dark irradiance cycle. To achieve a range of cell division rates, experiments were undertaken at four different temperatures – 16, 18, 20 and 22 °C – within the natural temperature range experienced by field populations of these three species (Ziveri et al., 2004).

For each temperature experiment, all three species were cultured simultaneously and in duplicate following a 'batch culture' procedure, where an initially low number of cells ml^{-1} are left to increase in density, using up nutrients, until initial nutrient levels are completely depleted and population growth ceases. This approach enables coccosphere geometry data to be collected from both nutrient-replete rapid cell division days and nutrient-deplete slowed cell division days towards the end of the experiment, as used successfully in the experiments of Gibbs et al. (2013) for *Coccolithus*. The initial starting density of cells for each experiment was very low at ~300 cells ml^{-1} (taken from acclimated cultures) added to 350 ml of sterilised and filtered natural seawater with added nutrients (low nutrient K/20 medium, modified from Keller et al., 1987, following Langer et al., 2006; Gerecht et al., 2014 and Daniels et al., 2014). Low nutrient media was specifically used to ensure that cultures reached nutrient limiting conditions before the occurrence of significant changes in carbonate chemistry (Daniels et al., 2014). The effect of increasing cell density on the carbonate chemistry of the media over the duration of the experiment was further minimised by using 650 ml polycarbonate flasks (Thermo Fisher Scientific) with vented lids to allow gas exchange between the culture media and the atmosphere outside the flask. After initial inoculation of the media, experiment cultures increase in cell number rapidly, termed the exponential growth phase, and were allowed to grow into stationary phase, at which point increasing nutrient limitation reduces growth rates such that the day-to-day increase in cells ml^{-1} decreases towards zero. The typical experiment duration between initial inoculation and the onset of stationary phase growth was 14-21 days.

3.2.2   Growth rate calculation

Daily cell abundance was determined from triplicate counts of cells ml^{-1} using a Sedgwick Rafter Cell (Pyser-SGI; following Langer et al., 2006) on a transmitted light microscope at

x100 magnification. As *H. carteri* is a motile species (cells have a flagella that enables motion), cell count samples for this species were spiked with 40 µl per ml (4% final volume) 10% formaldehyde to cease movement prior to counting to ensure accuracy. Daily growth rates were calculated as the natural log of the difference in cell density between the day in question and the day prior (Langer et al., 2006). The duration of the exponential growth phase was then established by visual examination of these daily growth rates and plots of cell abundance over time.

3.2.3   Coccosphere geometry

Samples for light microscope (LM) analysis were taken daily. 2-5 ml of each culture replicate was filtered onto cellulose nitrate filters (pore size 0.8 µm; Sartorius Stedim Biotech) and dried overnight at 50 °C. One half of each filter was then adhered between a glass microscope slide and a cover slip using Norland Optical Adhesive 74 (Norland Products Inc.) and cured under UV light exposure until set. The other half of each filter was stored for future scanning electron microscope (SEM) analysis or for additional replicate LM slides if needed. Coccosphere geometry data was obtained through LM following the same techniques applied by Gibbs et al. (2013), Daniels et al. (2014), and Sheward et al. (2014). All LM analysis was performed on a cross-polarised light microscope (Olympus BX51) with a colour camera attached (Olympus DP71). Random transects across the widest section of the filter hemisphere were performed until 30 individual coccospheres per slide were located from slides corresponding to alternate day or, in some instances, daily samples. After counting the number of coccoliths around each cell (C_N), in-focus images of the upper coccosphere surface and maximum cell cross-section were photographed from which biometric measurements (Figure 2.2) of coccolith length (C_L), coccosphere size (Ø; size including calcite covering) and cell size (Θ; size excluding calcite covering) were taken (Cell^D software, Olympus). Unlike the spherical coccospheres of *Coccolithus* and *Calcidiscus* species, *H. carteri* coccospheres are prolate spheroids in shape (Figure 3.4), so here we report cell and coccosphere sizes for this species as equivalent spherical diameters. Prolate spheroid volume is calculated as $V = (\pi/6)d^2h$, where d is short-axis cell/coccosphere diameter and h is long-axis cell/coccosphere height (Sun and Liu, 2003) and then this volume is used to calculate equivalent spherical radius. Particulate inorganic carbon (PIC) per cell was calculated following Young and Ziveri (2000), where PIC is a function of coccolith calcite and C_N. Coccolith calcite is a function of C_L and a

shape factor value that numerically describes species-specific coccolith morphology. Here we take the shape factors of $k_s = 0.08$ for *Calcidiscus* spp., $k_s = 0.05$ for *H. carteri*, and $k_s = 0.06$ for *Coccolithus* spp. published in Young and Ziveri (2000).

3.2.4 Additional experimental results from Gibbs et al. (2013) and Sheward et al. (2014)

In addition to the new experimental results for *Calcidiscus* and *Helicosphaera*, this study also reports coccosphere geometry and growth data for *Coccolithus* from two previously published studies. Gibbs et al. (2013) obtained coccosphere geometry data from a comparable batch culture experiment at a single temperature in *Coccolithus braarudii* strain RCC 1197. This data is presented for direct comparison with the three new species of this study, as much of the data was originally presented as Supplementary Information to accompany that paper. We also present results from a previously unanalysed dataset of exponential phase coccosphere geometry in *C. braarudii* strain RCC 1198 and *C. pelagicus* strain RCC 4092, published as Sheward et al. (2014) and available from http://pangaea.de (doi: 10.1594/PANGAEA.836841). For this study (further details of which can be found in Daniels et al., 2014), batch culture experiments were undertaken at multiple temperatures (6-12 °C in *C. pelagicus* and 12-19 °C in *C. braarudii*) and samples for coccosphere geometry analysis collected on a single mid-exponential phase experiment day. R. Sheward performed all coccosphere geometry measurements and analyses. In both Gibbs et al. (2013) and Sheward et al. (2014), the light microscope methods used to collect coccosphere geometry data were identical to those employed in this study.

3.3 Results

3.3.1 Growth rates

The four temperature experiments resulted in a modest range of daily and mean exponential growth rates (μ) across *Helicosphaera* and *Calcidiscus* species. The highest exponential growth rate for *C. quadriperforatus* was achieved at 22 °C (μ = 0.44 d⁻¹), for *C. leptoporus* at 20 °C (μ=0.44 d⁻¹), and for *H. carteri* at 20 °C (μ=0.45 d⁻¹). Mean exponential growth rates for *C. braarudii* at 15 °C was 0.68 d⁻¹. These exponential growth rates are well within the ranges reported in other studies carried out at similar temperatures for *Calcidiscus*

(Langer et al., 2006; Buitenhuis et al., 2008; Fiorini et al., 2010; Fiorini et al., 2011; Langer et al., 2012; Candelier et al., 2013; Müller et al., 2014) and *H. carteri* (Stoll et al., 2002a; Šupraha et al., 2015). Exponential growth rates of 0.4 to 0.5 d^{-1} signify that roughly half of the culture population undergoes cell division each day. Maximum cell density was ~100,000 cells ml^{-1} in *C. leptoporus* cultures, 60-100,000 cells ml^{-1} for *C. quadriperforatus*, ~30,000 cells ml^{-1} for *H. carteri* and ~25,000 cells ml^{-1} for *C. braarudii*.

3.3.2 Within-species range in coccosphere geometry across experiments

Coccosphere (Ø) and cell size (Θ), coccolith length (C_L) and number of coccoliths per cell (C_N) show clear species-specific differences (Figure 3.1). Coccosphere diameter shows a considerable range in all species, between a minimum of 15 μm and a maximum of 25 μm in *C. quadriperforatus*, and ranging between 10 and 15 μm in *H. carteri* and *C. leptoporus*. This is a slightly smaller coccosphere size range than observed in *C. braarudii* (15 to 30 μm), but very similar to *C. pelagicus* (12 to 22 μm; Figures 3.1d and p).

 Calcidiscus species and *H. carteri* show a much greater range in C_N compared to *Coccolithus* species (Figure 3.1a-d). The most frequently observed C_N is 16 in *H. carteri* cells, 18 in *C. quadriperforatus* cells, and 19 in *C. leptoporus* cells, with the maximum number of ~30 coccoliths in these species. In contrast, *Coccolithus* cells more typically have 11-12 coccoliths per cell up to a maximum of 20-23 coccoliths. In one *C. leptoporus* cell, the coccosphere was comprised of 45 coccoliths (Figure 3.4c). The relationship between C_N and Ø is subsequently noticeably different in *Coccolithus* compared to *Helicosphaera* and *Calcidiscus*, with the latter relationship showing a steeper gradient (Figure 3.1). Comparable coccosphere sizes but significantly greater number of coccoliths per coccosphere of *C. quadriperforatus* compared to *C. braarudii*, and *C. leptoporus* compared to *C. pelagicus*, suggests that *Calcidiscus* species can achieve a greater degree of coccolith overlapping compared with *Coccolithus* species. This is likely to be a result of the circular shape and narrower central tube structure of the placolith coccoliths formed by *Calcidiscus*. The coccolith shields are therefore able to overlap to a far greater extent in *Calcidiscus* and pack more tightly around the cell as C_N is increased, moderating a corresponding increase in Ø. The minimum C_N in *H. carteri* is similar to minimum C_N in *Coccolithus* (C_N = 6 and C_N = 5 - 7 respectively). The smallest cells with just 6 coccoliths observed in *H. carteri* formed cuboid coccospheres (Figure 3.4a). Cubiform coccospheres have also been reported in Bown et al. (2014) for
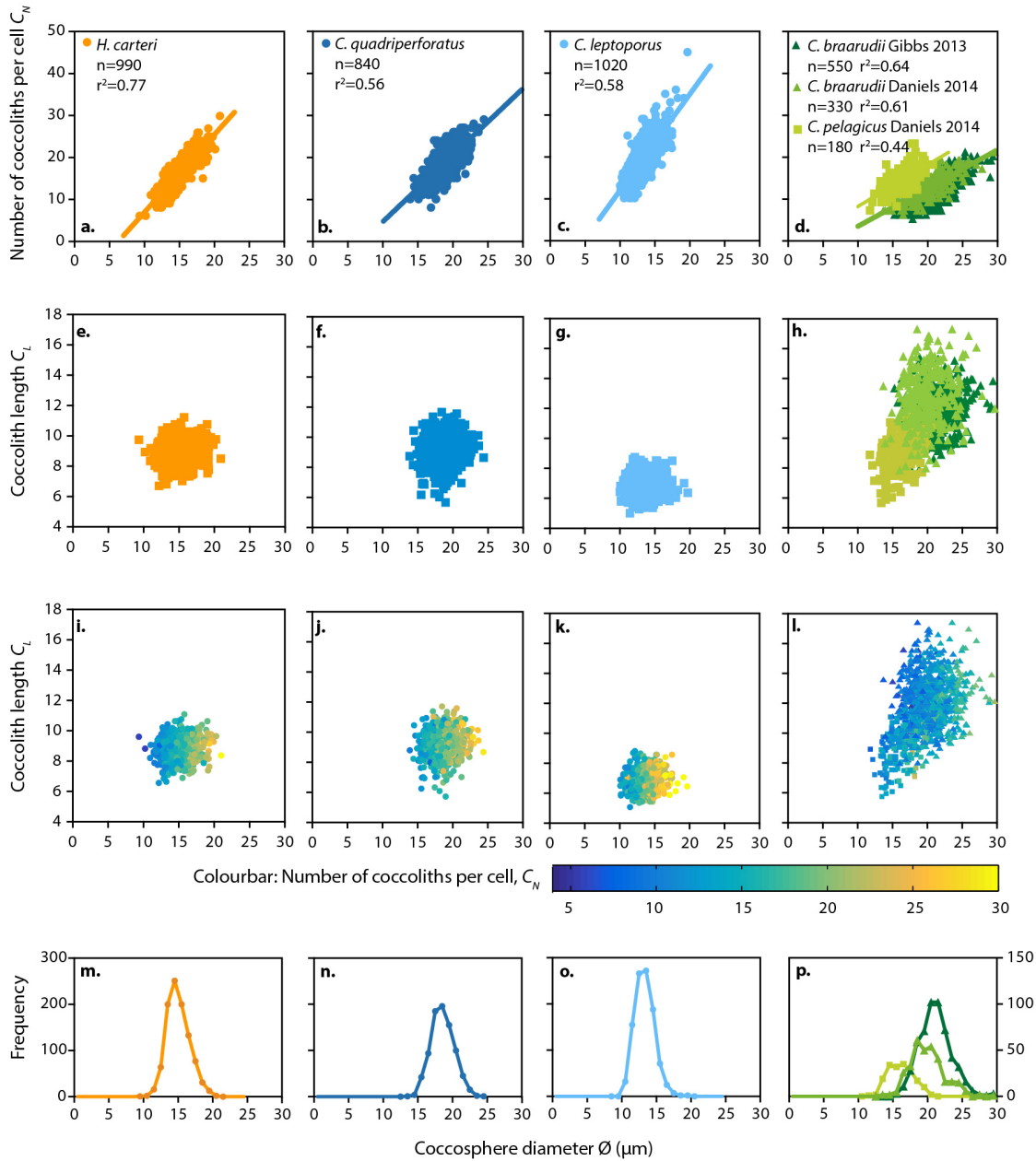
Figure 3.1: Full range of coccosphere geometry in *H. carteri*, *C. quadriperforatus* and *C. leptoporus*. **a. - d.** Number of coccoliths per cell (C_N) against coccosphere diameter (Ø) showing a strong and statistically significant (p<0.0001) positive relationship. **e. - h.** Coccolith length (C_L) showing no relationship with coccosphere diameter (Ø). **i. - l.** Coccolith length and coccosphere diameter, with data points coloured by C_N. **m. - p.** Histograms of coccosphere diameter, calculated for frequency bins of 1µm size. For comparison purposes, we include data for *C. braarudii* and *C. pelagicus* in plots **d.** and **l.** Note the different frequency scale in plot **l.** These datasets can be found in Gibbs et al. (2013) and Sheward et al. (2014) accompanying Daniels et al. (2014).

extinct Paleogene taxa *Toweius pertusus* and *Umbilicosphaera bramlettei* and 'boxy' coccospheres are also seen in several *Chiasmolithus* species.

Coccosphere geometry is not identical in the closely related species *C. quadriperforatus* and *C. leptoporus* (Figure 3.1b and c), with *C. leptoporus* producing coccospheres with a slightly greater number of coccoliths on average than *C. quadriperforatus*. This is in contrast with the two closely related species of *Coccolithus*, where the linear regression gradient between Ø and C_N is the same in both *C. pelagicus* and *C. braarudii*, although the gradients are offset from each other (Figure 3.1d). Both *Calcidiscus* species have previously been considered to be morphotypes (Knappertsbusch et al., 1997; Knappertsbusch, 2000) or sub-species (Geisen et al., 2002) but have since been shown to be genetically distinct species, similarly to *C. pelagicus* and *C. braarudii* (Saez et al., 2003; De Vargas et al., 2004). The species-specific coccosphere geometry within the *Calcidiscus* species identified here further supports the genetic distinction between these species alongside previously identified morphological differences (Knappertsbusch et al., 1997; Knappertsbusch, 2000; Geisen et al., 2002; Saez et al., 2003; Geisen et al., 2004).

Coccolith length varies between cells by up to 4.5 µm in *H. carteri*, 8.0 µm in *C. quadriperforatus*, and 3.7 µm in *C. leptoporus* but shows no relationship with coccosphere size within these culture populations (Figure 3.1e-l). A weak relationship between Ø and C_L appears to exist in *Coccolithus* (Figure 3.1h), but importantly only when data for both *C. pelagicus* and *C. braarudii*, as well as multiple clones, are combined (Figure 3.1h and also illustrated in culture and field data in Gibbs et al., 2013). In clonal populations where cell division is fully synchronised across cells, Ø and C_L are relatively restricted with no significant relationship (Figure 3.1e-g). Where C_N is superimposed onto plots of Ø against C_L (Figure 3.1i-l), it is clear that there is no overlying relationship between C_L and Ø but that Ø and C_N vary strongly. The combination of multiple growth-synchronised populations of two different species of *Coccolithus* shows that mixtures of populations can result in a relationship between C_L and Ø, an effect that is greatly amplified in fossil assemblages that integrate remains of surface populations over long time intervals (Figure 2.10; Figure 3a in Gibbs et al., 2013). In these culture populations, the principle coccosphere geometry relationship is between C_N and Ø rather than C_L and Ø, in agreement with Gibbs et al. (2013) for *C. braarudii* cultures (Figure 3.1d).
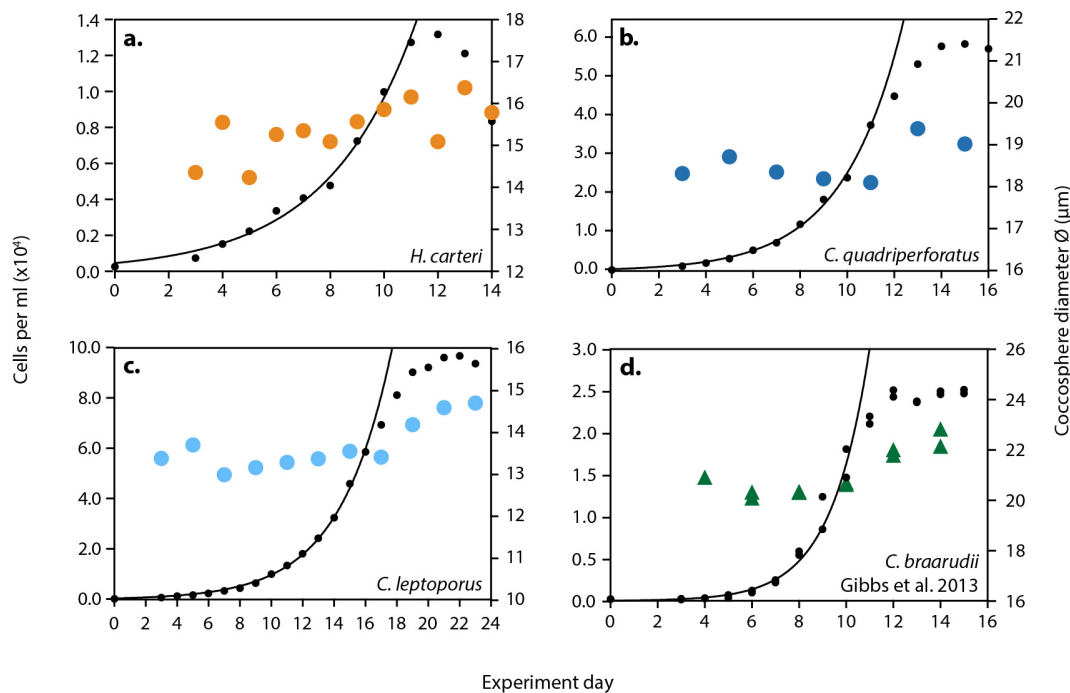
Figure 3.2: Mean coccosphere diameter and cell density with experiment day for the 22 °C experiment. Coloured data points are coccosphere diameter (right axis) and black data points are cells ml^{-1} (left axis). Where cells ml^{-1} begins to deviate from the black line exponential curve, the population is entering early stationary phase. Plot **d.** is a reproduction of SI Figure 1a. in Gibbs et al. (2013) for comparison.

3.3.3   Coccosphere geometry as a function of growth

This study demonstrates that coccosphere size is statistically smaller during experiment days of rapid, exponential phase growth than during days of slowed, early stationary phase growth in all species studied (Figures 3.2 and 3.3). Mean coccosphere diameter across all four temperature experiments during exponential phase growth is 14.8 μm in *H. carteri*, 18.4 μm in *C. quadriperforatus*, 13.1 μm in *C. leptoporus* and 20.5 μm in *C. braarudii* (Figure 3.3). Coccosphere diameter during non-exponential growth, i.e., stationary phase growth, is modestly but statistically (unpaired t-test) larger than during exponential phase growth, with mean coccosphere diameter 0.55 μm larger in *C. quadriperforatus* (t=3.324, df=839, p<0.001) and *H. carteri* (t=4.659, df=990, p<0.0001), and 0.7 μm larger in *C. leptoporus* (t=5.669, df=1020, p<0.0001). Mean coccosphere diameter in *C. braarudii* (Gibbs et al., 2013) shows a larger increase of 1.75 μm (t=9.216, df=548, p<0.0001) between exponential and early stationary growth. An increase in cell size has also previously been observed in response to
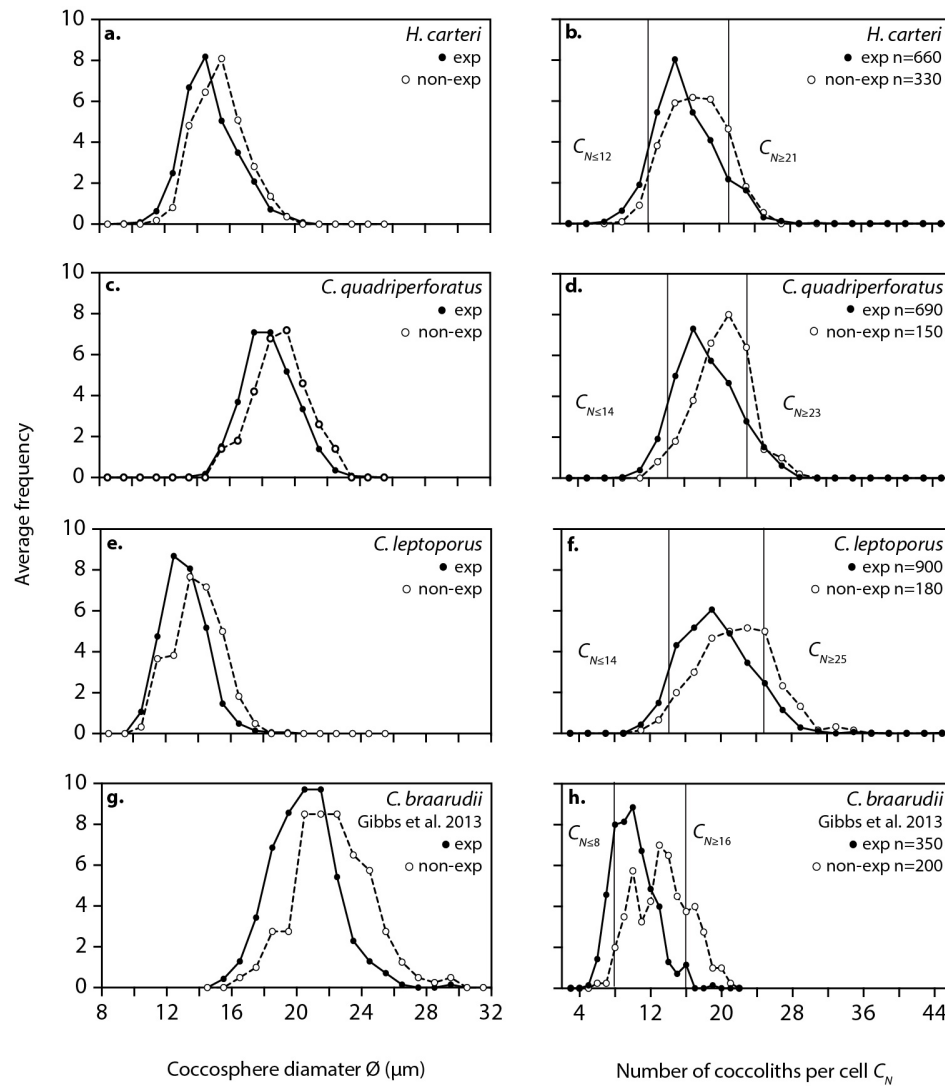
Figure 3.3: Frequency of coccosphere diameter (Ø) and number of coccoliths per cell (C_N) for experiment days in exponential growth (solid line) and experiment days no longer in exponential growth (dashed line), averaged across all temperature treatments. **a. - f.** *H. carteri*, *C. quadriperforatus*, and *C. leptoporus* data from this study. **g. - h.** is a reproduction of *C. braarudii* experiment data from Gibbs et al. (2013) SI Figure 1e. and 1.f for comparison purposes. The lines drawn on C_N plots indicate cells that are recently divided and ready-to-divide/non-dividing, based on the 10th and 90th percentiles of the complete species C_N data shown in Figure 3.1.

nutrient limitation in *Coccolithus* and *Helicosphaera* (Gerecht et al., 2014; Gerecht et al., 2015; Šupraha et al., 2015).

In addition to differences in size, coccospheres also typically consist of fewer coccoliths during exponential phase growth and a greater number of coccoliths during early stationary growth (Figure 3.3). Cells no longer able to maintain exponential rates of growth

have an average of 1-2 extra coccoliths per cell in *H. carteri* (t=5.067, df=990, p<0.0001) and *C. quadriperforatus* (t=5.451, df=840, p<0.0001), 2-3 extra coccoliths per cell in *C. leptoporus* (t=6.312, df=1020, p<0.0001) and 3-4 extra coccoliths per cell in *C. braarudii* (t=14.24, df=548, p<0.0001; Figure 3.3). The frequency distribution of C_N for each species (Figure 3.1m-p) can be used as a quantitative indicator of whether cells are in a recently-divided state (close to the minimum number of coccoliths per cell observed, $C_N \leq 10^{th}$ percentile of the data) or are in a ready-to-divide state (close to the maximum number of coccoliths per cell observed, $C_N \geq 90^{th}$ percentile of the data). These C_N 'thresholds' for recently-divided and ready-to-divide cells for each species are shown in Figure 3.3. Based on the species-specific geometry observed, recently divided cells typically have $C_N \leq 12$ in *H. carteri* and $C_N \leq 14$ in *Calcidiscus* spp., whilst cells that are ready to divide have $C_N \geq 21$, $C_N \geq 23$, and $C_N \geq 25$ in *H. carteri*, *C. quadriperforatus,* and *C. leptoporus* respectively (Figure 3.3). During exponential growth, the C_N of the population is typically closer to the minimum observed C_N. In contrast, populations exhibiting slowed growth are more likely to have cells in a ready-to-divide state (Figure 3.3).

3.4 Discussion

3.4.1 Physiological insights into coccosphere geometry

Within these experiments, coccosphere size (Ø) and the number of coccoliths per cell (C_N) varied depending on whether the culture population was increasing in cell numbers each day at a rapid rate (exponential growth phase) or a slowed rate (non-exponential growth phase). Across all four species investigated, coccosphere size was typically ~2 μm larger during non-exponential growth days (Figures 3.2 and 3.3), representing a statistically significant increase of 10-15% on exponential phase size. The transition from exponential into non-exponential phase growth was also clearly associated with a shift towards an increased abundance of cells with a greater C_N (Figure 3.3). C_N is not a frequently recorded variable and only a few culturing studies report limited ancillary C_N data (Balch et al., 1993; Paasche, 1998; Gerecht et al., 2014; Gerecht et al., 2015; Šupraha et al., 2015). Studies where Ø and C_N in nutrient replete and nutrient deplete cultures can be inferred from supplementary information are consistent with the extensive observations from these experiments for *Calcidiscus* and *H. carteri* and in Gibbs et al. (2013) for *C. braarudii*.

The relationship between growth phase, cell size and number of coccoliths per cell can be understood by considering the process of cell division and how it is affected by the depletion of nutrients that determines non-exponential phase growth. Both coccosphere size and number of coccoliths per cell vary as each cell progresses through the cell division cycle (unpublished observations; Taylor et al., 2007; Müller et al., 2008). Cells that have recently undergone division are small with approximately the minimum number of coccoliths required to form a complete cell covering (unpublished observations; Figure 3.4). After division, cells recommence coccolith production, which these experiments show increases C_N until the cell has sufficient coccoliths with which to cover two newly divided cells. Coccosphere diameter correspondingly increases alongside increasing C_N as the cell synthesises organic cellular products such as proteins, lipids and carbohydrates. Cultures that are able to maintain rapid rates of cell division (i.e., are growing exponentially) subsequently have a lower mean coccosphere/cell size and fewer coccoliths per cell on average as a large majority of cells within the culture are frequently in a 'recently divided' state (Figures 3.3 and 3.4). When cells are no longer able to maintain exponential rates of cell division, in this instance due to the decreasing availability of nutrients, more and more cells are dividing less frequently. This is observed in the later days of each experiment as an increase in the mean coccosphere/cell size and the number of coccoliths per cell (Figure 3.2) and this interpretation is consistent with the findings of Gibbs et al. (2013).

It may seem counterintuitive for cell size to increase under decreasing nutrient availability as nutrients are required for phytoplankton growth. Nitrate and phosphate are the two key nutrients required by most phytoplankton (Arrigo, 2005; Moore et al., 2013) and they fulfil different purposes within the cell. Phosphate limitation primarily impedes the production of RNA, phosolipids and DNA that are essential for cell replication and phosphate is a key component of cellular energy carriers (Zhao et al., 2015). Nitrate limitation particularly impacts the synthesis of proteins and pigments used in photosynthesis (Zhao et al., 2015). Nutrient limitation therefore suppresses cell division and growth from multiple angles. However, cell size and particulate organic carbon content (POC) have been consistently shown to increase under nutrient limited conditions (Müller et al., 2008) as the cell is still able to produce non-essential lipids and carbohydrates.

These experiments have identified a clear shift towards cells with a greater C_N during non-exponential phase growth (Figure 3.3), including the occurrence of some large coccospheres with very high C_N (Figure 3.4) that are apparently stuck in a high-C_N, ready-

a. Helicosphaera carteri

Recently divided cells C_N≤12
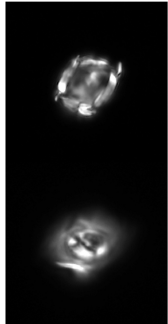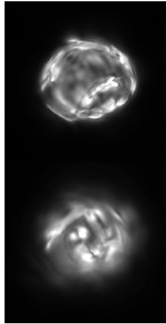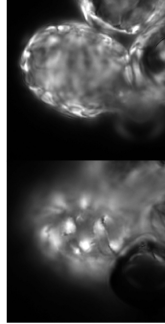
Ready to divide cells C_N≥21

22D5
C_N=6 Ø=9.3 µm

18D3
C_N=12 Ø=14.2 µm

18D7
C_N=18 Ø=16.0 µm
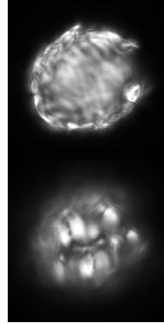
22D4
C_N=20 Ø=17.9 µm
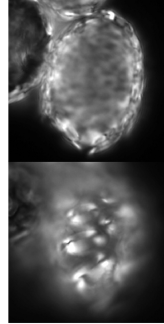
16D7
C_N=24 Ø=18.9 µm
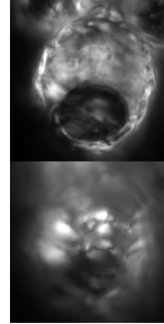
22D6
C_N=30 Ø=20.9 µm

b. Calcidiscus quadriperforatus

Recently divided cells C_N≤14
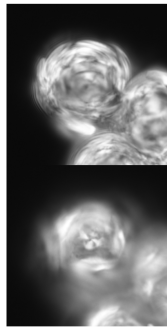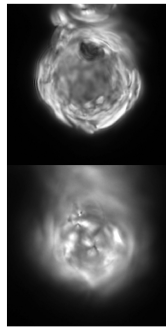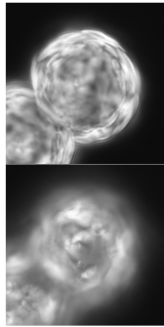
Ready to divide cells C_N≥23

22D3
C_N=8 Ø=16.8 µm

16D9
C_N=13 Ø=17.5 µm

20D9
C_N=16 Ø=18.6 µm
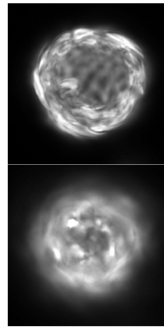
18D13
C_N=20 Ø=18.8 µm
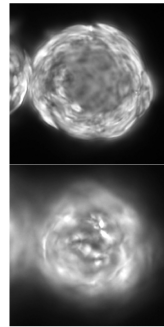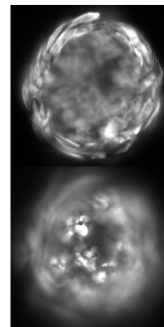
22D7
C_N=23 Ø=19.4 µm

22D5
C_N=29 Ø=24.4 µm

c. Calcidiscus leptoporus

Recently divided cells C_N≤14
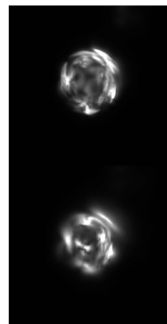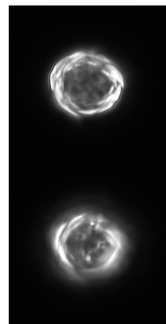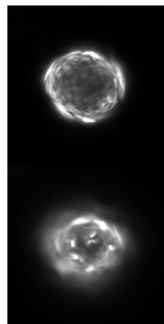
Ready to divide cells C_N≥25

22D7
C_N=10 Ø=11.3 µm

20D3
C_N=15 Ø=13.5 µm

22D5
C_N=20 Ø=14.4 µm
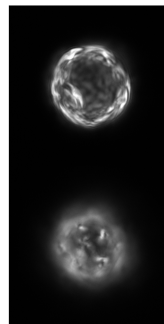
16D7
C_N=25 Ø=15.3 µm
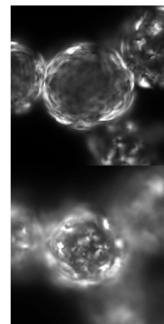
22D15
C_N=30 Ø=16.5 µm
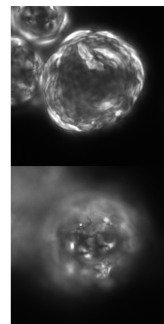
16D16
C_N=45 Ø=19.7 µm

Figure 3.4 (opposite): Range of cell geometry observed within cultures of **a.** *H. carteri*, **b.** *C. quadriperforatus*, and **c.** *C. leptoporus* at 16 - 22 °C. The upper image of each pair shows the cross-sectional view of the cell from which coccosphere diameter and cell diameter are measured. The lower image of each pair shows a coccolith-focused view of the cell from which coccolith length is measured. Values of number of coccoliths per cell (C_N) and coccosphere diameter (Ø) are given for each cell below the image. Values of C_N that characterise recently divided cells and cells that are ready to divide are the 10th and 90th percentiles of the full C_N dataset for each species, as shown in Figure 3.1. A reference code for the experiment day that the image was taken from is also given. 22D7 would be a cell from Day 7 of the 22 °C experiment as an example. All images are to the same scale.

to-divide state with more than enough coccoliths to cover two daughter cells. This is evidence that cellular calcification (coccolith production) is able to proceed uninterrupted despite decreasing nutrient availability. This implies that the process of calcification is less dependent on nutrient availability than cell division processes (Paasche, 1998). The dramatic overproduction of coccoliths by *E. huxleyi* under nutrient limitation (Balch et al., 1993; Paasche, 1998) would suggest that this is the case, even without new additional evidence from *Calcidiscus* and *Helicosphaera* (this study) and for *Coccolithus* (Gibbs et al., 2013). It has been suggested that phosphate limited cells become 'trapped' in the phase of the cell division cycle that enables calcification but not cell division (Müller et al., 2008), as evidenced by multi-layered coccospheres in *E. huxleyi*.

Although these experiments show a clear link between growth phase and coccosphere geometry, there was no clear pattern between Ø, Θ, C_L or C_N with daily or mean exponential growth rate. Growth rate quantifies the proportion of the culture that undergoes cell division between two days. During exponential phase growth, population density increases at an exponential rate each day but this can result from a range of growth rates, particularly if light levels or temperatures are varied. In these experiments, nutrient concentration was the key manipulated variable, which decreased growth rates to zero once levels become inhibiting to cell division. However, before nutrients become growth-limiting, growth rates during the exponential phase were regulated by temperature in these experiments (Figure A3.1). Temperature determines the rate of nutrient uptake and the rate of metabolic cell processes whereas light conditions affect photosynthetic rate, i.e., the rate at which the cell can produce energy. This means that temperature and light affect cell physiology differently to nutrient concentration, particularly that calcification is contingent on the rate at which nutrients can be supplied to the cell (temperature dependent) and processed into energy (light dependent). Growth rate would therefore not necessarily be

expected to influence coccosphere geometry in the same way as has been observed between nutrient-forced changes in growth phase. However, growth-limiting low light levels may result seasonally from deepening of the wind-mixed layer and photoinhibition (cellular damage under high light levels) could result from strong surface stratification in low latitude regions. As yet, no studies have investigated the response of cell size and/or coccosphere geometry under a range of optimum vs. limiting temperature or light conditions in coccolithophores.

3.4.2   Coccosphere geometry as a proxy for growth phase in the fossil record

The most notable finding of this study is that, whilst the coccosphere geometry (coccosphere size, coccolith length and coccoliths per cell) is specific to each species, coccosphere geometry responds identically to growth phase across four different species of *Calcidiscus, Coccolithus* and *Helicosphaera*. This study therefore strongly suggests that species within the major coccolithophore families Calcidiscaceae (*Calcidiscus leptoporus* and *C. quadriperforatus*) and Helicosphaeraceae (*Helicosphaera carteri*) respond to nutrient-driven changes in growth phase in the same way as species within the families Coccolithaceae (Gibbs et al., 2013) and Noelaerhabdaceae (Balch et al., 1993; Paasche, 1998; Gibbs et al., 2013). This is compelling evidence that coccolithophores, regardless of taxonomic affiliation, express a common physiological response to shifts between exponential and non-exponential (stationary) growth phase. This specifically results from the ability of the cell to maintain calcification processes during stationary phase, even when rates of cell division are suppressed by nutrient scarcity. This physiological response is manifested within the architecture of each coccosphere as a modest but significant increase in the average number of coccoliths per cell (C_N) within the population and a corresponding increase in mean population coccosphere size (Ø) when the population is no longer maintaining exponential rates of cell division (Figures 3.2 to 3.4).

The aim of this study was to further develop the interpretation of variability in fossil coccosphere geometry (**Chapter 2**) that was initially proposed by Gibbs et al. (2013) for *Coccolithus* and *Toweius*. In their study, culture experiments on modern *Coccolithus* and *Emiliania huxleyi* showed that Ø and C_N responded to growth phase and this was applied as a framework for interpreting coccosphere geometry records of *Coccolithus* and an ancestor of *E. huxleyi* called *Toweius* during the Paleocene-Eocene Thermal Maximum. Given the
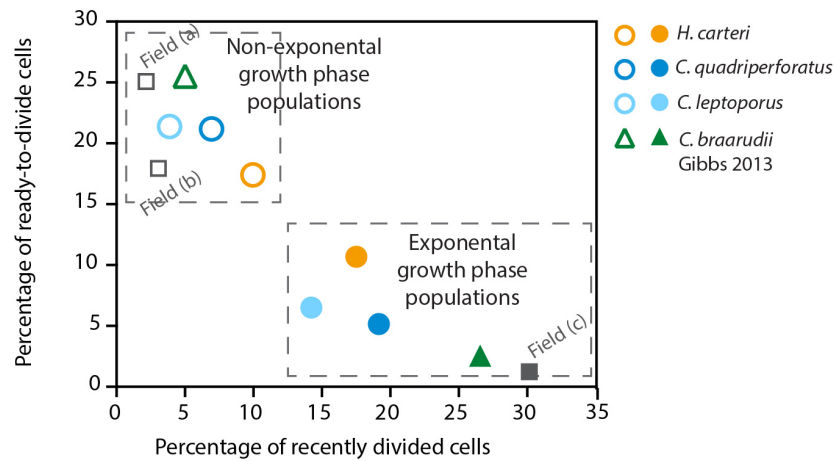
Figure 3.5: Contrasting exponential and non-exponential phase culture populations based on the percentage of recently divided and ready-to-divide cells within the population as characterised by C_N thresholds specific to each species. Recently divided cells fall within the 10th percentile of C_N data, such that $C_N \leq 12$ in *H. carteri*, $C_N \leq 14$ in both *Calcidiscus* species and $C_N \leq 8$ in *Coccolithus* (Figure 3.3). Ready to divide cells fall within the 90th percentile of C_N data, such that $C_N \geq 21$ in *H. carteri*, $C_N \geq 23$ in *C. quadriperforatus*, $C_N \geq 25$ in *C. leptoporus*, and $C_N \geq 16$ in *Coccolithus*. The mean percentages for exponential days are shown by the filled data points and the mean percentages for non-exponential experiment days are shown by the unfilled data points. Also indicated (grey squares) are the characteristic percentages of three field population datasets presented in Gibbs et al. (2013) - Field (a) is Scotland and Field (b) is Iceland non-bloom both experiencing slowed growth, and Field (c) is Iceland bloom experiencing rapid growth.

tendency of coccolithophores to show strong species- and strain-specific responses to external parameters, applying this same framework to any other fossil species would be extremely speculative based on data from only two modern species. The new experimental data presented in this study for *Calcidiscus* and *Helicosphaera*, in combination with previously published results for *Coccolithus* and *Emiliania* (Balch et al., 1993; Paasche, 1998; Gibbs et al., 2013; Gerecht et al., 2014; Gerecht et al., 2015), provides robust confirmation that coccosphere geometry persistently responds to growth phase in a common manner, regardless of species. Specifically, the number of coccoliths per coccosphere within the population increases under slowed growth in *Calcidiscus*, *Helicosphaera* and *Coccolithus*. These experiments have identified threshold values of C_N for recently divided cells and those that have sufficient coccoliths to be ready to divide (Figure 3.3) in *Calcidiscus* and *Helicosphaera* in addition to those reported by Gibbs et al. (2013) for *Coccolithus*. A rapidly dividing population during exponential growth phase has a greater percentage of recently divided cells, as defined by C_N (Figure 3.5), whereas a slowly dividing population in non-

exponential phase growth has a greater percentage of ready-to-divide cells. As C_N is easily quantified from fossil coccospheres as well as from modern cells (**Chapter 2**), this provides a robust method for identifying populations that are growing rapidly (>~15% population characterised by cells with C_N typical of recently divided cells) compared to populations that are growing slowly (>~15% population characterised by cells with C_N typical of ready to divide cells), as illustrated in Figure 3.5. In reality, the mixing of populations of different growth states in the fossil record will result in characteristic population C_N frequently lying between these two end-members (as shown by Gibbs et al., 2013; their Figure 4). However, relative changes in C_N characteristics within species through time can provide an indication of intervals where species may be experiencing environmental conditions that are more (towards exponential) or less (towards non-exponential) favourable for growth.

For fossil species that have no specific modern counterpart (e.g., *Chiasmolithus*), the general characteristics of rapidly growing populations consisting of smaller cells with fewer coccoliths relative to slowly dividing populations can be used as a qualitative indicator of changes in growth through time. For the species studied here, the C_N typical of recently divided and ready-to-divide cells can also be tentatively proposed based on the 10th and 90th percentiles of the full C_N dataset where substantial datasets of coccosphere geometry have been compiled for a species. Whilst we conclude that coccosphere geometry can now be used with confidence as a proxy of growth phase, we must be clear that the environmental and physiological signal recorded in field populations is always more complex than any laboratory experiment results. Populations may only experience a specific nutrient state for a few weeks or less before conditions change and the coccosphere geometry response of any individual cell to the experienced nutrient state is likely to be additionally complicated by temperature and light conditions that are also essential for growth. At present there is little to no experimental data to demonstrate the response of coccosphere geometry specifically to temperature or irradiance, or how changes in growth rate specifically (rather than growth phase) driven by these conditions may manifest in coccosphere geometry.

The fossil record of coccosphere geometry further compounds this issue, as remains are temporal integrations of many thousands of very short-lived population states. The coccosphere geometry signal of species populations transitioning between rapid and slowed growth phases as nutrient conditions change through time is therefore clearly going to become obscured and diluted by the mixing of population remains and subtle shifts in

species morphotypes and ecotypes as environmental conditions vary, as illustrated by Gibbs et al. (2013). However, the ability to define growth phase as a clear regulator of coccosphere geometry across coccolithophores generally and not just specific species, enables a defined link between the physiology of an individual cell and the long-term response of species to changes in nutrient conditions.

3.4.3 Implications of growth-driven cellular PIC and POC for calcite production

Coccolithophores are major calcite producers, contributing significantly to carbon export to the deep ocean (Broecker and Clark, 2009). *Coccolithus*, *Calcidiscus* and *Helicosphaera* have the potential to be major regional calcite producers in both the modern ocean (Daniels et al., 2014) and in the past (Ziveri et al., 2007) as they are some of the larger, most heavily calcified modern species with distributions throughout sub-Polar (*C. pelagicus*), temperate (*C. braarudii*), and sub-tropical (*Calcidiscus* and *Helicosphaera*) waters (Ziveri et al., 2004). The process of biogenic calcification is thought to be responsive to climate and particularly sensitive to changes in ocean carbonate chemistry (for reviews see Riebesell and Tortell, 2011; Bach et al., 2015; Meyer and Riebesell, 2015). The experiments presented here have illustrated that a significant change in calcite per cell can additionally result from nutrient availability by means of variability in the number of coccoliths in the coccosphere with growth phase. This has been known for some time for *E. huxleyi,* which produces multi-layered coccospheres and sheds excess coccoliths into the surrounding waters (Langer et al., 2013), but has not been known for other species. Calcite production, a function of cellular calcite (particulate inorganic carbon, PIC) and growth rate, could therefore change considerably with environmental conditions through time with implications for the biogeochemical cycling of carbon in the ocean. PIC can be calculated directly from the extensive dataset of coccosphere geometry collated for this study by multiplying C_N by coccolith calcite. Coccolith calcite is calculated following the method of Young and Ziveri (2000) as coccolith volume (C_L^3) multiplied by a 'shape factor' (k_S) that estimates species-specific coccolith thickness and cross-sectional shape, and the density of calcite (2.7 pg/μm^3). In the following, the impact of a shift between exponential phase and stationary phase growth on calcite production is discussed.

Mean cellular PIC is 11-15 pmol C cell^{-1} in *C. leptoporus* and 16-18 pmol C cell^{-1} in *H. carteri*, whilst mean calcite per cell is higher in *C. quadriperforatus* and *C. braarudii* at ~30 pmol
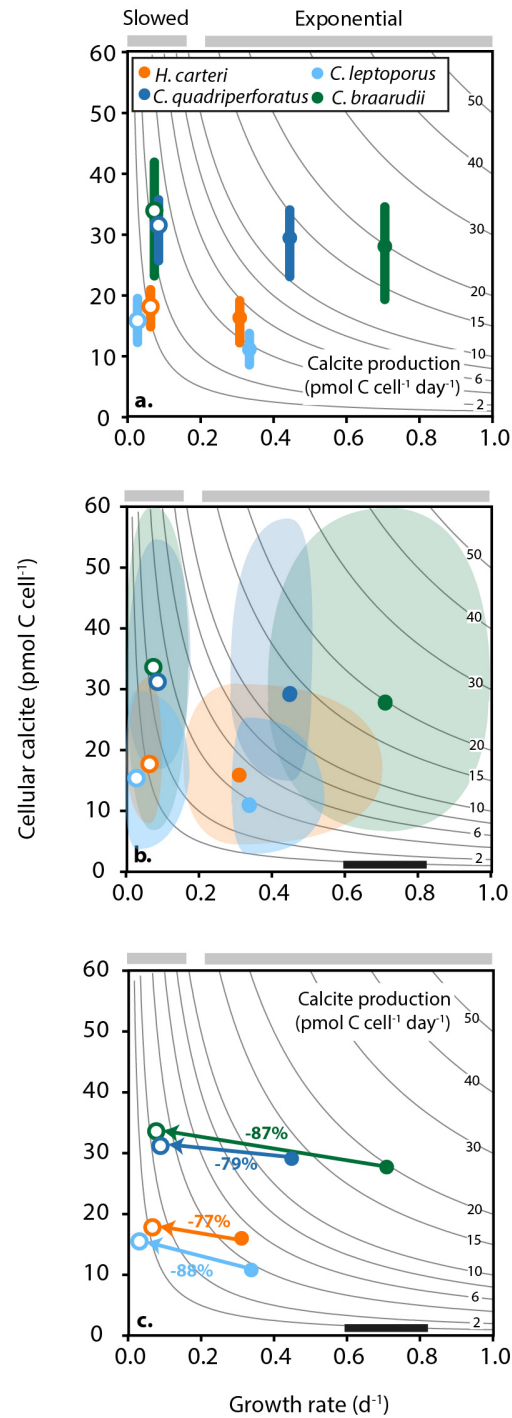
Figure 3.6: Calcification rates in *Coccolithus*, *Calcidiscus* and *Helicosphaera* at 22 °C. **a.** mean and 25th to 75th percentile of cellular calcite for cultures dividing exponentially (filled circles) and cultures no longer maintaining exponential growth (unfilled circles). **b.** Range in cellular calcite, growth rates and calcite production observed across the experiment. **c.** Percentage decrease in mean calcite production when cultures can no longer divide exponentially. The black box in **b.** and **c.** represents typical calcite production rates (~0.2-0.8 pmol C cell^{-1} day^{-1}) for *E. huxleyi* for comparison (Balch et al., 1996, Poulton et al., 2010).

C cell^{-1} (Figure 3.6a). Mean PIC increases in non-exponential experiment days in all species due to an average increase of 2-4 coccoliths per cell (Figure 3.3). The 25th and 75th percentiles are also clearly shifted towards higher cellular PIC in cells no longer growing exponentially (Figure 3.6a). *Calcidiscus* 25th percentile increases 50-60%, with *C. braarudii* and *H. carteri* increasing 20-25%. The increase in 75th percentile is not as large but is still considerable in *C. leptoporus* and *C. braarudii* at 36% and 24% respectively, with *C. quadriperforatus* and *H. carteri* showing more modest increases of 6% and 11%.

Calcite production per cell per day is calculated by multiplying cellular calcite by growth rate. Calcite production in these four species is 6-20 times higher than in *E. huxleyi* at a comparable growth rate (Figure 3.6; Balch et al., 1996; Poulton et al., 2010), therefore these heavily calcified species, where the calcite of one *C. braarudii* cell is equivalent to ~78 cells of *E. huxleyi*, do not necessarily need to maintain similar comparative growth rates or be present in high abundances within the community to dominate calcite production (Daniels et al., 2014). A dramatic difference in calcite production can be seen between populations growing exponentially and those no longer growing exponentially, with reductions of 77-88% in all species due to the approximate order of magnitude decrease in growth rates (Figure 3.6c). In field populations, growth rates can reach as low as <0.2 d^{-1} (Poulton et al., 2014), similar to culture populations in slowed growth shown in Figure 3.6, therefore these shifts to such low calcite production per cell per day are approximate minimum calcite production values for these species. However, it is clear that rates of calcite production can be altered by up to 50% for even a moderate change of growth rate of 0.1-0.2 d^{-1}, for example where coccolithophore populations experience changes in nutrient supply, temperature or light that no longer support optimal rates of cell division (Poulton et al., 2014).

The majority of studies attribute the response of calcite production to environmental change to changes in calcite per coccolith through coccolith size, thickness or malformation (e.g., Beaufort et al., 2011; Horigome et al., 2014). However, C_L would need to increase by roughly 5-20% to achieve the same change in cellular calcite as produced by the increase of just 2-4 coccoliths per cell. Changes in C_N with growth phase are therefore very important when considering the impact of environmental parameters such as nutrient availability on cellular PIC. The dominant control of growth rates on calcite production is an important consideration that is often overlooked when investigating the impact of

climate on long-term calcite production, carbon export, and sequestration and should be accounted for alongside growth phase changes in calcite.

3.4.4   Novel observations of living *Calcidiscus* and *Helicosphaera* cells

In addition to the main aim of the study to investigate coccosphere geometry with growth phase, the extensive LM analysis of culture material has also highlighted several interesting and novel observations concerning the active growth of these coccolithophore species. Firstly, proto-coccoliths at various stages of development were frequently observed within the cell in all species (Figure 3.7a). Proto-coccoliths are coccoliths still undergoing crystal growth onto a nucleation 'template' within a Golgi-body-related vesicle (Young et al., 1999). When growth is complete, the fully formed coccolith is extruded from the cell to join the coccosphere. Notably, cells of *Helicosphaera* and *Calcidiscus* species containing more than one proto-coccolith at once (up to three) were observed (Figure 3.7a). To our knowledge, this has not been previously reported and in fact, Paasche (2001) suggests that coccoliths are formed one at a time and Taylor et al. (2007) observed the sequential production of single coccoliths in *C. braarudii*. Coccoliths of *Calcidiscus*, *Helicosphaera* and *Coccolithus* are particularly heavily calcified and are likely to take a comparatively long time to fully form inside the cell. As coccospheres must have sufficient coccoliths to cover two newly divided cells before division occurs (Taylor et al., 2007), it may be that heavily calcified cells frequently need to start the production of a new coccolith before the previous is completed and extruded in order to produce sufficient coccoliths in the timespan between divisions. For these species with a minimum C_N of 8-10 (Figure 3.1), each cell must produce a further 8-10 coccoliths before dividing to ensure a complete cell covering of the daughter cells. At exponential growth rates of $\mu = 0.4$ d^{-1} (~1.7 days division^{-1}), new coccoliths must be produced at least every ~2.0-2.5 hours, as the majority of calcification is thought to be restricted to the light phase (Müller et al., 2008).

We also observed mid-division cells in all species during the daylight phase (Figure 3.7b). This was slightly unexpected, as the typically consensus is that DNA replication and cell division (mitosis) occurs during the dark period (e.g., Müller et al., 2008) and justifies performing cell counts 4-6 hours after the light period begins to ensure accuracy of cells ml^{-1}. It is possible that the mid-division cells observed are incapable of completing division due to errors during mitosis. We further observed that *H. carteri* cells in culture show strong
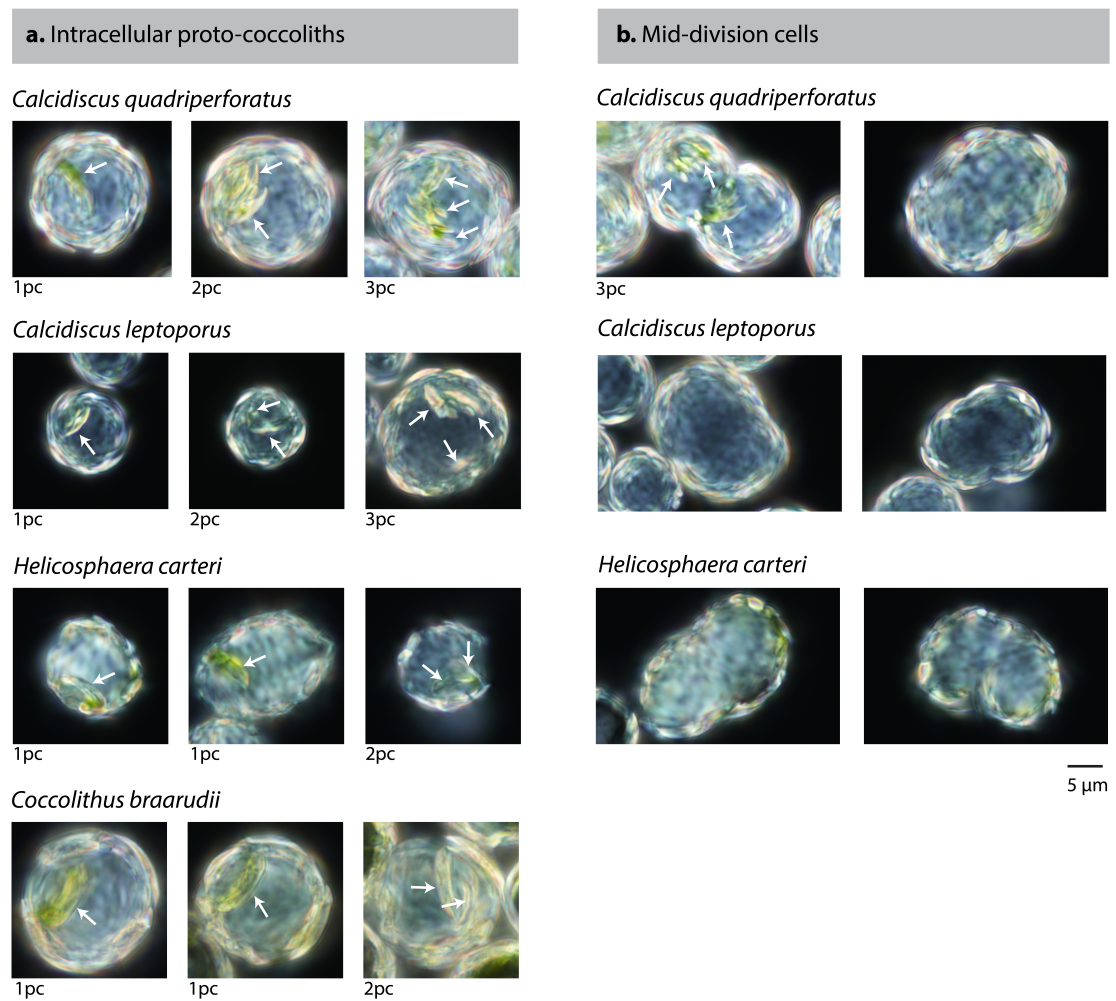
Figure 3.7: Observations of coccolithogenesis and active cellular division in four key modern coccolithophore species – *Calcidiscus quadriperforatus*, *C. leptoporus*, *Helicosphaera carteri*, and *Coccolithus braarudii*. **a.** Cells showing the presence of partially-formed intra-cellular new coccoliths (proto-coccoliths). All species show that more than one proto-coccolith may be present within the cell. Arrows identify the location of the proto-coccolith and the number present is below the image, e.g., 2pc means 2 protococcoliths observed. **b.** Cells in mid-division show a 'dumbbell' shape as the cells pull apart. *H. carteri*, with a non-spherical coccosphere shape, shows division along both the long and short axis. These images were taken ~5 hours into the light phase, by which time all cell division should be complete.

positive phototaxis, persistently clustering closest to the incubator light source. This indicates that *H. carteri* cells may have eyespots associated with their chloroplast in order to enable irradiance detection. Phototactic behavior has been reported in other motile coccolithophore species, including *Algirosphaera robusta*, *Jomonlithus littoralis*, the coastal coccolithophorid *Ochrosphaera neapolitana* and the haploid phase of *Coccolithus* (Billard and Inouye, 2004; Fresnel and Probert, 2005; Probert et al., 2007; Probert et al., 2014).

67

3.5   Conclusions

Experiments on modern coccolithophore species of *Calcidiscus* and *Helicosphaera* identify differences in coccosphere geometry under exponential phase growth (nutrient replete conditions) and non-exponential phase growth (nutrient depleted conditions) identical to those previously observed in *Coccolithus* and *Emiliania huxleyi*. The extension of these previously published findings into two additional coccolithophore families strongly demonstrates that the decoupling of cell division and calcification is a core physiological response to nutrient depletion. This is revealed in coccosphere geometry as an increase in coccoliths per cell and coccosphere size across all families. With due consideration, coccosphere geometry can now be applied as a proxy for growth phase in the geological record, as well as sediment trap and modern field population samples, with the expectation that populations of any coccolithophore species experiencing growth-limiting nutrient conditions will have a greater number of larger cells with more coccoliths per cell. The variability of coccosphere geometry with growth, specifically calcite production through the production of coccoliths, identifies coccoliths per cell as an equally important parameter as calcite per coccolith in determining cellular calcite. Growth rate is the principal driver of calcite production rather than cellular calcite, highlighting the need for accessing growth information in the geological record in order to explore the impact of future climate change scenarios on calcite production and export.

Chapter 4:
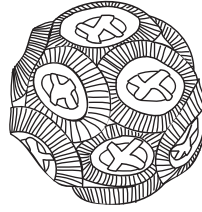
The response of coccolithophore community cell size structure to Paleogene climate variability

Rosie M. Sheward, Samantha J. Gibbs, Alex J. Poulton, Paul R. Bown

Abstract

The cell size structure of phytoplankton communities is an important determinant in the production and export of biomass and therefore plays a key role in biogeochemical cycles and energy transfer through food webs. Community cell size structure is the net result of bottom-up biotic and environmental controls on the biogeography and relative abundance of species with different cell size ranges. The cell size distribution of Paleogene taxa has been determined for specific time intervals using new coccosphere geometry data from fossil coccospheres. Combined with information about the relative abundance of taxa within different Paleogene coccolithophore communities, community cell size structure has been reconstructed at different latitudes for the first time in the geological record. Generally, coccolithophore community cell size structure is broadly similar across latitudes and time intervals, showing a peak of cells with <12 μm cell diameters and a low abundance of cells spread across large cell size classes up to 40 μm. Between the 'greenhouse' of the Early Eocene and the 'icehouse' of the Early Oligocene, community composition transitions towards the inclusion of larger cell sizes, primarily in the morphologically diverse group *Reticulofenestra*. This major change in community composition substantially increased relative community biovolume and biomass, which, in conjunction with the presence of larger cells, supports a hypothesis of increased oceanic nutrient availability by the Late Eocene. The shift in the partitioning of biomass from smaller to larger cells may have significant implications for carbon cycling and export and affect size-specialized grazers in higher trophic levels. Patterns in coccolithophore community cell size structure are therefore linked to the interactions of cell size with physiology that drives the ecological and evolutionary response of coccolithophores to environmental change.

4.1   Introduction

Phytoplankton community structure is established through the interactions of species with their abiotic environment – temperature, nutrients, light, chemistry – and biotic factors including predator-prey relationships and competition for resources (Margalef, 1978). Abiotic conditions determine the species composition of each community, as each species has a fundamental ecological niche of preferred temperature, nutrient and light conditions that sustain growth (Hutchinson, 1957). The relative abundance of species within each community results from competition between species for resources and from relative grazing pressure from zooplankton (Tilman, 1982). Phytoplankton community structure therefore exhibits strong spatial variability in response to niche dynamics and hydrography (e.g., Haq and Lohmann, 1976; Winter et al., 1994; Ziveri et al., 2004; Boyd et al., 2010; Cermeño et al., 2010).

As each species within a community has a specific distribution of cell sizes, a predictable outcome of the biogeographic variability in species composition and relative abundance is that the overall cell size structure of communities also exhibits spatial variability. The cell size structure of each community will be sensitive to environmental variability through time, responding to the evolving biogeographic distribution and abundance of species of different sizes as conditions in the marine environment change (e.g., Li et al., 2009). Changes in the size structure of phytoplankton communities is therefore a likely response to climate change, which could have broader implications for biogeochemical cycles, as different species composition, abundance and cell sizes affect the production of organic and inorganic elements such as carbon and nitrogen (Geider and La Roche, 2002; Finkel et al., 2010). Particle size and composition may also affect the balance between export and remineralisation of organic material (Michaels and Silver, 1988) due to its relationship with sinking velocities and aggregate formation (Guidi et al., 2008).

The cell size structure of phytoplankton communities during different climate states in geological time can be assessed from the fossilised remains of mineralised phytoplankton groups, providing the opportunity to assess the net responses of phytoplankton communities to climate variability in the past. Of particular relevance to predicted future climate conditions are similarities and differences between phytoplankton communities during geological periods of 'greenhouse' conditions, such as the Paleogene period ~66 to 23 million years ago, and the 'icehouse' conditions of 23 million years ago (Ma) to present

(Zachos et al., 2008; Norris et al., 2013). During the last ~66 Ma, the global fossil records of multiple plankton groups show trends in body size through time, largely associated with changing abiotic conditions, notably nutrient availability, as the climate shifted from a greenhouse background state into an icehouse background state. These trends include decreases in the mean frustule size of marine diatoms (Finkel et al., 2005) and the cyst size of marine dinoflagellates (Finkel et al., 2007), as well as increases in the largest foraminiferal test sizes (Schmidt et al., 2004b) over the same era. Whilst there are some records of coccolith size changes through the Paleogene (Herrmann and Thierstein, 2012; Bordiga et al., 2015), a complementary record of cell size in geological time is notably absent for the coccolithophores, a widespread and globally abundant calcifying phytoplankton group that evolved during the Late Triassic ~225 Ma (Bown et al., 2004). This is primarily because the calcite cell covering (coccosphere) of coccolithophores typically disarticulates into its component parts (coccoliths) following cell death. The extensive fossil record of coccolithophores therefore conspicuously lacks 'body fossils' from which the cell size of all cells within a fossil assemblage can be easily measured. Studying the cell size structure of an entire fossil coccolithophore assemblage therefore presents significant challenges compared to diatoms, dinoflagellates and foraminifera.

In this study, the cell size structure of fossil coccolithophore communities is reconstructed at multiple sites using a novel approach that utilises the extensive new database of cell geometry data from intact fossil coccospheres of Paleogene (~66–23 Ma) age presented in **Chapter 2**. This dataset represents the 'state of the art' of our knowledge of coccolithophore cell size in the fossil record. These reconstructions of coccolithophore community cell size structure specific to different sites and time intervals provide insights into community-level cell size responses to climate variability through intervals spaced throughout the Paleogene period. This period is of particular palaeoclimatic interest as it encompasses a long-term transition between Early Eocene peak greenhouse conditions and the newly established icehouse state of the Early Oligocene (e.g., Zachos et al., 2008), during which atmospheric CO_2 levels and global temperatures gradually fell (Pagani et al., 2005; Beerling and Royer, 2011; Zhang et al., 2013). Together, these trends have been shown to increase the vertical and latitudinal thermal gradients of the ocean (Liu et al., 2009; Inglis et al., 2015). Such considerable environmental restructuring led to long term changes in the marine system that are expected to drive shifts in phytoplankton community composition, and possibly within-species cell size, that will ultimately be reflected in the

size structure of the reconstructed coccolithophore communities.

4.2   Methods

4.2.1   Site descriptions

Coccolithophore community size structure was reconstructed at six locations distributed across a range of latitudes and ocean basins (Figure 4.1; Table 4.1). Each site provides a continuous coverage of calcareous nannofossil remains of Paleocene to Oligocene age from drilled deep-sea sediments. Detailed records of species relative abundance at each site had previously been published in Schneider et al. (2011) and the original assemblage counts were generously provided by Leah LeVay, formerly Schneider (Texas A&M University), for this study. For the purposes of this study, species abundance in each sample was averaged across the nannoplankton zones of Martini (1971).

4.2.2   Community cell size reconstruction intervals

This study focuses on coccolithophore community cell size structure at five intervals spaced throughout the long-term cooling trend (Zachos et al., 2001; Zachos et al., 2008) between the peak warmth of the Early Eocene Climatic Optimum (EECO, 53-50 Ma; Zachos et al., 2008) and the new icehouse background state of the Early Oligocene (Liu et al., 2009).

(1)   The Early Eocene reconstruction represents coccolithophore communities ~54-53 Ma during Paleogene Nannoplankton (NP) zone NP11 (Martini, 1971) immediately prior to EECO (53-50 Ma) at each site.

(2)   The Early-Mid Eocene reconstruction represents an interval of major evolutionary turnover between the coccolithophore genus *Toweius* and the expansion of the *Reticulofenestra* genus. The age and duration of overlap between these genera varies between sites (Schneider et al., 2011) but typically falls within the latter half of zone NP12 (~52-50 Ma).

(3)   The Mid Eocene reconstruction represents communities ~41-42 Ma during zone NP16.

(4)   The Late Eocene interval reconstructs communities during zone NP20-19 (~34.5-37 Ma), prior to the major global cooling step at the Eocene-Oligocene boundary (~33 Ma; Liu et al., 2009).
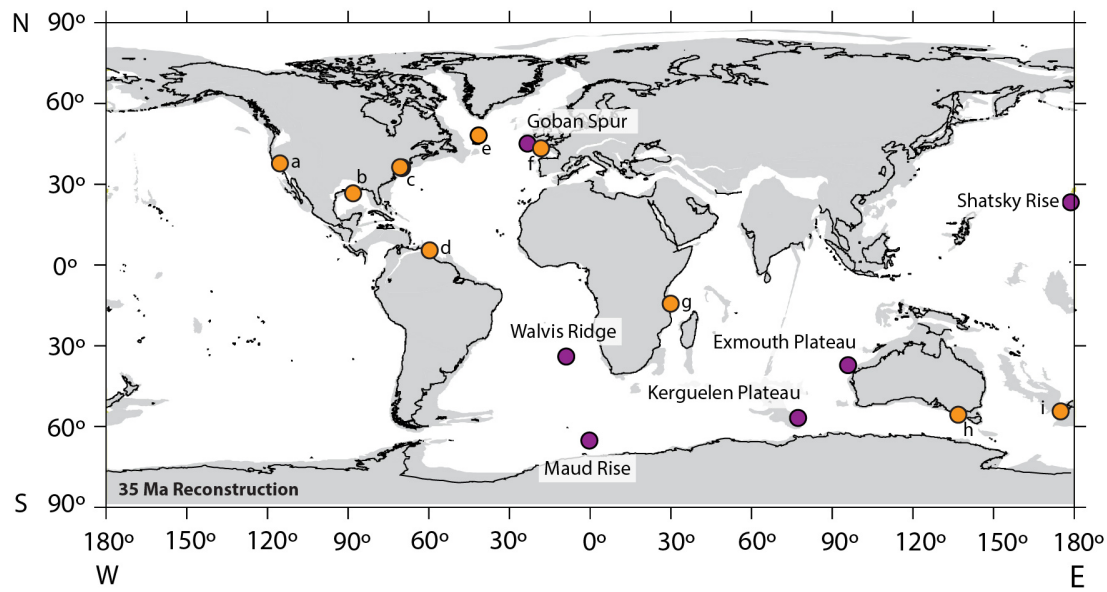
Figure 4.1: Locations of sites where community size structure has been reconstructed (purple dots; Table 4.1) and sites from which coccosphere geometry measurements (**Chapter 2**) have been used for modelling the cell size distribution of *Chiasmolithus*, *Coccolithus*, *Coccolithus formosus*, *Cyclicargolithus*, *Reticulofenestra*, and *Toweius* (orange dots). a. Lodo Gulch, b. Mississippi, c. New Jersey Shelf (Bass River and Wilson Lake), d. Trinidad and Puerto Rico, e. Labrador Sea, f. Bay of Biscay, g. Tanzania, h. Australia, i. New Zealand. See Table 2.1 for detailed site descriptions.

Site	DSDP/ODP	Ocean	Palaeolatitude	Biogeography
Shatsky Rise	ODP Leg 198 Site 1210	North Pacific	18-22 °N	Topical
Walvis Ridge	ODP Leg 208 Site 1263	South Atlantic	30°S	Sub-tropical
Goban Spur	DSDP Leg 80 Site 549	North Atlantic	45°N	Temperate
Exmouth Plateau	ODP Leg 122 Site 762	Indian	40-45°S	Sub-tropical
Kerguelen Plateau	ODP Leg 183 Sites 1135, 1137	Southern Ocean, Indian sector	60°S	Sub-polar
Maud Rise	ODP Leg 113 Sites 689, 690	Southern Ocean, Atlantic sector	65°S	Sub-polar

Table 4.1: Overview of sites used for coccolithophore community reconstructions in this study. Palaeolatitudes are estimated from tectonic plate reconstruction maps at each of the specified intervals (Ocean Drilling Stratigraphic Network, odsn.de). Biogeography refers to the biogeographic zone denoted to each site by Schmidt et al. (2004a), except for Shatsky Rise, which is tentatively assigned as tropical due to its low palaeolatitude.

(5)   The final reconstruction interval is for the earliest Oligocene ~33-32 Ma following the major global climate perturbations of the Eocene-Oligocene boundary.

4.2.3   Calculating community cell size from fossil coccosphere data

The distribution of cell sizes within a coccolithophore community is dependent on two main factors:

(1)   The frequency distribution of cell sizes within each species in the community.

(2)   The relative abundance of each species in the community.

In this study, we develop a method that uses the fossil coccosphere geometry dataset (cell and diameter, coccolith length and number of coccoliths per cell) presented in **Chapter 2** to calculate the cell size structure of coccolithophore communities of different ages. For the purposes of this study, we consider only the coccolith proportion of the calcareous nannoplankton assemblage, i.e., we exclude holococcolith taxa that represent a separate coccolithophore life-cycle stage and nannolith taxa that lack definite coccolithophore affinities.

From the coccolithophore assemblage, the reconstructed coccolithophore community is then simplified to comprise of six coccolithophore groups (Figure 4.2) – *Chiasmolithus* spp. (undivided), *Coccolithus pelagicus*, *Coccolithus formosus* (called *Ericsonia formosus* by some authors), *Cyclicargolithus floridanus*, *Reticulofenestra* spp. (divided, see below), and *Toweius* spp. (undivided) – for which we have already amassed a substantial number of fossil coccosphere geometry measurements (these six groups account for 91% of the fossil coccosphere data collected and presented in **Chapter 2**). These six groups dominate Paleogene coccolith assemblages, including those that are being used in this study to reconstruct coccolithophore community cell size structure (>90% of coccolith assemblage in many time intervals; Appendix Table A4.2; Schneider et al., 2011). For the purposes of this study, we have subdivided *Reticulofenestra* into small, medium and large defined 'species' groupings. As such, the reconstructions refer to *Reticulofenestra minuta* (defined as C_L <3 μm), *Reticulofenestra umbilicus* (here C_L >14 μm and therefore also including *R. stavensis*), and *Reticulofenestra dictyoda* (C_L = 3-14 μm) that encompasses the remaining diversity of *Reticulofenestra* species.

Chiasmolithus

— 2 μm
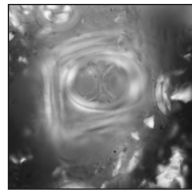
Chiasmolithus oamarensis
NP20-19 Australia
COLN 51
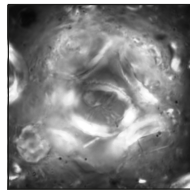
Chiasmolithus expansus
NP17 Labrador Sea
647A 46-4 85-87 cm
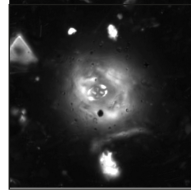
Chiasmolithus nitidus
NP15 Tanzania
TDP 6 9/1 85 cm
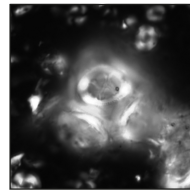
Chiasmolithus solitus
NP16 Labrador Sea
647A 49-5 108-110 cm
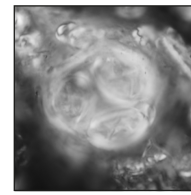
Chiasmolithus bidens
NP10 Bay of Biscay
401 14 3 20 cm

Coccolithus pelagicus

Coccolithus formosus
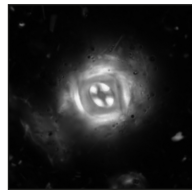
Coccolithus pelagicus
NP11 Tanzania
TDP 3 12/1 62-63
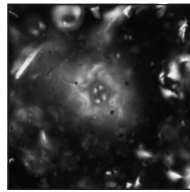
Coccolithus pelgicus
NP17 Labrador Sea
647A 46-7 17-19 cm
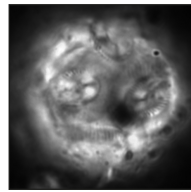
Coccolithus pelagicus
NP21 Tanzania
TDP 12 9/1 20-21 cm
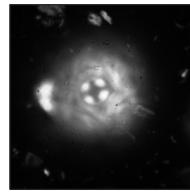
Coccolithus formosus
NP15 Tanzania
TDP 2 25/1 62 cm
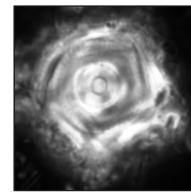
Coccolithus formosus
NP21 Mississippi

Cyclicargolithus floridanus
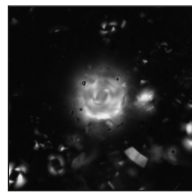
Reticulofenestra

Cyclicargolithus floridanus
NP16 New Zealand
HB 205
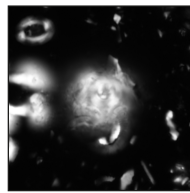
Cyclicargolithus floridanus
NP20-19 Labrador Sea
647A 34-1 104 cm
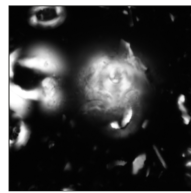
Cyclicargolithus floridanus
NP20-19 Labrador Sea
647A 34-1 104 cm
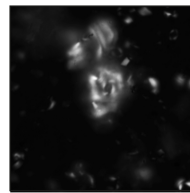
Reticulofenestra minuta
NP16 New Zealand
HB 205
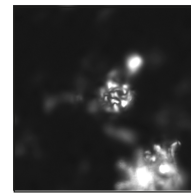
Reticulofenestra minuta
NP20-19 Australia
COLN 51
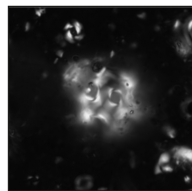
Reticulofenestra dictyoda
NP16 New Zealand
HB 205
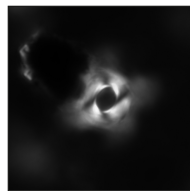
Reticulofenestra dictyoda
NP16 Labrador Sea
647A 49-1 137-139 cm
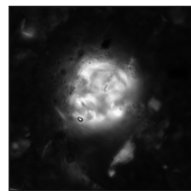
Reticulofenestra bisecta
NP15 Tanzania
TDP LIN 99-17
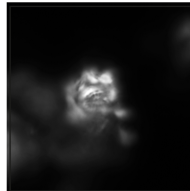
Reticulofenestra daviesii
NP20-19 Labrador Sea
647A 32-2 13 cm
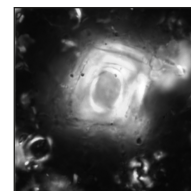
Reticulofenestra dictyoda
NP16 Labrador Sea
647A 51-1 7-9 cm

Toweius
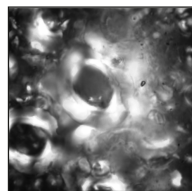
Reticulofenestra umbilicus
NP16 Labrador Sea
647A 49-3 45-47 cm
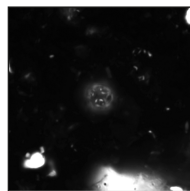
Toweius pertusus
NP12 Lodo Gulch
LO-03-13
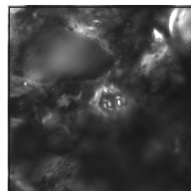
Toweius pertusus
NP5 Tanzania
TDP 27 7/1 46-48 cm
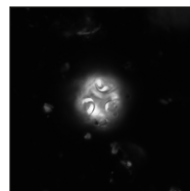
Toweius pertusus
NP12 Lodo Gulch
LO-03-13
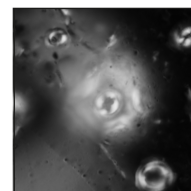
Toweius pertusus
NP9 Bass River
BR 81

Figure 4.2: Light microscopy images of selected coccolithophore species used in the reconstruction of cell size distributions of six Paleogene genera. All images are to the same scale (2 μm scale bar is indicated).

For each time interval (**Section 4.2.2**), the following steps are taken to reconstruct the cell size distribution of each community:

(1)   Derive the frequency distribution of cell sizes within each taxonomic group, specific to each reconstruction time interval.

(2)   Normalise each histogram to the relative cellular abundance of each taxonomic group at each site.

(3)   Combine the abundance-normalised histograms of each taxonomic group to generate the cumulative cell size frequency of the community.

Initially, we plot the frequency histograms of fossil coccosphere cell size for each genus during each reconstruction time interval (Figure 4.3a) from our dataset of fossil coccosphere geometry (**Chapter 2**). By comparing the coccolith length of these fossil coccospheres to the frequency distribution of coccolith lengths in loose coccolith material (Figure 4.3b) within the same samples, it is, not unexpectedly, clear that our fossil coccospheres data are somewhat biased towards preferentially representing smaller size classes with correspondingly smaller coccoliths. As such, the abundance of cell sizes within larger size classes is under represented in our coccosphere dataset in all genera. Simplistically, it would be easiest to merely use cell size histograms plotted directly from fossil cell size data as the basis of our community cell size reconstructions. However, this would introduce an obvious size bias. Instead, we use coccolith size data measured from loose coccoliths, which are arguably less size biased, alongside our fossil cell size data to reconstruct a more realistic cell size distribution histogram for our purposes.

To do this, we have developed a novel method for calculating cell size based on robust relationships between cell size, coccolith length and number of coccoliths per cell that we have identified (**Chapter 2**). This allows us to calculate cell size for the complete range of coccolith lengths observed in a sample. Existing techniques to calculate cell size rely solely on a linear relationship between cell size and coccolith length (Henderiks and Pagani, 2007; Henderiks, 2008), which although is a reasonable indicator of cell size (Figure 2.6), ignores the inherent variability in cell size that is related to number of coccoliths per cell, C_N. For some genera, coccolith length, C_L, is a particularly poor predictor of cell size that greatly over- or underestimates true size based solely on coccolith size (Figure 2.8a, 2.9a).
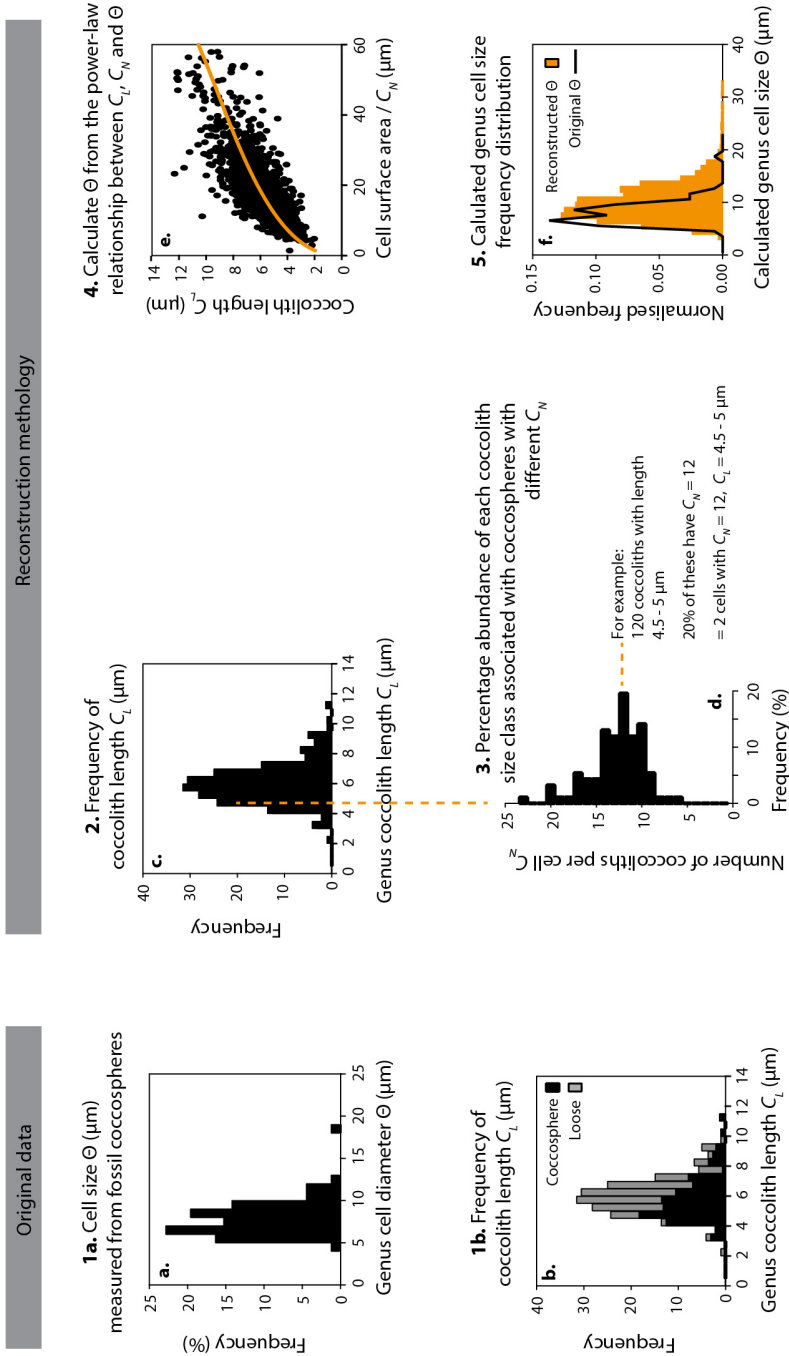
Figure 4.3: Illustrative schematic of the method used to reconstruct the frequency distribution of genus cell size within each interval (in this example for *Coccolithus* in the Early-Mid Eocene) using fossil coccosphere geometry data specific to each interval. All data shown in black are size measurements taken from fossil coccospheres (**Chapter 2**). Data shown in orange is modelled based on the original data (1a and 1b). The calculated frequency distribution of genus cell size (orange, f) clearly shows that his method calculates the additional cell size range that is not captured by the original coccosphere dataset (black line).

For each genus, we firstly plot the frequency distribution of C_N from fossil *coccosphere* geometry data in samples of the same age as the reconstruction interval (Figure 4.3d). From the same samples, we plot the frequency distribution of coccolith length (C_L) measured from loose coccolith data (Figure 4.3c) and assume that the C_N frequency plot would theoretically apply across each C_L size bin, comparable to the distribution of C_N we observe across coccosphere size classes (Figure 2.6). In other words, the distribution of C_N is consistent for all coccolith length size bins. For example (Figure 4.3d), if 20% of the coccoliths with length 4.5–5 μm (e.g., 24 coccoliths out of a total of 120 coccoliths in this size bin) are associated with cells that have 12 coccoliths per cell, this would represent 2 cells of 12 coccoliths that are 4.5–5 μm in length. Of the remaining 96 coccoliths, the C_N histograms tells us that 18 coccoliths (15%) would be associated with cells that have 10 coccoliths per cell, thus representing 1.8 cells. This is repeated for all of the C_L size bins until we know how many cells in the genus population have x number of coccoliths of x μm in length. The cell size of these cells is then calculated using the power-law relationship that exists between cell size, coccolith length and number of coccoliths per cell specific to each genus, as shown in Appendix Figure A.4.1 and illustrated in Figure 4.3e. Following this method for each coccolith length size class calculates the cell size data of each genus (Figure 4.3f).

To reconstruct the frequency distribution of cell sizes within the whole community, the cell size distributions for each genus are normalised to the relative abundance of cells (rather than coccoliths) in the community. Cellular abundance is calculated from coccolith relative abundance using the mean C_N observed on coccospheres of each genus of the same age as the reconstruction interval. The normalised cell size frequency distribution of each genus is then combined to produce a reconstructed cell size distribution for a coccolithophore community comprised of *Chiasmolithus* spp., *Coccolithus pelagicus*, *Coccolithus formosus*, *Cyclicargolithus floridanus*, *Reticulofenestra* spp., and *Toweius* spp. A detailed description of how this methodology was implemented can be found in **Appendix Chapter 4**.

4.3   Results

4.3.1   Cell size characteristics of each genera and its variability through time

The basis for reconstructing coccolithophore community cell size structure is the specific cell size distribution for each genus during each time slice that we calculate directly from
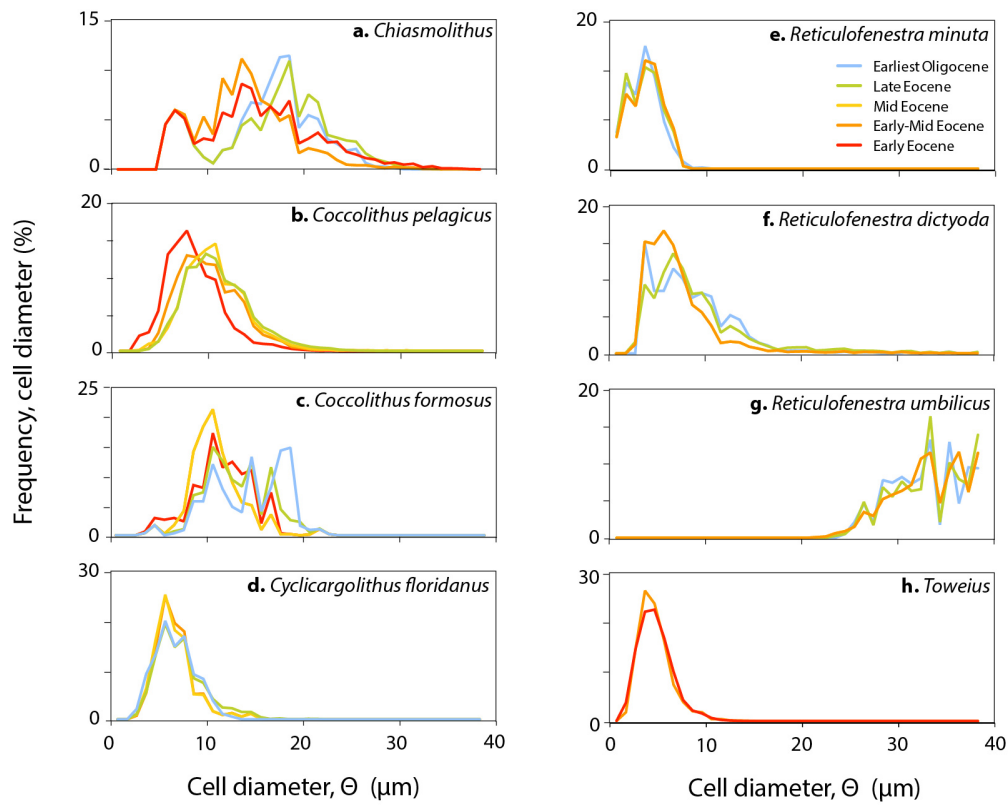
Figure 4.4: Frequency distribution of cell size within each genus specific to each reconstruction time interval. Note the different range on the frequency axis for each genus.

coccosphere geometry measurements (Figure 4.4). The smallest taxonomic groups are *Reticulofenestra minuta* and *Toweius*, with 95% of their cell size less than 7 μm and 8 μm respectively. *Reticulofenestra umbilicus* is by far the largest coccolithophore taxon, with a minimum cell size of 23 μm and largest cells up to 39 μm. The range in cell size is relatively small in *Reticulofenestra minuta* (0.5 to 10.5 μm), *Reticulofenestra umbilicus* (24.5 to 38.5 μm), *Toweius* (1.5 to 14.5 μm) and *Cyclicargolithus floridanus* (2.5 to 16.5 μm) compared to the cell size range of 19 μm in *Coccolithus pelagicus* up to 36 μm in *Reticulofenestra dictyoda*. Maximum cell size is almost double the size of the 95th percentile of the data (Θ_{95}) in *Reticulofenestra dictyoda* and *Coccolithus pelagicus*, indicating that the largest 5% of cells within each genus are distributed in very low abundances across a large number of size classes. The distribution of cell sizes in *Toweius*, *Coccolithus*, *Reticulofenestra minuta* and *Reticulofenestra dictyoda* is broadly unimodal. In contrast, the distribution of cell sizes in *Chiasmolithus*, *Coccolithus formosus* and *Reticulofenestra umbilicus* shows multiple peaks throughout the size classes. This is likely to

80

result from a mixing of species or morphospecies with discrete ranges in coccosphere geometry that do not intergrade smoothly.

Cyclicargolithus floridanus, *Reticulofenestra minuta* and *Toweius* show a high degree of similarity in cell size distribution through time (Figure 4.4). A moderate shift of the frequency distribution towards larger size classes in the later Eocene and earliest Oligocene is observed in *Chiasmolithus*, *Coccolithus pelagicus* and *Coccolithus formosus* but this involves little change in the smallest or largest cells (Θ_5 and Θ_{95}) except in *Coccolithus formosus*. In *Reticulofenestra dictyoda*, there is an increase in the abundance of cells between 8 μm and 20 μm in size and a corresponding decrease in the <8 μm size classes between the Mid Eocene reconstruction and the Late Eocene reconstructions (Figure 4.4f).

4.3.2 Spatial and temporal variability in community cell size structure

The reconstructed community cell size structure (for a community of 100 cells) at six different sites located at a range of palaeo-latitudes and ocean basins aims to highlight any spatial variability in community cell size structure that may result from biogeographic variability in community composition and abundances (Figure 4.5). Perhaps the most interesting feature is the broad similarities in community cell size structure between sites and reconstruction intervals (Figure 4.6) despite the significant range in latitudes between the six sites (65 °S to 45 °N; Figure 4.1). Community cell size structure is consistently skewed away from larger size classes, with the vast majority of cells (80-95%) between 2 and 15 μm in all reconstructions. In addition, all communities exhibit a long 'tail' that represents a low abundance of cells distributed across a wide range of larger cell size classes between 15 and 30 μm, becoming a more pronounced feature of the community (hosting an increased proportion of the community) at all sites as the Eocene progressed. As such, by the Late Eocene the largest 25% of cells are distributed in low abundances across size classes >14 μm and the largest 10% of cells between 27 and 35 μm in cell diameter (Figures 4.5 and 4.6).

Superimposed on these broadly similar cell size structures are modest spatial and temporal differences that result predominantly from differences in the composition and abundance of the different genera (Figure 4.5) with different cell size structures (Figure 4.4). Spatial variability is not a particularly pronounced feature of the cell size structure of these communities. However, during specific intervals some sites have a cell size structure
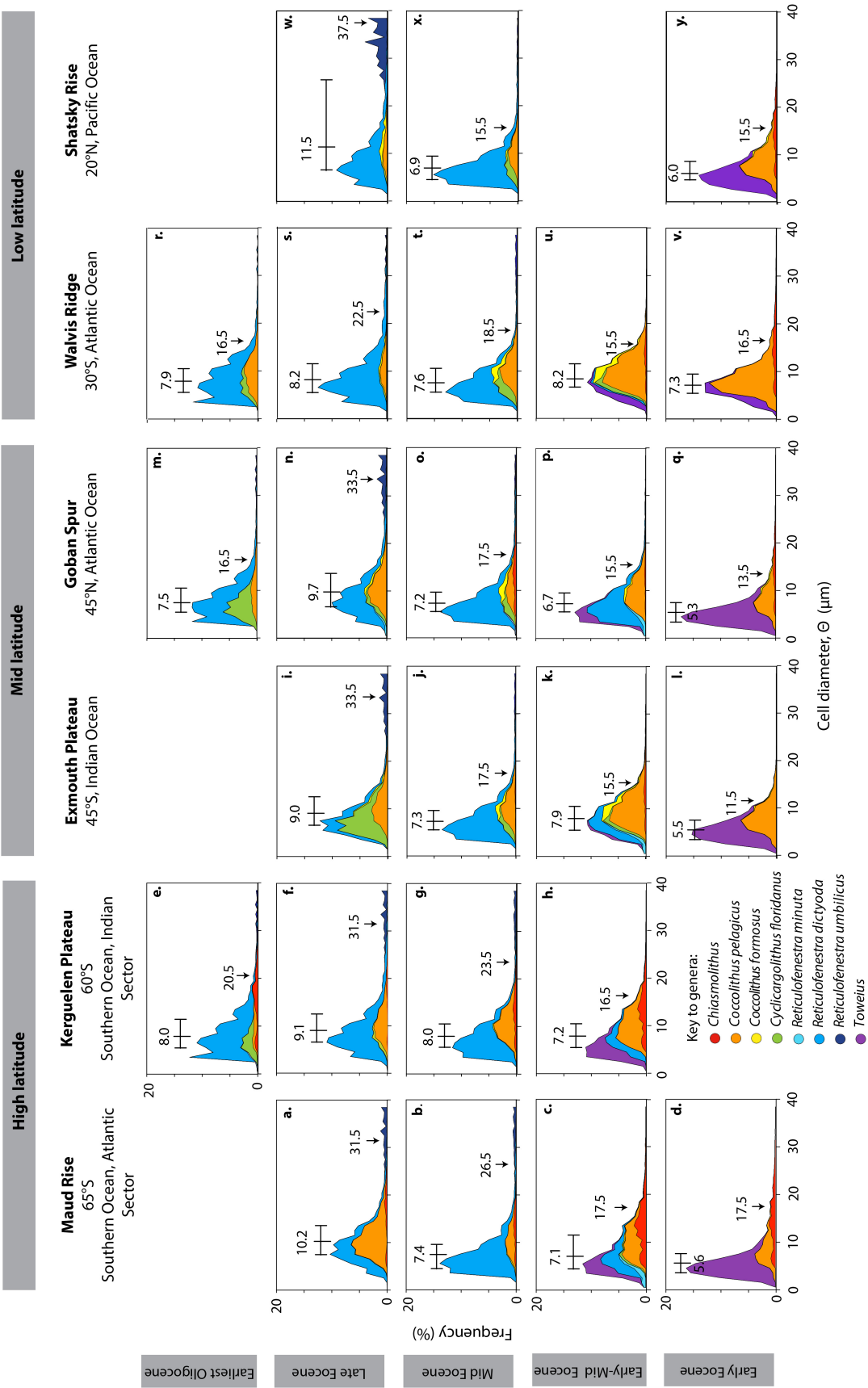
Figure 4.5 (opposite): Reconstructed community cell size distributions at each site (left to right) and by reconstruction interval (top to bottom). High latitude sites **a. - d.** Maud Rise (65 °S) and **e. - h.** Kerguelen Plateau (60 °S). Mid-latitude sites **i. - l.** Exmouth Plateau (45 °S) and **m. - q.** Goban Spur (45 °N). Low latitude sites **r. - v.** Walvis Ridge (30 °S) and **w. - y.** Shatsky Rise (20 °N). See Figure 4.1 for map locations. Reconstruction intervals are shown from the youngest (earliest Oligocene or Late Eocene depending on site, top) to the oldest (Early Eocene, bottom). The 'whisker' bar on each plot shows (from left to right) the 25th percentile, geometric mean cell size of the community (displayed), and 75th percentile of the model. The arrow marks the 95th percentile (Θ_{95}). Details of the descriptive statistics for each site interval are shown in Table 4.3. Early-Mid Eocene reconstruction is the interval across which *Toweius* and *Reticulofenestra* co-occur and is variable by site (see. Appendix Figure A4.2 and A4.3).

that is notably distinct from other sites. For example, the most abundant cell size class at Early Eocene Walvis Ridge is 6 to 9 μm compared to ~3 to 6 μm at other latitudes (Figure 4.5), which can be attributed to the overall larger cell size of *Coccolithus pelagicus* relative to the other highly abundant Early Eocene taxa *Toweius* and its high abundance at Walvis Ridge (73%; Figure 4.5v) relative to its abundance elsewhere (20-40%). Maud Rise has the largest Θ_{95} of the Early Eocene reconstructions (17.5 μm) due to the higher abundance of *Chiasmolithus* cells at Maud Rise and Kerguelen Plateau during the Early, Early-Mid Eocene and earliest Oligocene. This adds a low abundance of cells into size classes >15 μm, resulting in a larger Θ_{95} than observed at other sites during these intervals.

Temporal changes in cell size structure are largely a reflection of the change in cell size distribution that occurs with the decline and extinction of *Toweius* and origination and expansion of *Reticulofenestra* after the Early Eocene, increasing peak cell size by up to 5 μm by the Late Eocene and earliest Oligocene (Figure 4.5). During the Late Eocene, the presence of higher abundances of *Reticulofenestra umbilicus* elongates the upper tail of the histograms such that Θ_{95} doubles to triples relative to the Early Eocene and is >30 μm at all sites except Walvis Ridge, where *Reticulofenestra umbilicus* is <1% of the community.

4.3.3   Community biovolume

The biovolume structure of each community can be calculated by multiplying the cell volume of each cell size class (cell volume = $(4/3)*\pi*$cell radius^3 as the coccospheres of these genera are spherical) by the frequency of cells in the same size class. Community biovolume structure (Figure 4.7) shows a striking contrast to the shape of the cell size structure (Figure 4.5) as lower abundances of larger cells make a disproportionately large contribution to total community biovolume relative to their cell diameter. In the Early and Mid Eocene reconstruction intervals, cell biovolume accumulates in medium to large cell
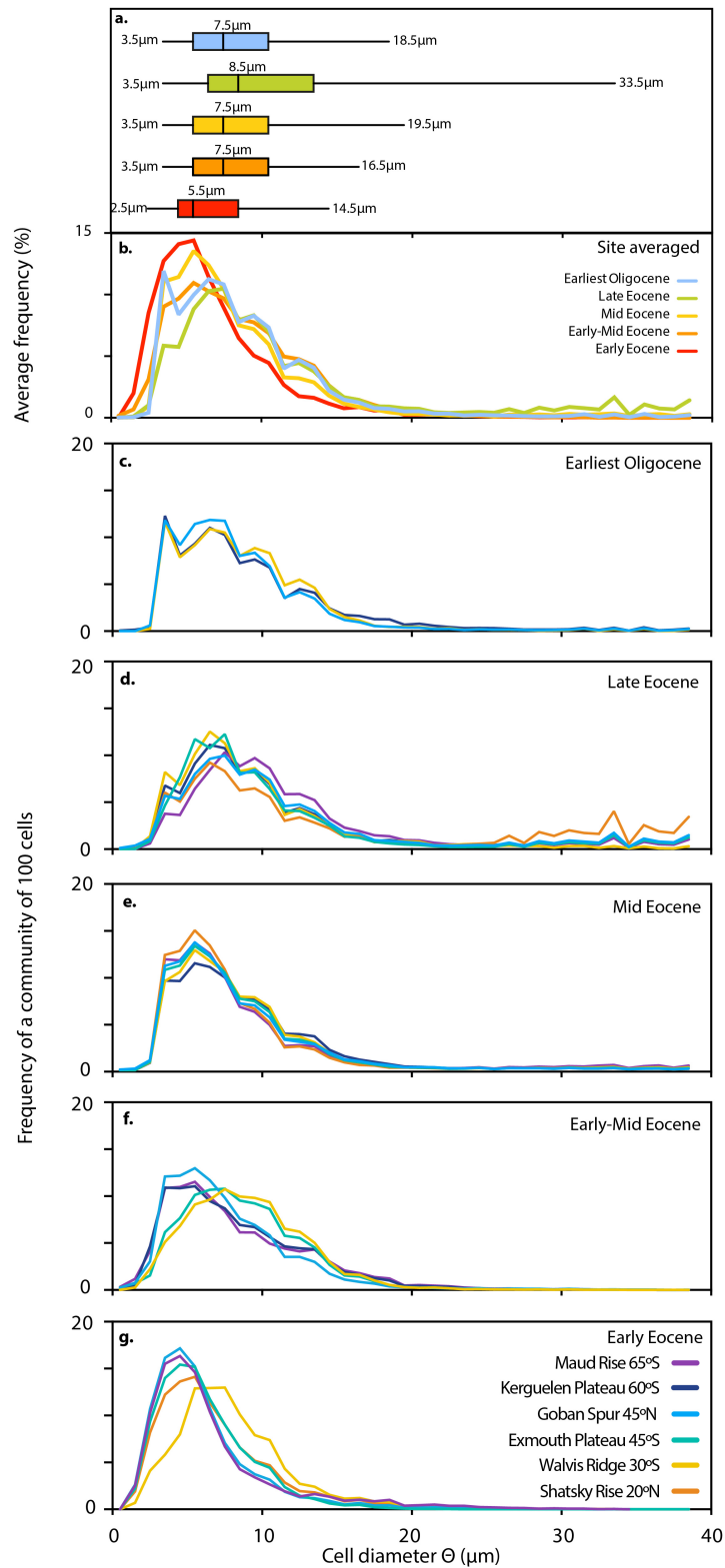
Figure 4.6: a. and **b.** Community cell size structure by reconstruction interval averaged across all six sites. Box and whisker plots showing the 25th to 75th percentiles of each distribution (box) with the 5th to 95th percentiles of the data (whiskers, labelled) and the median of the data (labelled). **c. - g.** Community cell size distribution by site during each reconstruction interval from **c.** youngest interval (earliest Oligocene) to **g.** oldest interval (Early Eocene).

size classes (5 to 25 μm) as *Coccolithus pelagicus* and *Chiasmolithus* constitute the largest proportion of community biovolume (15–70% and 43–74% respectively), despite their relatively minor abundance in the community (<13%). Conversely *Toweius*, the dominant component of all Early Eocene sites except Walvis Ridge, only represents ~10-20% of community biovolume. The biovolume structure of Early and Early-Mid Eocene communities is remarkably different to the very amplified profile in size classes >25 μm that characterises the Mid Eocene onwards. This predominantly results from the presence of *Reticulofenestra umbilicus*, which has substantially larger cell sizes (Figure 4.4) than other genera within the community. Their significantly larger cell biovolumes therefore dominate the biovolume of the community despite their relatively low abundances (<10%).

4.4   Discussion

4.4.1   Biogeographic patterns in community cell size structure as a function of community composition and abundance

Coccolithus pelagicus, *Reticulofenestra* and *Toweius* are cosmopolitan in latitudinal distribution, despite the inferred warm-water palaeoecology of *Coccolithus pelagicus* (Haq and Lohmann, 1976; Wei and Wise, 1990) and cool, mesotrophic preference of *Reticulofenestra* (Kalb and Bralower, 2012) and, to a certain extent, *Toweius* (Bralower, 2002; Gibbs et al., 2006b; Schneider et al., 2011). The wide biogeographic distribution and significant proportion of each community accounted for by *Coccolithus pelagicus*, *Toweius* and *Reticulofenestra* explains the broad consistency in community cell size structure across latitudes during each time interval (Figures 4.5 and 4.6).

The main features of the spatial and temporal variability in community cell size structure result primarily from the evolutionary transition from *Toweius*- to *Reticulofenestra*- dominated communities and the heterogeneous abundance of *Chiasmolithus* that is a more common presence at higher latitude sites. The coincident decline of *Toweius* and origination of *Reticulofenestra* during NP12 (our Early-Mid Eocene reconstruction interval; Appendix Figures A4.2 and A4.3) occurred as the initiation of global cooling prompted the cooling of sea surface temperatures (Zachos et al., 2008; Schneider et al., 2011). These conditions appear to have better suited to the cool, mesotrophic palaeoecology of *Reticulofenestra* rather than *Toweius*, which is proposed to have a tolerance for warmer, more oligotrophic conditions than *Reticulofenestra* (Kalb and Bralower, 2012). *Toweius* may therefore have been
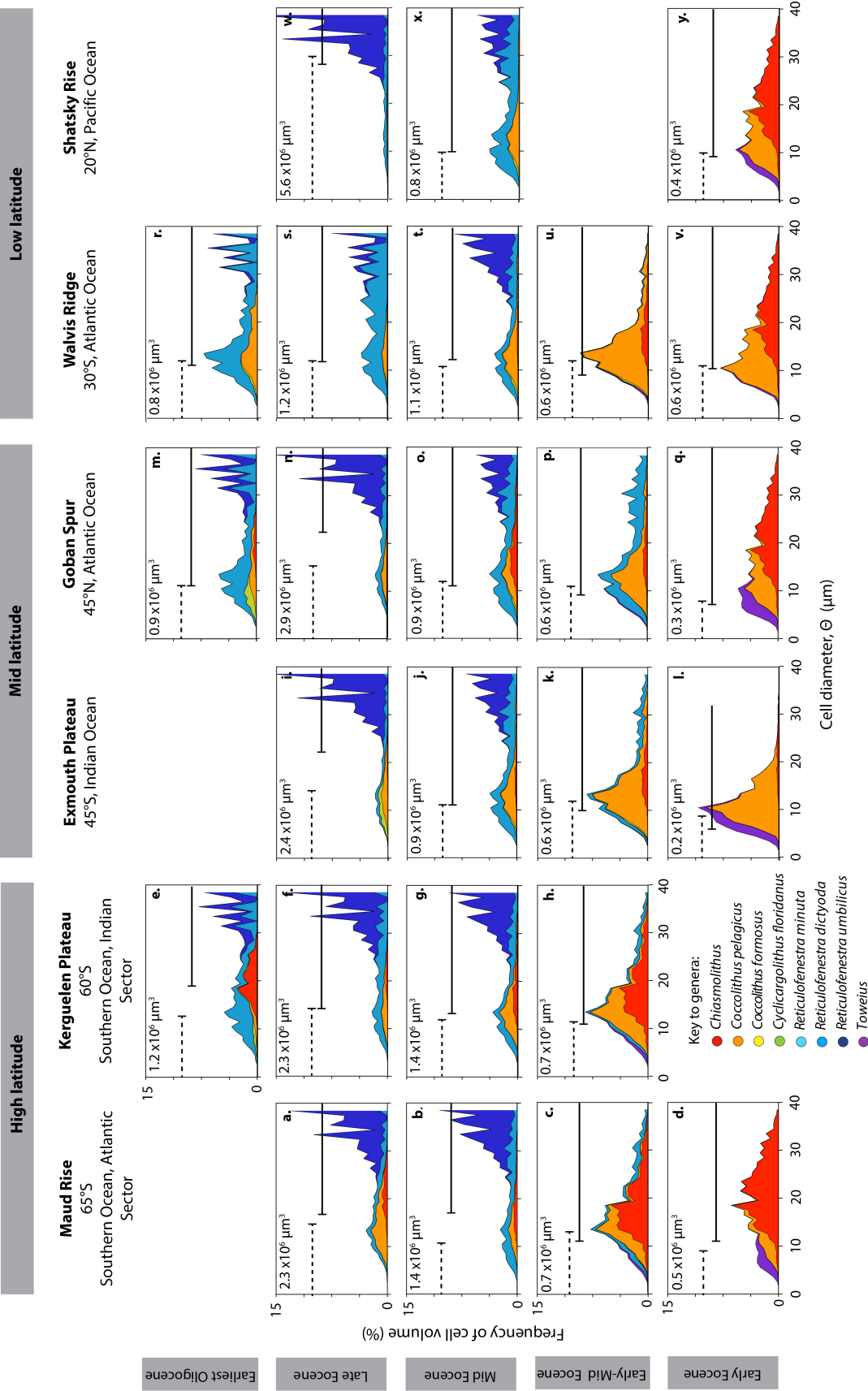
Figure 4.7 (opposite): Reconstructed community biovolume distributions at each site (left to right) and by reconstruction interval (top to bottom). Biovolume (μm^3) is calculated for each cell diameter size class and multiplied by frequency then displayed by original cell size class. High latitude sites **a. - d.** Maud Rise (65 °S) and **e. - h.** Kerguelen Plateau (60 °S). Mid-latitude sites **i.-l.** Exmouth Plateau (45 °S) and **m. - q.** Goban Spur (45 °N). Low latitude sites **r. - v.** Walvis Ridge (30 °S) and **w. - y.** Shatsky Rise (20 °N). See Figure 4.1 for map locations. Reconstruction intervals are shown from the youngest (earliest Oligocene or Late Eocene depending on site, top) to the oldest (Early Eocene, bottom). Early-Mid Eocene reconstruction is the interval across which *Toweius* and *Reticulofenestra* co-occur and is variable by site (see. Appendix Figure A4.2 and A4.3).

more competitive during the warmer Early Paleogene period then out-competed by *Reticulofenestra,* perhaps leading to the ecological marginalisation of *Toweius* prior to its extinction. The primary significance of the initial *Toweius-Reticulofenestra* transition for community cell size structure was an increased abundance of cells into the ~12-18 µm cell size classes followed by low abundances of *Reticulofenestra umbilicus* during the Mid Eocene onwards, dramatically increasing the cell size range of the community owing to its very large cell sizes (20-40 µm).

The progressive cooling of the marine environment during the Eocene is associated with decreased abundances of inferred warm-water *Coccolithus* and an overwhelming dominance of cool, mesotrophic *Reticulofenestra* at all latitudes. Additionally, *Chiasmolithus* is a persistent component of (southern) high latitude communities at Maud Rise and Kerguelen Plateau in agreement with the inferred cool to cold-water, mesotrophic preference of this genus (Wei and Wise, 1990; Firth and Wise Jr, 1992; Persico and Villa, 2004; Tremolada and Bralower, 2004; Persico and Villa, 2008; Villa et al., 2008). The additional occurrence of *Reticulofenestra umbilicus* at Maud Rise and Kerguelen Plateau results in a stronger temporal change in community cell size structure between the Early and Mid Eocene in the high latitudes compared to the mid- and low latitudes. By the Late Eocene, *Reticulofenestra umbilicus* has migrated even to low latitudes (Schneider et al., 2011; Figure 4.5), implying that sea surface temperatures were cooling even at lower latitudes and flattening cell size structure at all sites. Palaeoceanographic trends towards cooler and potentially more mesotrophic conditions through the Eocene therefore appear to drive changes in community composition that shift the cell size structure of coccolithophore communities towards an overall broader distribution of cells in the <20 µm size classes and increased cell size diversity in size classes >15 µm (Figures 4.5).

Post-Eocene-Oligocene transition communities indicate greater biogeographic differentiation between high and low latitudes by the earliest Oligocene (Figure 4.5). Low latitude Walvis Ridge has higher abundances of supposed warm-water *Coccolithus pelagicus* relative to other groups and mid-latitude Goban Spur has reduced abundances of *Coccolithus pelagicus* but higher abundances of *Cyclicargolithus floridanus*, inferred to have a temperate, eutrophic preference (Villa and Persico, 2006; Villa et al., 2008). Despite the difference in composition, the earliest Oligocene community cell size structure at Goban Spur and Walvis Ridge remains comparable due to the similar cell size distribution of these genera (Figure 4.4). The primary distinction in cell size structure therefore results from the presence of larger *Chiasmolithus* at Kerguelen Plateau. The insignificant abundance of *Reticulofenestra umbilicus* at all latitudes by the earliest Oligocene just prior to its extinction means that the overall community cell size structure is more similar to Mid Eocene communities than Late Eocene communities.

There is a generally-held assumption that modern phytoplankton communities are dominated by small species in stratified, tropical oligotrophic regions and increase in cell size towards the temperate and sub-polar regions as nutrient availability increases (Falkowski, 1998). However, coccolithophore-specific biogeographic patterns in community cell size structure are unfortunately virtually unknown for modern communities. Although the composition and relative abundance of some coccolithophore communities has been quantified through several oceanographic research programmes, for example the Atlantic Meridional Transect (AMT), robust cell size data for the majority of the ~200 extant modern coccolithophore species is lacking. This is particularly the case for the species-diverse families within the order Syracosphaerales, for species that are not obviously related to well-defined orders, and for holococcolith taxa, which are collectively likely to contribute significantly to both the diversity and absolute abundance of extant coccolithophore communities (e.g., Boeckel and Baumann, 2008). Systematic documentation of the mean and range of cell sizes observed within both field and cultured populations should therefore be a future priority in order to enable the cell size structure of modern coccolithophore communities to be compared to communities during different climate states such as the Paleogene greenhouse or during past intervals of rapid climate perturbation such as the PETM. Documenting species cell size for the entire diversity within modern coccolithophore communities would also enable a more comprehensive assessment of the proportion of community cell size structure that can be attributed to taxa

with a lower preservation potential, particularly non-placolith species (murolith, planolith, holococcolith morphologies), that are likely to be generally underrepresented in community-level coccolithophore studies. Additionally, datasets of cell size and coccosphere geometry across the full diversity of modern species would prove to be invaluable in accurately assessing current biogeographic patterns in biomass and calcite production and investigating how this may change if species distributions and abundances are altered by climate change.

4.4.2 Potential environmental drivers of evolution in coccolithophore community size and biovolume structure during the Eocene

The main features of the observed changes in community cell size structure over the long time interval considered here are driven most significantly by the addition of new species in the *Reticulofenestra* genus, resulting in a substantially greater cell size range than other genera. Some aspects of the temporal trends in our reconstructed community cell size structures are additionally driven by the varying abundances and biogeographic distributions of existing taxa with different cell size distributions. Environmental conditions, predominantly nutrients, temperature, light, and CO_2 can therefore affect community cell size structure through the regulation of species biogeographies and also by acting as evolutionary drivers that open new environmental niches that could promote speciation. This could facilitate out-competition of existing species by newer, larger species, such as observed in the extinction of *Toweius* and the origination of *Reticulofenestra*.

The size implications of the decline of *Toweius* and replacement by *Reticulofenestra* can be observed most obviously by contrasting the community biovolume structure between the Early and Late Eocene. In all reconstruction intervals, 80% of community cell size is smaller than 8 to 15 μm (Figure 4.5). However, an average of 80% of cell biovolume exists in cells greater than 10 to 20 μm (Figure 4.7). Cell biovolume is an important regulator of cellular carbon content and the cellular demand for nutrients, particularly nitrate and phosphate (Geider and La Roche, 2002). Cell biovolume also regulates diffusive uptake rates of micro- and macronutrients, as surface area to volume ratio decreases rapidly with cell size (Figure 4.8a). The dramatic expansion of community biovolume between the Early and Late Eocene into very large size classes that have correspondingly higher demands for resources could therefore suggest that the supply of nutrients and/or carbon was potentially greater in the Late Eocene compared to the Early Eocene. Is it therefore
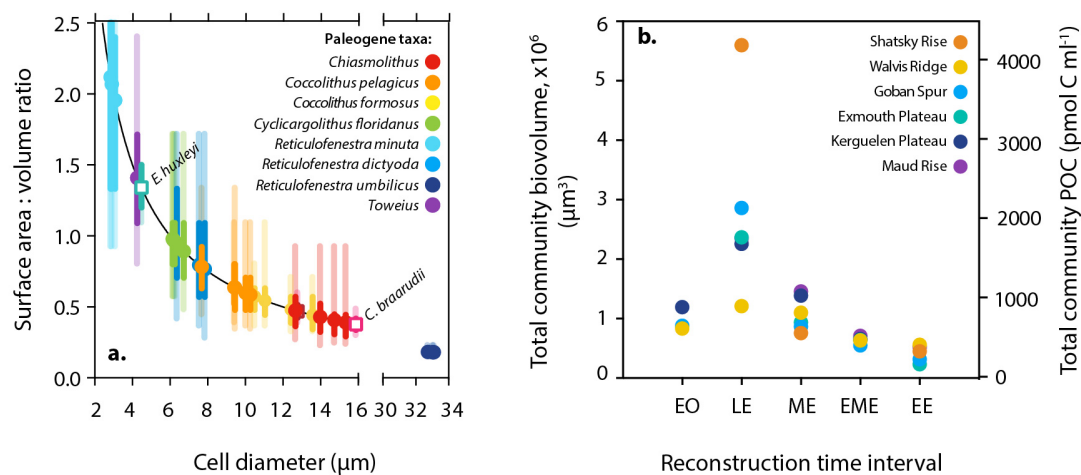
Figure 4.8: a. The surface area to volume ratio of the cell decreases with increasing cell size. Shown are the mean (dot), 25th to 75th percentile (solid line) and 5th to 95th percentile of the cell size of each genus used within the community reconstructions. For reference, the ranges of data observed experimentally in modern *E. huxleyi* and *Coccolithus* (Sheward et al., 2014) are also shown. **b.** The total biovolume and total biomass (organic carbon) of a hypothetical community of 1000 cells ml^{-1} is shown based on the biovolume structure of the community. Cellular carbon is calculated from biovolume following Menden-Deuer and Lessard (2000), where POC (pg C cell^{-1}) = 0.216 x volume$^{0.939}$. This is then multiplied by the frequency of cells in each size class. EO – Early Oligocene (most recent reconstruction), LE – Late Eocene, ME – Mid Eocene, EME - Early-Mid Eocene, EE – Early Eocene (oldest reconstruction interval).

reasonable to hypothesise that the changes we see in reconstructed community cell size and biovolume structure are driven by trends in the availability of CO_2 and/or nutrients caused by long-term climate changes during the Eocene and Oligocene?

4.4.2.1   Nutrient availability as a driver of abundance patterns and the evolution of new species sizes

Consider that each of our community cell size reconstructions represents an idealised sample of 1000 cells ml^{-1}. The theoretical total biovolume that would be produced by each community based on its cell size structure can then be evaluated and the biomass (organic carbon) that it represents calculated following the linear conversion of Menden-Deuer and Lessard (2000) (Figure 4.8b). The nutrient demand (organic nitrate and phosphate content) of the cell is assumed to vary proportionally with cellular carbon content, traditionally in the ratio 106 C: 16N: 1P (Geider and La Roche, 2002). Currently, published data for the elemental stoichiometry of modern coccolithophores is insufficient to determine whether coccolithophores generally deviate from this 'Redfield' ratio or whether there are strong

species-specific differences in stoichiometry. However, calculating community biomass for a given community cell size structure assuming Redfield stoichiometry allows us to initially explore whether the increase in community biovolume observed globally between the Early and Late Eocene would be reliant upon increased nutrient supply.

If we assume this idealised scenario of a community of 1000 cells ml^{-1}, total community biovolume in the Early and Early-Mid Eocene would be less than 1×10^6 μm^3 (Figure 4.8b), increasing by an order of magnitude at Shatsky Rise, Goban Spur and Exmouth Plateau by the Late Eocene due to the significant accumulation of biovolume of cells within size classes >25 μm. Total community biovolume then decreases to similar-to-Early Eocene values in the earliest Oligocene due to the diminished abundance of *Reticulofenestra umbilicus*. Organic carbon per ml^{-1} (for our idealised community of 1000 cells ml^{-1}) mirrors these trends, increasing from 2–4 nmol C ml^{-1} in the Early Eocene to Late Eocene values of ~20–42 nmol C ml^{-1} at mid- and low latitude sites Shatsky Rise, Goban Spur and Exmouth Plateau.

However, there are two end-member scenarios to be considered. Firstly, calculation of community biomass shown in Figure 4.8b assumes that the number of cells within the community remains constant but shifts towards larger cell sizes. This scenario would necessitate an increase in nutrient availability to accompany the increase in community cell biovolume as the cellular carbon, nitrate and phosphate demand of the entire community would have increased. A scenario of increasing nutrient supply between the Early and Late Eocene would also support the inclusion of very large taxa by the Late Eocene that otherwise might have been competitively excluded from the community due to the dependence of diffusive uptake on surface area to volume ratios (Figure 4.8b).

An alternative end-member scenario could assume that nutrient availability and nutrient utilisation by cells does not change through time. To maintain constant biomass production despite the change in cell biovolume structure that we observe between the Early and Late Eocene reconstructions, the number of cells within each community must decrease in order to support the increased nutrient demands of the larger cells. If all Early Eocene communities represent 1000 cells ml^{-1} and nutrients remain at constant concentrations, the shift towards larger cell biovolume structure (Figures 4.7 and 4.8b) would necessitate a dramatic decrease in community cell numbers by 50 to 90% by the Late Eocene, representing only 220 cells ml^{-1} at Maud Rise, 290 cells ml^{-1} at Kerguelen Plateau,

99 cells ml^{-1} at Exmouth Plateau, 110 cells ml^{-1} at Goban Spur, 462 cells ml^{-1} at Walvis Ridge, and 80 cells ml^{-1} at Shatsky Rise.

The same biomass production by a community of fewer, larger cells rather than a community of more abundant smaller cells is therefore one possible interpretation of the community biovolume increase that is observed between the Early and Late Eocene. A shift in the partitioning of community biomass from smaller to larger cell size classes could have implications for both ecology and trophic energy transfer, as zooplankton are thought to be size-selective grazers, with larger cells predated on by correspondingly larger zooplankton (Bergquist et al., 1985; Hansen et al., 1994). Communities of larger phytoplankton are therefore thought to be associated with shorter food chains, reducing the energy loss between trophic levels (Berglund et al., 2007; Finkel, 2007). In the context of biogeochemical cycling, the biomass of communities dominated by high abundances of small cells is rapidly recycled within the microbial loop whereas larger cell sizes are likely to contribute more to carbon export to the deep ocean (Michaels and Silver, 1988). Reduced efficiency of biomass recycling and greater export may subsequently be a consequence of a shift towards communities where biomass production is dominated by larger cells. However, the relevance of size-selective grazing and the biogeochemical implications of shift in community cell size structure within the cell size range of coccolithophores (~2 to 40 μm) rather than the cell size range across all phytoplankton groups (<2 to 2000 μm) remains speculative.

In reality, the most likely interpretation of the substantial increase in cell biovolume seen in these community reconstructions between the Early and Late Eocene will lie somewhere between these two end-member scenarios. Cell numbers within the community are highly unlikely to remain constant through time and cells of larger species could occur even if nutrient concentrations remained fairly constant providing they had more efficient nutrient utilisation strategies and/or lower nutrient demands than other, smaller species. Unfortunately, the specific ratios of cellular nitrate and phosphate to cellular carbon for fossil species must be assumed and there is currently little experimental stoichiometry data for modern coccolithophore species in different families from which to suggest potential differences between the nutrient demand of the different genera in these reconstructions.

What can be concluded is that nutrient availability is very likely to have been altered by the gradual but fundamental transition between the warm, high-CO_2 'greenhouse' of the

Early Eocene to the cool, lower CO_2 'icehouse' of the Early Oligocene (Zachos et al., 2008; Beerling and Royer, 2011; Norris et al., 2013). Stable isotope records suggest that there was a weak latitudinal temperature gradient during the Early Eocene that strengthened due to high latitude cooling as the Eocene progressed (Bijl et al., 2013; Sijp et al., 2014; Inglis et al., 2015). Deep-sea temperatures were also believed to have been very warm relative to the modern ocean during the Early Eocene (Lear et al., 2000; Pearson et al., 2007), such that the global overturning circulation was likely to have been weaker, followed by substantial deep-sea cooling throughout the ocean (Huber and Sloan, 2001; Inglis et al., 2015). These changes in ocean temperature conditions are likely to have altered water column stability, increased the strength of overturning circulation and wind-driven mixing (Caballero and Huber, 2013; John et al., 2014; Sijp and England, 2015). Enhanced nutrient delivery into the euphotic zone globally as the Eocene progressed is therefore a reasonable inference that would have supported the increase in biovolume and nutrient demand that is observed at all latitudes between the Early and Late Eocene.

4.4.2.2 CO₂ concentrations as a driver of the evolution of new species sizes

The above scenario assumes that the presence of larger cells in the community is limited by lower nutrient availability during the Early Eocene, the implication being that all coccolithophore cells would be larger if nutrients were available in sufficient concentrations. However, based on the data we have measured from fossil coccospheres for these reconstructions, a clear cell size diversification is really only observed within the *Reticulofenestra* genus. All other genera in these reconstructions arguably remain fairly consistent in size, even though the inferred mesotrophic palaeoecologies of *Chiasmolithus*, *Toweius* and *Cyclicargolithus floridanus* (Bralower, 2002; Tremolada and Bralower, 2004; Gibbs et al., 2006b; Persico and Villa, 2008; Villa et al., 2008) would suggest that higher nutrient availability would be advantageous. Is there then a second environmental driver of the evolution of larger species that might explain the cell size expansion within *Reticulofenestra* but not in other genera?

It has been suggested that CO_2 concentrations can exert an evolutionary selective pressure on coccolithophore cell size (Henderiks and Pagani, 2007; Henderiks and Pagani, 2008; Pagani et al., 2011; Hannisdal et al., 2012; Bolton and Stoll, 2013) because the diffusive uptake capacity of cells is size-dependent. Larger cells are therefore theoretically disadvantaged compared to smaller cells under lower CO_2 conditions, which is broadly

supported by coccolith length evidence that coccolithophores were larger during the higher pCO_2 conditions of the Paleocene and Eocene compared to the lower pCO_2 conditions of the Pliocene and Pleistocene (Hannisdal et al., 2012). Certainly the largest cells in *Reticulofenestra* and *Chiasmolithus* observed as fossil coccospheres (20 to 30 μm; **Chapter 2**) and calculated from coccosphere geometry (up to 40 μm; Figure 4.4) are not cell sizes typically reached by modern placolith species (e.g., Figure 3.1). We might therefore expect that community cell size would have been at its largest during the Early Eocene under higher $CO_{2(aq)}$ and other dissolved carbonate ions for photosynthesis (and calcification) relative to the Late Eocene and Early Oligocene. However, the modest increases in the abundance of cells within the 10-20 μm size classes and a diversification into >20 μm size classes through the Eocene translates to substantial increases in community biovolume structure as atmospheric CO_2 concentrations are falling. If global CO_2 concentrations were an important driver of macroevolutionary change in coccolithophore cell size, we would more likely expect to see a change in the range of cell sizes within the majority of genera rather than changes restricted to a single genus.

The degree of cell size evolution in *Reticulofenestra* relative to other key genera could therefore suggest that it has specific physiological advantages over other coccolithophores that greatly increase its competitiveness under a range of environmental conditions. Physiological strategies could include a greater efficiency of carbon and nutrient utilisation in larger cells that enables them to remain competitive whilst also having a greater surface area to volume ratio. For example, the evolution of carbon acquisition strategies to reduce the dependence of larger cells on diffusive $CO_{2(aq)}$ uptake would be an advantageous adaptation if not possessed by other families. However, a recent study suggests that carbon acquisition strategies in coccolithophores may not have evolved until as recently as the Late Miocene, 5-7 Ma (Bolton and Stoll, 2013). Alternatively, *Reticulofenestra* may have had a lower cellular nitrate and/or phosphate requirement relative to cell volume enabling it to tolerate lower nutrient conditions than other species of a similarly large size. Whilst little species-specific stoichiometry data exists for modern coccolithophores, some experimentally-derived particulate organic carbon (POC) and particulate organic nitrate (PON) ratios in *Emiliania huxleyi* and *Gephyrocapsa oceanica*, modern descendents of the *Reticulofenestra* lineage, suggest that these taxa require less PON per unit POC than the Redfield ratio (Ho et al., 2003; Kaffes et al., 2010; Jones et al., 2013). In contrast, *C. braarudii* may approach Redfield ratios of POC:PON as pCO_2 increases (Rickaby et al.,

2010). Finally, the notable range in cell sizes observed in *Reticulofenestra* (Figure 4.4; **Chapter 2**) may additionally suggest extensive genetic diversity within this genus, similar to their modern descendent *E. huxleyi* (Read et al., 2013). This may have enabled a greater degree of environmental specialism and continual microevolution in response to progressively changing environmental conditions that were not achieved to the same degree in other genera.

4.5   Conclusions

Coccolithophore community cell size structure is reconstructed for the first time between the peak greenhouse conditions of the Early Eocene and the newly-established icehouse conditions of the Early Oligocene. The trend towards the inclusion of larger cells within all communities between the Early and Late Eocene can be primarily attributed to the *Reticulofenestra* genus, which becomes the dominant taxa within our community cell size reconstructions from the Mid Eocene onwards. Substantial increases in relative community biovolume and biomass result from this transition in community composition, which would indicate an accompanying dramatic decrease in community cell numbers or, alternatively, a concurrent increase in nutrient availability and/or utilisation. Certainly, an increase in nutrient availability is a plausible hypothesis for this interval of the Paleogene and is supported by the species composition of the communities, including *Reticulofenestra*, *Chiasmolithus* and *Cyclicargolithus floridanus* that are inferred to have mesotrophic palaeoecologies. The appearance of larger-celled species within *Reticulofenestra* also suggests that the environment must have had sufficient nutrient concentrations to support the high nutrient demands of larger cells. Shifts in the partitioning of biomass production from smaller to larger size classes, as seen between the Early and Late Eocene, may have consequences for the efficiency of carbon export and the transfer of energy to higher trophic levels. Trends in coccolithophore community size structure therefore provide novel insights into the ecological and evolutionary response of communities interacting with bottom-up controls on cellular-level physiological requirements, abundance and biogeographic distribution.

Chapter 5:

Conclusions and future perspectives

5.1 Conclusions

In this thesis I have investigated how the coccosphere geometry of coccolithophores can be used as a valuable tool for exploring the response of coccolithophore cells, species, and communities to environmental change.

5.1.1 Coccosphere geometry as a recorder of cellular-level physiology

Substantial variability in the relationship between cell and coccosphere size, coccolith length and the number of coccoliths per cell in fossil coccolithophores is documented in **Chapter 2**. Within the range of coccosphere geometry observed in species-specific populations, how can variability in coccosphere geometry be interpreted? This research has shown that the cell size and number of coccoliths per cell are intimately linked with cellular growth and physiology, which has proven to be invaluable in developing a growth proxy for fossil coccolithophores (**Chapter 3**). I present new data from culture experiments on four important modern coccolithophore species with long evolutionary records – *Calcidiscus leptoporus*, *C. quadriperforatus*, *Coccolithus braarudii* and *Helicosphaera carteri* – that show that, across several taxonomic orders of coccolithophores, relationships between coccosphere size and number of coccoliths per cell are strongly regulated by growth phase, specifically whether a population is able to maintain exponential growth. Within the range of coccosphere geometry specific to each species, populations that are dividing exponentially have, on average, smaller cells with fewer coccoliths per cell compared to populations no longer able to maintain exponential rates of growth. The crucial features of coccosphere size and number of coccoliths per cell can be clearly identified and measured in fossil coccospheres. Species exhibiting smaller cells with fewer coccoliths within fossil communities can therefore be interpreted as likely to be experiencing intervals of more optimal growth conditions than during periods where within-species coccosphere size and number of coccoliths per cell is increased. Assessing the coccosphere geometry response to controlled laboratory conditions has therefore furthered our understanding of the physiological regulation of coccosphere geometry that can be directly applied to fossil data as a valuable new tool for exploring the impact of past environmental changes on coccolithophore growth in the geological record.

5.1.2　The role of cell size in coccolithophore responses to Paleogene environmental change

Through this research I have collected an unprecedented quantity of coccosphere geometry measurements in many Paleogene taxa. From this data, the cell size structure of fossil coccolithophore communities can be reconstructed for the first time to explore how the physiological response of species to environmental change is manifested at the level of communities. The cell size structure of coccolithophore communities between the Early Eocene and Early Oligocene trends towards larger mean cell sizes by the Late Eocene, which can primarily be attributed to the ecological replacement of the small, cosmopolitan coccolithophore genus *Toweius* by the highly size-diverse genus *Reticulofenestra*. The accompanying diversification of coccolithophore communities into larger cell size classes implies that increased nutrient availability is a plausible consequence of the long-term cooling of the Eocene and Oligocene, facilitating the size evolution of larger cells with correspondingly higher nutrient requirements. Interestingly, the appearance of larger cells is largely restricted to the genus *Reticulofenestra*, perhaps suggesting that this genus possesses specific physiological strategies that increase its competitiveness and enabled progressive environmental specialism under continually changing environmental conditions.

Given the important regulation of cellular nutrient requirements and nutrient uptake rates by cell volume, community cell size evolution in response to changes in background nutrient availability are not unexpected. However, the broad consistencies in overall community cell size through this interval of considerable climatic upheaval and the inconsistent cell size response of different genera suggest that there is considerable scope for species-specific adaptation strategies to environmental change on longer timescales.

5.2　Future directions of research

The fossil coccosphere data presented in this thesis presents the opportunity to explore other avenues of research that preliminary data suggests will be highly informative but that I have not yet investigated in detail. Here, I highlight just two examples of future research that can be addressed using this dataset.

5.2.1 Macroevolutionary trends in coccosphere geometry and cell size

The extensive coccosphere geometry record collected for *Toweius*, *Reticulofenestra* and *Coccolithus*, as well as many other species, throughout the Paleogene enables traditional assemblage approaches to species evolution to also be considered from a cellular perspective. The species *Coccolithus pelagicus* is particularly intriguing, as it is one of the only species to have existed throughout the entire Paleogene and it has done so with little morphological variability. From my data, the precise interrelationship between cell size, coccolith length and number of coccoliths per cell (C_N) in *C. pelagicus* is variable through the Paleogene but exhibits no overall systematic trends in coccosphere geometry (Figure 5.1). This is in stark contrast to the Noelaerhabdaceae *Toweius-Reticulofenestra* lineage that undergoes dynamic speciation and extinctions and substantial diversification in size over the same period (**Chapter 4**). The continued existence of *Coccolithus* in modern oceans and its persistence over the last ~66 Ma is testament to its ability to weather both rapid and long-term climate variability but the overall similarities that I see in coccosphere geometry throughout the dataset could imply that it has different adaptation strategies relative to other species.

The coccosphere geometry record of *Coccolithus* and other taxa thereby provide additional means by which to investigate micro- and macroevolutionary trends in coccolithophore species. Firstly, coccosphere geometry may be a useful tool to refine the taxonomic classification of fossil *Coccolithus* (and other species), which shows significant within species variability in coccosphere geometry (Figure 2.10b) that is likely to represent multiple 'cryptic species' that are difficult to distinguish based on coccolith morphologies. Further taxonomic classification of *Coccolithus* and other species based on coccosphere geometry data and the potential to take detailed measurements of coccolith morphology (coccolith length:width ratios, number of elements, central area size and any axial cross features) using scanning electron microscopy of the same samples could prove highly effective at assessing whether spatial and temporal patterns in cell size result from within-species/morphospecies size trends or ecological replacement of species/morphospecies of different sizes.

Secondly, the coccosphere geometry proxy for growth phase developed in **Chapter 3** allows records of coccosphere size and number of coccoliths to be interrogated for likely intervals where *Coccolithus* was experiencing more or less favourable environmental
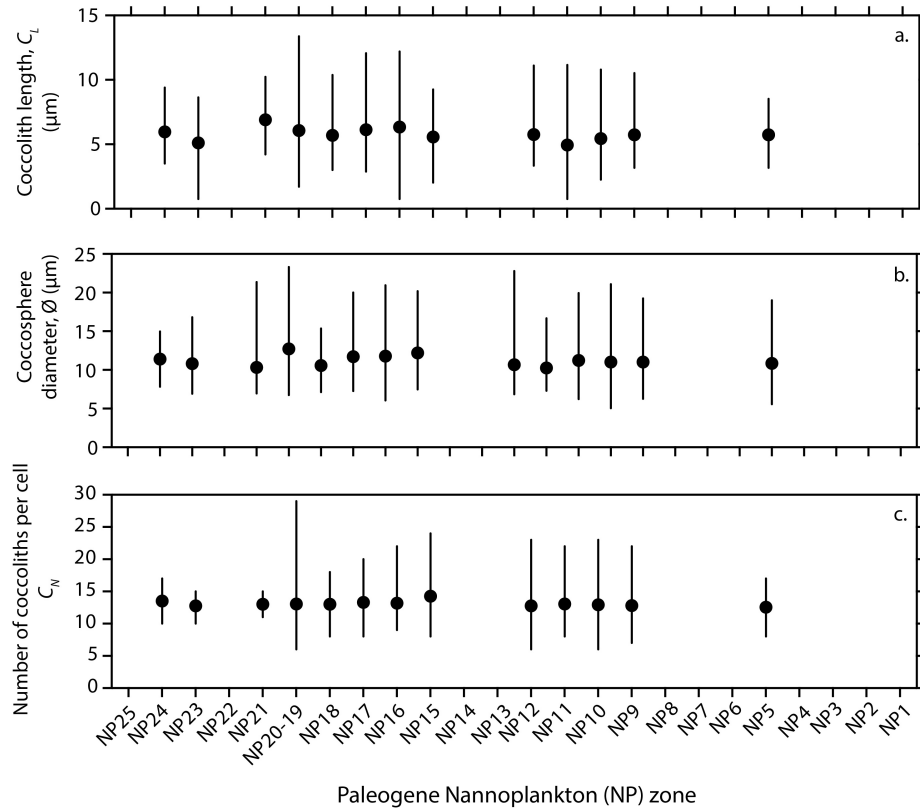
Figure 5.1: Coccosphere geometry in *Coccolithus* from the samples studied in this thesis. Data is combined within Paleogene Nannoplankton (NP) zones of Martini (1971).

conditions for growth. An example of this is shown for *Coccolithus* at Labrador Sea Site ODP 647A during the Mid-Late Eocene from coccosphere data presented in this study (Figure 5.2). The growth proxy further developed in this thesis from Gibbs et al. (2013) enables us to estimate intervals of less favourable growth conditions based on the number of coccospheres that have a C_N that is characteristic of non-exponential growth ($C_N > 16$ for *Coccolithus* based on the experimental evidence presented in **Chapter 3**). For example, two Labrador Sea samples are conspicuous for their high proportion (30-40%) of coccospheres with $C_N > 16$ that may indicate slowed rates of cell division at this time. Whilst this is a very preliminary perspective, it demonstrates how the extensive dataset of coccosphere geometry presented here can be used to investigate changes in growth that may be associated with environmental variability on longer timescales, as explored during the Paleocene-Eocene Thermal Maximum in Gibbs et al. (2013) and O'Dea et al. (2014). Additionally, the fossil coccosphere sizes observed in the Paleogene are smaller than modern *Coccolithus pelagicus* and *C. braarudii* (shown for comparison in Figure 5.2), which are
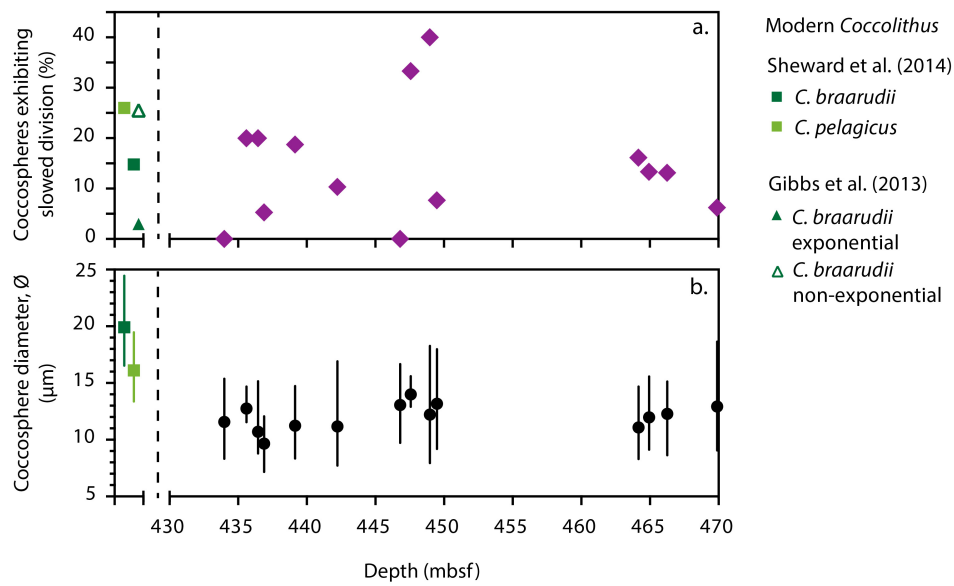
Figure 5.2: The record of fossil *Coccolithus* coccosphere geometry at Labrador Sea Site ODP 647A (data from this thesis) during NP16 to NP18. **a.** The proportion of coccospheres exhibiting number of coccoliths (C_N) typically identified with cells experiencing non-exponential growth (C_N >16; Chapter 3) and **b.** the mean and 5th to 95th percentile of coccosphere size within the same sample. Shown for comparison (green symbols) is the proportion of cells with C_N>16 in exponentially growing cultures of modern *Coccolithus braarudii* (dark green) and *Coccolithus pelagicus* (light green) and non-exponentially growing cultures of *C. braarudii* (dark green unfilled triangle) and their associated coccosphere size from Sheward et al. (2014) and Gibbs et al. (2013).

restricted primarily to the high latitude and temperate Atlantic Ocean respectively (Ziveri et al., 2004). It would therefore be interesting to investigate the coccosphere geometry of *Coccolithus* with new data through the Neogene 'icehouse' to explore whether coccosphere geometry can provide valuable insights in the evolution and changing ecology of this taxon.

Whilst I have discussed *Coccolithus* as an interesting starting point, this approach can be applied to scrutinise linkages between coccosphere geometry and growth phase, environmental variability and evolution in other species or lineages. Combining modern cellular physiological regulation of coccosphere geometry with the coccosphere geometry of fossil species can therefore provide valuable insights into species responses to environmental variability from which we may be able to infer their specific evolutionary strategies that could elude to the potential response of different coccolithophore species to future climate change.

5.2.2   Cellular calcification

The physiology of coccolithophore calcification has received widespread attention in recent years as researchers attempt to understand the sensitivity of the calcification process to future 'ocean acidification' scenarios, with the majority of evidence coming from shorter-term laboratory experiments that identify strain-specific responses to tightly controlled parameters (e.g., Müller et al., 2010; Bach et al., 2011; Langer and Bode, 2011; Lohbeck et al., 2014; Schlüter et al., 2014). To fully understand the potential response of coccolithophores to complex future climate change it is necessary to consider the cellular-level physiology of calcification and species-specific calcification alongside population- to ecosystem-level responses (Ridgwell et al., 2009). Fossil coccospheres are a unique archive of biotic responses to different magnitudes and timescales of environmental change that offer an exciting avenue into understanding cellular calcification in fossil coccolithophore populations.

Coccospheres provide a record of cellular calcite and cellular organic carbon quotas, providing a new means to estimate cellular particulate inorganic carbon (PIC) and cellular organic carbon (POC) that can be directly estimated from my coccosphere geometry data. This is based on the assumption that cell size is directly proportional to organic carbon content (Menden-Deuer and Lessard, 2000) and by calculating the inferred calcite content of the coccoliths making up the coccosphere (Young and Ziveri, 2000). Preliminary estimates shown in Figure 5.3 based on the fossil and modern coccosphere data presented in this thesis reveal that cellular calcite relative to cellular organic carbon is highly variable both within and between different species, which reflects the diversity of fossil coccosphere geometries that have been identified throughout this thesis. Although many modern coccolithophore species are held in culture collections, the majority of experimental studies investigating calcite in coccolithophores concern only *Emiliania huxleyi* and, increasingly, *Coccolithus* and *Calcidiscus* species. In contrast, the fossil record of coccospheres includes more than 40 species with the potential to greatly advance our understanding of the remarkable diversity in coccolithophore cellular calcite.

An important finding of **Chapter 3** is that the regulation of number of coccoliths per cell by growth phase can result in changes in calcite production (calcite per cell multiplied by growth rate) that potentially far outweigh changes in calcification that result from changes in coccolith calcite. Changes in the growth phase of different species in the
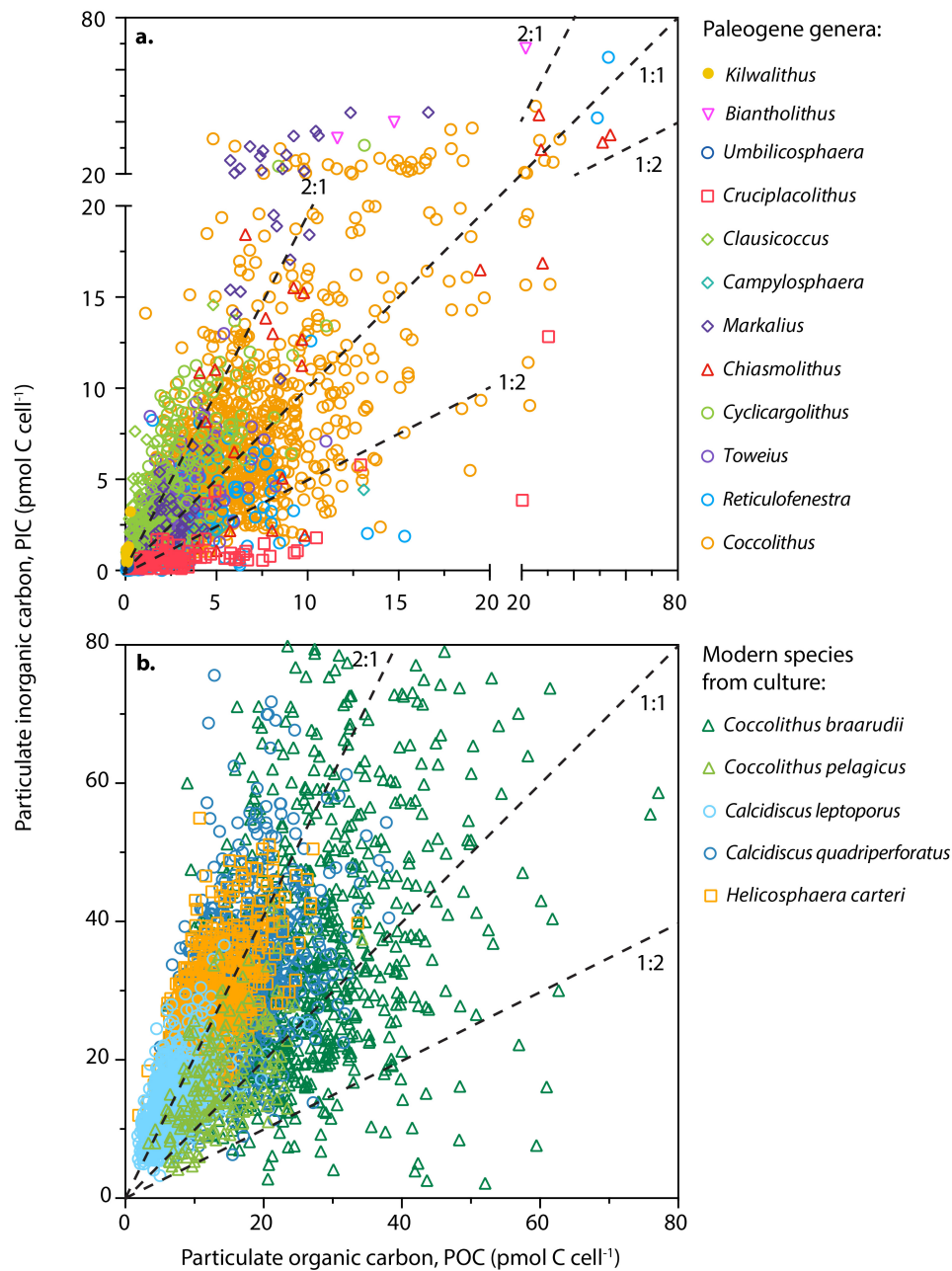
Figure 5.3: Particulate organic carbon (POC) and inorganic carbon (PIC) calculated for each coccosphere. **a.** For fossil coccospheres of Paleogene age (Chapter 2) and **b.** for coccospheres of the five modern species discussed in Chapter 3. Note the different axes of the two figures. POC was calculated from cell diameter using Menden-Duer and Lessard (2000), where POC (pmol C cell^{-1}) = (0.216 x cell volume $^{0.939}$)/12. PIC is calculated from the number of coccoliths per cell (C_N) multiplied by coccolith calcite, which can be calculated from coccolith length following Young and Ziveri (2000) - coccolith calcite = 2.7 x C_L^3 x Ks. Ks is a shape factor that estimates species-specific coccolith thickness and cross-sectional shape. Here I use Ks values of 0.06 for *Coccolithus* (fossil and modern) and Ks = 0.08 for *Calcidiscus* and *Helicosphaera* based on Young and Ziveri (2000). Shape factors for the other taxa were estimated based on coccolith morphology: Ks = 0.08 in *Cyclicargolithus*, Ks = 0.07 for *Markalius* and *Biantholithus*, Ks = 0.06 in *Chiasmolithus*, Ks = 0.055 in *Toweius*, Ks = 0.3 in *Cruciplacolithus*, *Clausicoccus*, *Campylosphaera* and *Biscutum*, and Ks = 0.015 in *Umbilicosphaera*. Dashed lines show PIC:POC ratios of 1:1, 2:1 and 1:2. At a PIC:POC ratio of 1:1, cellular inorganic and organic carbon are equal.

community as nutrient availability varies could therefore result in considerable changes in calcite production through time (Figure 3.6). Combined with cellular calcite estimates from fossil coccospheres, the growth phase proxy (**Chapter 3**) enables this to be explored in geological time, which was done for the first time for *Coccolithus* and *Toweius* during the PETM (O'Dea et al., 2014) but not yet during different time intervals or with other taxa.

This cellular perspective on cellular calcite and calcite production in the fossil records provides the tools needed to explore species-specific roles in community-level calcite production, including intriguing questions about how relative growth rates, abundances and cellular calcite between different species determines the dominant calcite producer in the community. This has been explored in modern field populations using cellular calcite data collected for this study from modern *Coccolithus pelagicus* coccospheres (Sheward et al., 2014) to show that it is the major source of calcite in the Iceland Basin relative to *Emiliania huxleyi*, despite being present in lower relative abundances, because of the substantially greater calcite per coccosphere of *Coccolithus* (Daniels et al., 2014). This coccosphere data can additionally be used to show how changes in community composition can impact community calcite production and its ratio with organic carbon production. This in turn could have important implications for the role of coccolithophores in the biogeochemical cycling of carbon.

The coccosphere geometry data presented for both fossil and modern coccolithophores in this thesis and the development of a proxy for growth phase in the fossil record therefore have the potential to provide unprecedented insights into rates of calcite production through time by different species in the community. Coccosphere geometry is also clearly a very useful approach for considering calcite production in modern species. The integration of modern and fossil coccosphere data and approaches therefore has great potential to further explore fundamental questions about coccolithophore calcification and its response to climate change in the future.

Appendices

Taxonomic Appendix

Order ISOCHRYSIDALES Pascher, 1910

Family PRINSIACEAE - Hay & Mohler, 1967 emend. Young & Bown, 1997.

Toweius callosus - Perch-Nielsen, 1971.

Toweius eminens – (Bramlette & Sullivan, 1961) Perch-Nielsen, 1971.

Toweius gammation – (Bramlette & Sullivan, 1961) Romein, 1979.

Toweius occultatus – (Locker, 1967) Perch-Nielsen, 1971.

Toweius pertusus - (Sullivan, 1965) Romein, 1979.

Toweius rotundus - Perch-Nielsen et al., 1978.

Toweius serotinus – Bybell & Self-Trail, 1995.

Family NOELAERHABDACEAE - Jerkovic, 1970 emend. Young & Bown, 1997

Reticulofenestra dictyoda - (Deflandre in Deflandre & Fert, 1954), Stradner in Stradner & Edwards, 1968.

Reticulofenestra minuta - Roth, 1970.

Reticulofenestra umbilicus - (Levin, 1965) Martini & Ritzkowski, 1968. Size >14 μm.

Reticulofenestra wadeae - Bown, 2005.

Reticulofenestra daviesii - (Haq 1968) Haq, 1971.

Reticulofenestra lockeri - Müller, 1970.

Reticulofenestra westerholdii – Bown and Dunkley Jones, 2012.

Cyclicargolithus floridanus - (Roth & Hay, in Hay et al., 1967) Bukry, 1971.

Cyclicargolithus luminis - (Sullivan, 1965) Bukry, 1971.

Reticulofenestra bisecta - (Hay et al., 1966) Roth, 1970.

Order COCCOLITHALES Schwarz, 1932.

Family COCCOLITHACEAE - **Poche, 1913 emend. Young & Bown, 1997.**

Kilwalithus cribum – Bown, 2010.

Coccolithus pelagicus - (Wallich, 1877) Schiller, 1930.

Coccolithus eopelagicus - (Bramlette & Riedel, 1954) Bramlette & Sullivan, 1961.

Coccolithus foraminis – Bown 2005.

Coccolithus formosus – (Kamptner, 1963) Wise, 1973.

Coccolithus latus – Bown, 2005.

Coccolithus pauxillus - (Bown, 2005) Bown, 2010.

Campylosphaera dela – (Bramlette & Sullivan, 1961) Hay & Mohler, 1967.

Campylosphaera eroskayi - (Varol, 1989) Bown, 2005.

Chiasmolithus bidens – (Bramlette & Sullivan, 1961) Hay & Mohler, 1967.

Chiasmolithus eoaltus – Persico & Villa, 2008.

Chiasmolithus expansus – (Bramlette & Sullivan, 1961) Gartner, 1970.

Chiasmolithus nitidus - Perch-Nielsen, 1971.

Chiasmolithus oamaruensis – (Deflandre, 1954) Hay et al., 1966.

Chiasmolithus solitus - (Bramlette & Sullivan, 1961) Locker, 1968.

Cruciplacolithus asymmetricus – van Heck & Prins, 1987.

Cruciplacolithus edwarsii – Romein, 1979.

Cruciplacolithus frequens – (Perch-Nielsen, 1977) Romein, 1979.

Cruciplacolithus latipons – Romein, 1979.

Cruciplacolithus primus – Perch-Nielsen, 1977.

Clausicoccus fenestratus - (Deflandre & Fert, 1954) Prins 1979.

Clausicoccus subdistichus - (Roth & Hay in Hay et al., 1967) Prins, 1979.

Clausicoccus vanheckiae - (Perch-Nielsen, 1986) de Kaenel & Villa, 1996.

Family CALCIDISCACEAE - **Young & Bown, 1997.**

Cryptococcolithus mediaperforatus – (Varol, 1991) de Kaenel and Villa, 1996.

Umbilicosphaera bramlettei – (Hay & Towe, 1962) Bown et al., 2007.

Umbilicosphaera protoannulus – (Gartner, 1971) Young & Bown 2014.

Nannolith families *incertae sedis.*

Family BRAARUDOSPHAERACEAE – Deflandre, 1947

Braarudosphaera bigelowii – (Gran & Braarud, 1935) Deflandre, 1947.

Nannolith genera incertae sedis.

Biantholithus australis – Steinmetz & Stradner, 1984.

Goniolithus fluckigeri – Deflandre, 1957.

Mesozoic survivors sensu – Young & Bown, 1997.

Family BISCUTACEAE

Biscutum braloweri – Bown et al., 2014.

Markalius apertus – Perch-Nielsen, 1979.
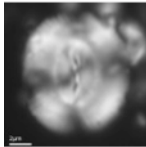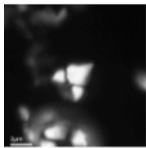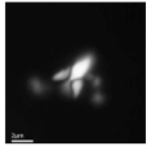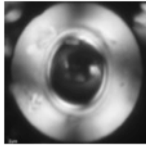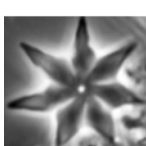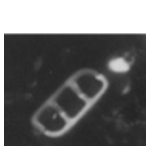
Markalius inversus - (Deflandre and Fert 1954) Bramlette and Martini 1964.
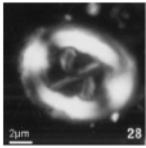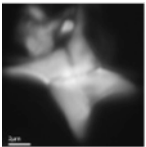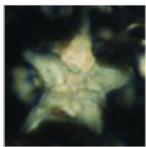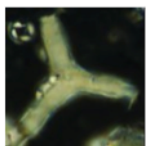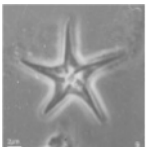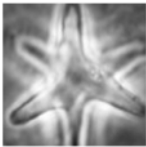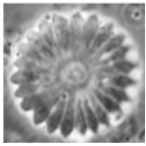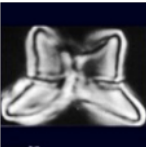
Appendix Chapter 2

Table A2.1: List of samples at each site from which coccosphere geometry was collected during this study. See Table 2.1 for site descriptions.

Labrador Sea	Bay of Biscay	Lodo Gulch	Bass River		Wilson Lake
647A 49-1 137-139cm	14 3 99cm	LO 03 27 47	BR 100	BR 25	WL 318/5
647A 49-2 64-66cm	14 4 20cm	LO 03 27 10	BR 103	BR 28	WL 338/4
647A 49-3 45-47cm	14 4 3cm	LO 03 27 0	BR 110	BR 30	WL 352/37
647A 49-5 108-110cm	14 4 50cm	LO 03 27 130	BR 73	BR 31	WL 356/85
647A 51-1 7-9cm	14 4 9cm	LO 03 27 160	BR 74	BR 34	WL 319/75
647A 46-4 85-87cm	14 1 105cm	LO 03 28	BR 77	BR 35	WL 321/16
647A 46-5 91-93cm	14 1 4cm	LO 03 32	BR 78	BR 38	WL 326/21
647A 46-6 92-94cm	14 2 55cm	LO 03 14	BR 81	BR 40	WL 329/54
647A 46-7 17-19cm	14 3 0cm	LO 03 21	BR 82	BR 42	WL 335/27
647A 47-3 107-109cm	14 3 20cm		BR 84	BR 44	WL 339/35
647A 47-3 30-32cm	14 3 50cm		BR 85	BR 49	WL 343/9
647A 47-4 147-150cm	14 3 59cm		BR 86	BR 51	
647A 47-4 97-99cm			BR 87	BR 57	
647A 46-2 29-31cm			BR 88	BR 61	
647A 46-3 8-10cm			BR 89	BR 67	
647A 46-2 114-116cm			BR 90	BR 70	
647A 46-1 19-21cm			BR 91	BR 72	
647A 32-3 13cm			BR 92	BR 10	
647A 34-1 104cm			BR 94	BR 12	

Mississippi	Puerto Rico	Trinidad	Tanzania	Australia	New Zealand
Miss BSWID BW 1.12	PR 139/9	PP07/T6	TDP 27 7/1 46-48cm	COLN 51	HB 205
	PR 139/14		TDP 27 6/1 56cm		HB 215
	PR 139/17		TDP 37 6/1 17cm		HB 245
			TDP 14 7/1 80cm		
			TDP 14 8/3 67-69cm		
			TDP 14 11/2 20-22cm		
			TDP 14 6/1 40-42cm		
			TDP 14 4/1 19-20cm		
			TDP 8 1/1 30cm		
			TDP 3 12/1 62cm		
			TDP 3 12/1 62cm		
			TDP 3 4/3 52-53cm		
			TDP 6 8/1 62cm		
			TDP 6 8/1 63cm		
			TDP 9/1 85cm		
			TDP MPC 25/1 62cm		
			TDP MPC 25/2 62cm		
			TDP LIN 99-17		
			TDP 12 26/2 62cm		
			TDP RAS 99-42		

Figure A2.2: Marker taxa and descriptions for Paleogene nannoplankton zone boundaries, following Martini (1971). Images and text description taken from Nannotax3 web database (Young et al., 2014).

Zone
NN1
NP25
NP24
NP23
NP22
NP21
NP20-19
NP18
NP17

LO *Reticulofenestra bisecta* **>10μm**

Large to very large (>10 μm) reticulofenestrid coccoliths with a solid central plug.

LO *Sphenolithus distentus*

Small with narrow, tapering, typically monocrystalline spine and basal 'feet' that encroach on the spine; the angle between the top and bottom surface of the feet is up to 90° and the basal W/H ratio is 1.7-2.5.

FO *Sphenolithus ciperoensis*

Small with relatively large basal 'feet' (~half the height of the sphenolith and basal W/H <1.7) with low spine that typically appears monocrystalline, and at 45° a birefringent structure passes between the 'feet'.

LO *Reticulofenestra umbilicus* **(low-mid latitudes)**

Very large (>14 μm) elliptical reticulofenestrids, with delicate proximal nets that cannot be resolved in light microscope or are missing.

LO *Coccolithus formosus*

Large circular Coccolithus with narrow central area.

LO *Discoaster saipanensis*

Discoasters with 5-8 (normally 6 or 7) straight or curved rays joined through half their length and which then taper to a point. A central stem and distinct radial sutural ridges and depressions are visible in some specimens.

FO *Isthmolithus recurvus*

Narrowly elliptical to oblong (or parallelogram-like), relatively high muroliths with two parallel transverse bars.

FO *Chiasmolithus oamaruensis* **(common)**

Large to very large *Chiasmolithus* with broad centro-distal cycle, wide central area and straight, narrow, symmetrical diagonal bars, which join at a relatively acute angle along the minor axis.

NP17

LO Chiasmolithus solitus

Chiasmolithus with broad centro-distal cycle, narrow central area and broad diagonal bars, two that curve and are offset where they meet. Bars are birefringent and may show median extinction lines. |
| **NP16** | |
| |

LO Nannotetrina fulgrens

Large to very large *Nannotetrina* with arms that taper to a point. |
| **NP15** | |
| |

FO Nannotetrina fulgrens

Large to very large *Nannotetrina* with arms that taper to a point. |
| **NP14** | |
| |

FO Discoaster sublodoensis

Five (less commonly 6) rayed *Discoaster* with a small stem on one side and sharply tapering, straight, pointed rays joined along half their length. |
| **NP13** | |
| |

LO Tribrachiatus orthostylus

Large, single-cycle tri-radiate nannoliths with little or no ray end bifurcation (<25% of the total arm length). |
| **NP12** | |
| |

FO Discoaster lodoensis

Large to very large stellate *Discoasters* with a central boss on one side and 5-7 (typically 6) curving rays joined along 1/2 to 1/3 their length with a ridge on one side. |
| **NP11** | |
| |

LO Tribrachius contortus

Tri-radiate forms with long ray tip bifurcations that deviate strongly from the plane of the nannolith, giving the appearance of two asymmetrically offset and superimposed tri-radiate cycles. |
| **NP10** | |
| |

FO Tribrachius bramlettei / Rhomboaster bramlettei

Nannolith with the appearance of two symmetrically offset and superimposed tri-radiate cycles. Three-dimensional but flatter than *Rhomboaster cuspis*. |
| **NP9** | |
| |

FO Discoaster multiradiatus (common)

Large to very large rosette-shaped *Discoasters* with 16-35 rays joined along most of their length with simple ray tips. |
| **NP8** | |
| |

FO Heliolithus riedelii

Heliolith with two high, birefringent cycles, the narrower cycle is around two thirds of the width of the broader. |
| **NP7** | |

NP7
NP6
NP5
NP4
NP3
NP2
NP1
NC23
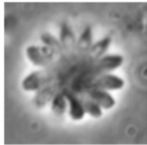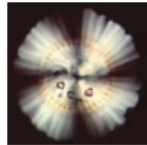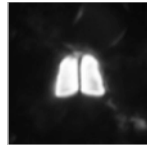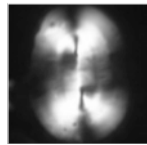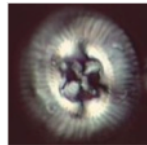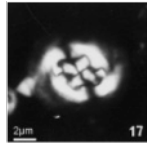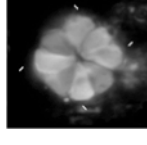
FO *Discoaster mohleri*

Medium sized rosette-shaped *Discoasters* with 9-16 rays joined along most of their length with simple broad ray tips.

FO *Heliolithus kleinpellii*

Large, heliolith with two thin birefringent cycle. The narrow cycle is around 3/4 of the width of the wider cycle.

FO *Fasciculithus tympaniformis*

Small to medium sized, squat cylindrical fasciculith, almost square in side view, with gently convex upper surface. Appears to lack fenestrae.

FO *Ellipsolithus macellus*

Moderate to large elliptical to oblong *Ellipsolithus* with conjunct, birefringent central area plate.

FO *Chiasmolithus danicus*

Small to moderate *Chiasmolithus* with diagonal cross formed from two curving and two straight bars; two of the bars are offset. High degree of variability reported.

FO *Cruciplacolithus tenuis*

Medium size to large (>7 µm) *Cruciplacolithus* with axial cross-bars that have disjunct, birefringent blocks ('feet') where they meet the rim.

FO *Biantholithus sparsus* & flood of Calcispheres

Biantholithus with 8-12 visible elements/rays in LM.

Figure A2.3: Comparison between **a.** Paleogene fossil coccosphere geometry data and **b.** the coccosphere geometry data measured from modern cultures of *Coccolithus pelagicus*, *Coccolithus braarudii*, *Calcidiscus quadriperforatus*, *Calcidiscus leptoporus* and *Helicosphaera carteri* shown in **Chapter 3**.
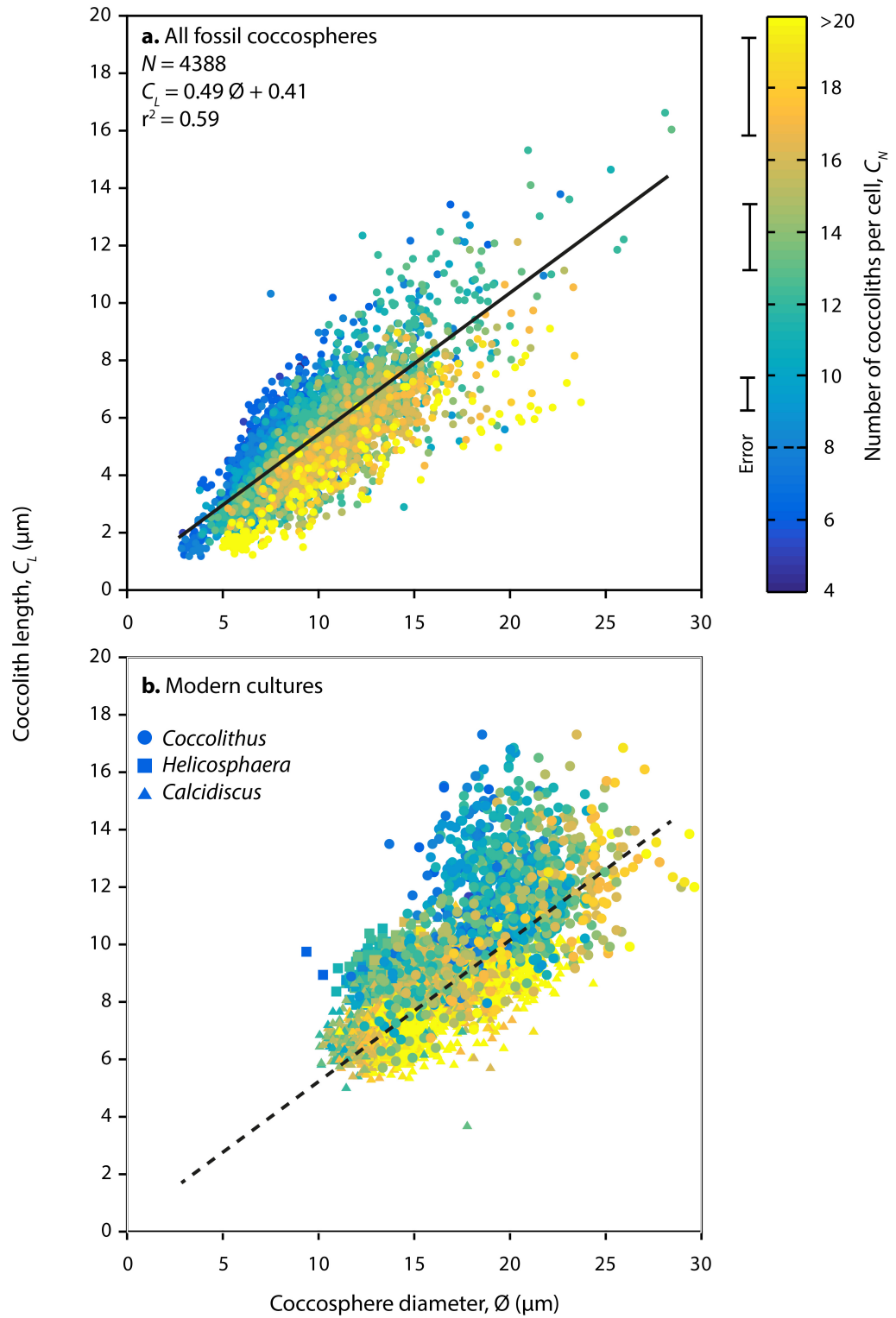
Table A2.4: Approximate coccosphere geometry measurements (coccosphere diameter, number of coccoliths per cell and coccolith length) for a selection of extant coccolithophore species. ImageJ freeware (v1.50i) was used to make measurements from individual scanning electron microscope (SEM) images sourced from Nannotax3 (Young et al. 2014). This data was used to plot Figure 2.8b.

Species	Coccosphere diameter, Ø (µm)	Number of coccoliths per cell, C_N	Coccolith length, C_L (µm)
Order: Isochrysidales			
Family: Noelaerhabdaceae			
Emiliania huxleyi	5.5	16	3.2
Gephyrocapsa ericsonia	3.0	14	2.1
Gephyrocapsa muellerae	5.6	16	3.4
Gephyrocapsa oceanica	4.8	14	4.1
Gephyrocapsa ornata	4.0	26	2.5
Reticulofenestra parvula	5.0	18	2.8
Order: Coccolithales			
Family: Coccolithaceae			
Coccolithus pelagicus	14.1	12	9.0
Coccolithus braarudii	19.9	12	11.8
Family: Calcidiscaceae			
Calcidiscus leptoporus	13.3	19	6.7
Calcidiscus quadriperforatus	18.6	18	9.1
Hayaster perplexus	42.0	80	4.0
Oolithotus antillarum	7.6	26	5.0
Oolithotus fragilis	17.1	30	4.2
Umbilicosphaera anulus	16.2	62	4.5
Umbilicosphaera hulburtiana	6.8	26	4.5
Umbilicosphaera sibogae	24.2	136	4.3
Order: Zygodiscales			
Family: Helicosphaeraceae			
Helicosphaera carteri	15.0	16	8.9
Helicosphaera hyalina	11.3	26	6.6
Helicosphaera pavimentum	11.3	28	5.0
Helicosphaera wallichii	22.0	24	6.5
Family: Pontosphaeraceae			
Pontosphaera syracusana	24.9	14	15.5
Scyphosphaera apsteinii	20.5	33	8.0

Table A2.4 continued

Species	Coccosphere diameter, Ø (µm)	Number of coccoliths per cell, C_N	Coccolith length, C_L (µm)
Order: Syracosphaerales			
Family: Syracosphaeraceae			
Coronosphaera binodata	13.7	46	4.0
Coronosphaera maxima	31.5	222	4.5
Coronosphaera mediterranea	17.2	78	3.7
Syracosphaera ampliora	8.1	32	3.0
Syracosphaera anthos	8.0	30	2.5
Syracosphaera bannockii	9.6	36	1.7
Syracosphaera borealis	7.5	34	2.8
Syracosphaera didyma	13.5	54	3.5
Syracosphaera dilatata	9.0	56	2.8
Syracosphaera epigrosa	10.3	34	2.8
Syracosphaera exigua	9.8	84	2.6
Syracosphaera hastata	8.0	44	2.3
Syracosphaera histrica	8.9	56	2.5
Syracosphaera leptolepis	7.3	52	2.3
Syracosphaera marginaporata	6.7	55	1.8
Syracosphaera molischii	9.1	66	3.0
Syracosphaera nana	5.0	58	1.5
Syracosphaera nodosa	7.7	48	2.4
Syracosphaera orbiculus	7.3	50	2.3
Syracosphaera ossa	5.8	36	2.5
Syracosphaera protrudens	10.0	70	2.4
Syracosphaera pulchra	13.7	38	5.5
Syracosphaera squamosa	7.0	44	2.7
Family: Calciosoleniaceae			
Alveosphaera bimurata	8.5	66	2.9
Calciosolenia murrayi	5.0	68	3.5
Family: Rhabdosphaeraceae			
Acanthoica acanthos	7.0	114	2.2
Acanthoica quattrospina	9.4	50	2.8
Algirosphaera robusta	11.8	92	3.5
Rhabdosphaera clavigera	9.6	22	4.5

Table A2.4 continued

Species	Coccosphere diameter, Ø (µm)	Number of coccoliths per cell, C_N	Coccolith length, C_L (µm)
Coccolith families inc. sed.			
Family: Alisphaeraceae			
Alisphaera gaudii	6.8	108	2.0
Alisphaera ordinata	7.4	156	1.5
Alisphaera pinnigera	9.8	294	1.5
Alisphaera unicornis	10.4	104	2.7
Family: Umbellosphaeraceae			
Umbellosphaera irregularis	16.3	18	9.0
Umbellosphaera tenuis	9.8	16	5.0

Appendix Chapter 3

Table A3.1: Culture strain details.

Strain	Other names	Species	Isolation	Other studies
RCC 1323	AC419, NS2-2	*Helicosphaera carteri*	S. Atlantic (2000), I. Probert	
RCC 1130	AC370, NS10-2, NIES-2694, CCMP3392	*Calcidiscus leptoporus*	S. Atlantic (2000), I. Probert	Sáez et al., 2003; Gussone et al., 2007; Buitenhuis et al., 2008; Fiorini et al., 2010; Franklin et al., 2010; Fiorini et al., 2011; Diner et al., 2015
RCC 1135	AC365, NS6-1	*Calcidiscus quadriperforatus*	S. Atlantic (2000), I. Probert	Langer et al., 2006; Langer and Bode, 2011; Langer et al., 2012; Müller et al., 2014
RCC 1197	AC615, IFAS-6	*Coccolithus braarudii*	English Channel, I. Probert	Sáez et al., 2003; Gibbs et al., 2013
RCC 1198	AC387, PLY182g	*Coccolithus braarudii*	English Channel (1958), M.Parke	Sáez et al., 2003; Daniels et al., 2014
RCC 4092	CD3.1b	*Coccolithus pelagicus*	C. Daniels	Daniels et al., 2014

Figure A3.1: Mean exponential phase growth rates (d^{-1}) with culture temperature in *Calcidiscus* leptoporus, *C. quadriperforatus* and *Helicosphaera carteri* from this study, plus mean exponential growth rates for *Coccolithus braarudii* (Gibbs et al. 2013) and for a wider temperature range for *C. pelagicus* and *C. braarudii* from Daniels et al. (2014).

Appendix Chapter 4

Table A4.1: Summary of samples from which coccosphere geometry data was used in community reconstructions. Coccosphere data is used to determine relationships between cell size, coccolith length and number of coccoliths per cell (Figure A4.1) and to calculated the predicted frequency of each cell size based on the frequency of C_N and C_L occurrence in samples of the same nannoplankton zone as the reconstruction intervals. An asterisk (*) next to the sample number denotes samples for which an additional 30-50 measurements of C_L were taken for each genus to ensure no size bias in the coccosphere data used.

Reconstruction interval	Nannoplankton Zone	Site	Samples used for coccospheres
Earliest Oligocene	NP21	Tanzania	* TDP 12 9/1 20-21
	Post-EOT	Labrador Sea	* 647A 27-1 95.0
Late Eocene	NP20-19	Labrador Sea	* 647A 32-2 13.0
			* 647A 34-1 104.0
		Tanzania	* TDP 12 26/2 62
		Australia	* COLN 51
		Mississippi	* Mississippi BW1.12
	NP18	Labrador Sea	647A 46-1 19-21
			647A 46-2 29-31
			* 647A 46-2 114-116
			* 647A 46-3 8-10
Mid Eocene	NP16 (not MECO)	Labrador Sea	* 647A 49-2 64-66
			647A 51-1 7-9
			* 647A 49-1 137-139
			* 647A 49-3 45-47
			647A 49-5 108-110
		Hampden Beach	HB 205
			* HB 215
			HB 245
	NP15	Tanzania	* TDP 2 25/2 62
			* TDP 2 25/1 62
			* TDP 6 9/1 85
			* TDP 6 8/1 63
Early-Mid Eocene	NP12	Lodo	* LO-03-21
			LO-03-14
			* LO-03-13
			LO-03-11
Early Eocene (post PETM)	NP11	Tanzania	TDP 3 12/1 62
			* TDP 3 4/3 52
		Bass River	BR 12
			BR 10
	NP10 Post CIE	Bay of Biscay	* 401 14 1 4
			401 14 1 105
		Tanzania	TDP 8 1/1 30
			TDP 14 4/1 19-20

| | Low Latitude | | | Mid Latitude | | | High Latitude | | | | |
| | Shatsky Rise 20 °N | | Walvis Ridge 30 °S | | Goban Spur 45 °N | | Exmouth Plateau 45 °S | | Kerguelen Plateau 60 °S | | Maud Rise 65 °S | |
	Rec	Others	**Rec**	Others	**Rec**	Others	**Rec**	Others	**Rec**	Others	**Rec**	Others
Early Eocene	**40.0**	60.0	**55.0**	45.0	**54.2**	45.8	**76.3**	23.7			**90.3**	9.7
Early-Mid Eocene			**21.9**	78.1	**59.0**	41.0	**47.2**	52.8	**64.2**	35.8	**88.9**	11.1
Mid Eocene	**70.2**	29.8	**53.4**	46.6	**74.5**	25.5	**70.8**	29.2	**91.2**	8.8	**99.5**	0.5
Late Eocene	**26.8**	73.2	**74.1**	25.9	**76.9**	28.1	**76.7**	23.3	**95.1**	4.9	**96.8**	3.2
Early Oligocene			**86.4**	13.6	**86.4**	73.6			**93.3**	6.7		

Table A4.2: Combined percentage of coccoliths of *Chiasmolithus*, *Coccolithus*, *Coccolithus formosus*, *Cyclicargolithus*, *Reticulofenestra*, and *Toweius* genera (Rec - used for reconstructions) compared to coccoliths of all other taxa (Others) within each interval (from the assemblage counts of Schneider et al. 2011). In the two high latitude locations, these six genera constitute upwards of ~90% of the entire calcareous nannoplankton assemblage., with the contribution of other taxa to the assemblage increases with decreasing latitude.

Figure A4.1: Geometric relationships between coccolith length, C_L, cell surface area, and number of coccoliths per cell, C_N, used in calculating cell diameter from C_L and C_N in each genus. Genus-specific constants α and β from the power-law relationship between C_L and surface area/C_N are used in **Chapter 4** Equations 4.1 and 4.2. The contours in the right hand plots shows the cell size calculated for each combination of C_L and C_N using Equation 4.2 and is used to calculate the genus histograms during each reconstruction interval.
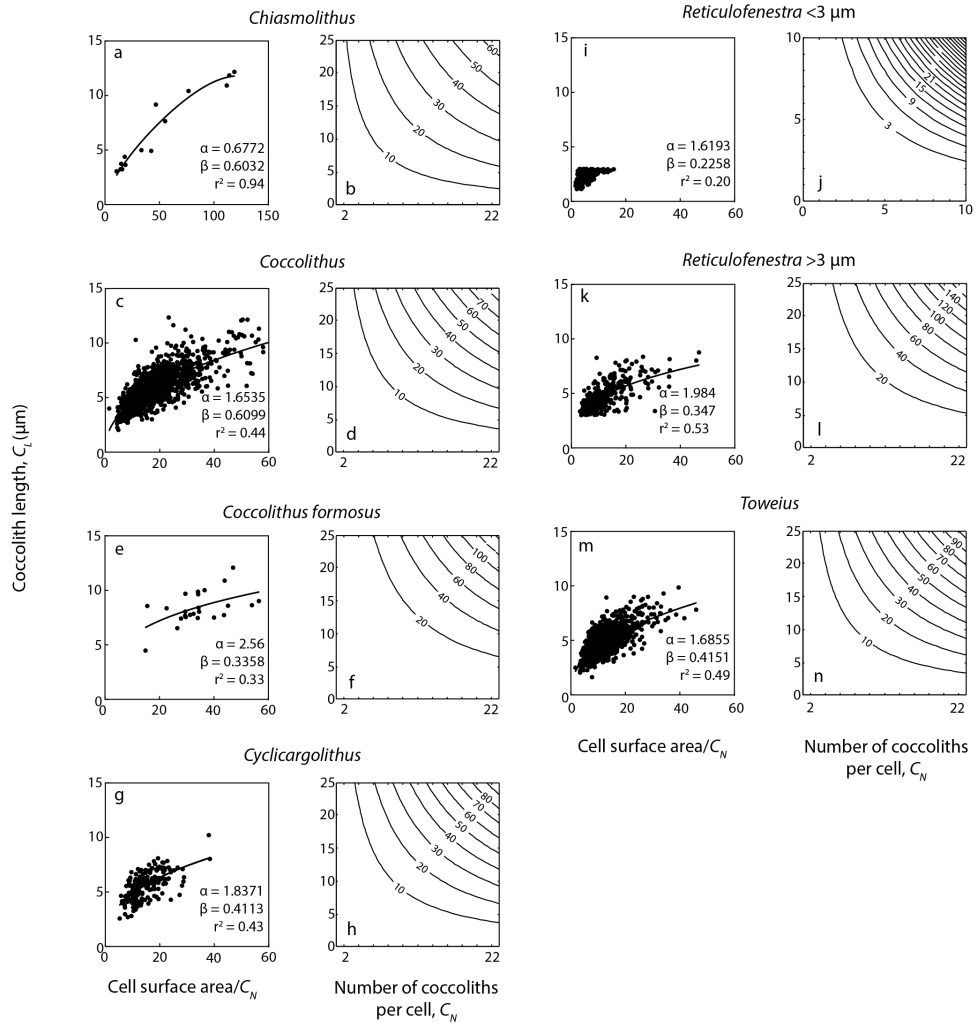
Detailed methodological procedure used to reconstruct the cell size distribution of coccolithophore communities.

Step 1.1: Derive the relationship between Θ, C_L and C_N for each genus.

There is a strong relationship between cell size (Θ), coccolith length (C_L) and the number of coccoliths per cell (C_N) within coccolithophores, as shown by the extensive dataset of more than 4000 cellular measurements from fossil coccospheres of Paleogene age presented in **Chapter 2** (Figure 2.6). The relationship between Θ, C_L and C_N is specific to each genus (Figures 2.8 and 2.10) and can be described as a power-law equation:

$$C_L = \alpha \left(\frac{SA}{C_N}\right)^{\beta}$$

Eqn. 4.1

where C_L is coccolith length in µm, SA is cell surface area ($SA = 4\pi(\Theta/2)^2$), C_N is number of coccoliths per cell, and α and β are constants specific to each genus (Appendix Figure A4.1).

Step 1.2: Calculate the Θ that would result from a range of C_L and C_N combinations based on this relationship.

Cell size, Θ, for any combination of C_L and C_N can be calculated for each genus by re-arranging Equation 4.1 as follows:

$$\Theta = \sqrt[2]{\frac{C_N \times \sqrt[\beta]{\frac{C_L}{\alpha}}}{4\pi}}$$

Eqn. 4.2

Using Equation 4.2, cell size was calculated for each combination of C_L between 0 µm and 25 µm (at 0.5 µm size bins) and C_N between 1 and 23 coccoliths cell[-1]. This resulted in a 23 (C_N) x 50 (C_L) matrix consisting of 1150 calculated cell sizes, which was repeated for each genus using the genus-specific relationship between Ø, C_L and C_N derived in Step 1.1.

Step 1.3: Calculate the expected frequency that each combination of C_L and C_N will occur within a sample of each interval age.

Each genus is comprised of individual species with specific ranges in C_L, C_N and Θ. The species within a genus will change through time such that the cell size range of a genus may not remain constant between reconstruction intervals. To account for this, the frequency

distribution of C_N and C_L in fossil coccospheres can be used to calculate the expectation that any combination of C_N and C_L will occur in a community of that age. For example, this could mean that there are 120 coccoliths of length 7 μm (from C_L histogram) and 20% of these would be associated with a coccosphere of 6 coccoliths (from C_N histogram). Therefore there would be an expected frequency of 4 cells with a C_N of 6 and a C_L of 7 μm (20% of 120 coccoliths equals 24 coccoliths, each cell has 6 coccoliths). In addition to the C_L frequency distribution obtained from fossil coccospheres, this step also incorporates the C_L frequency distribution measured from loose coccoliths in samples of the same age. This ensures that the cell size frequency distribution does not inadvertently reflect any size bias due to taphonomic processes, such as the preferential disarticulation of very large coccospheres. The samples from which loose coccolith length measurements were taken in addition to coccosphere geometry are indicated in Appendix Table A4.1.

Step 1.4: Collate the expected frequencies of each cell size into a genus cell size frequency histogram.

Each cell size (combination of C_L and C_N) is 'matched' to the expected frequency that those combinations of C_L and C_N will occur, then the resulting frequencies are collated into 1 μm cell size bins. At this stage, all genus cell size histograms are normalised to sum to a total frequency of 1. The cell size frequency of each genus for each reconstruction interval is shown in Figure 4.4.

Step 2: Normalise each histogram to the relative abundance of each genus at each site.

The relative abundance of each genus in each community is typically determined based on coccolith abundance counts (c.f., Schneider et al. (2011) for relative abundance of genera based on coccoliths for this dataset). However, some genera typically have a greater number of coccoliths per coccosphere (Figure 2.9 b). For this study, the coccolith abundance of each genus (as a percentage of the assemblage) is divided by the mean C_N of that genus during that time interval to give the mean number of 'cells' in the community. From this, a cellular-based percentage abundance is then calculated for each genus. The frequency distribution of each genus histogram is finally normalised to the relative cellular abundance of the genus at each site in order to reflect the site-specific characteristics of species composition.

Step 3: Combine the abundance-normalised histograms of each genus to generate the cumulative cell size frequency of the community.

A cumulative frequency histogram that 'stacks' each genus histogram together then reveals how the size distribution of each genus affects the overall cell size distribution of the coccolithophore community through time at each site.

Figure A4.2: Relative abundance of the six genera used for community size reconstructions at Maud Rise, Kerguelen Plateau and Exmouth Plateau by sample age (lines) with the relative cellular abundance of the genus during each interval shown as black dots. The relative coccolith abundance is a selective reproduction of Figure 3 in Schneider et al. (2011) and cellular relative abundance was calculated from this by dividing by the typical number of coccoliths per cell of that genus specific to each time interval reconstruction. Note the different x-axis scale for each genus.
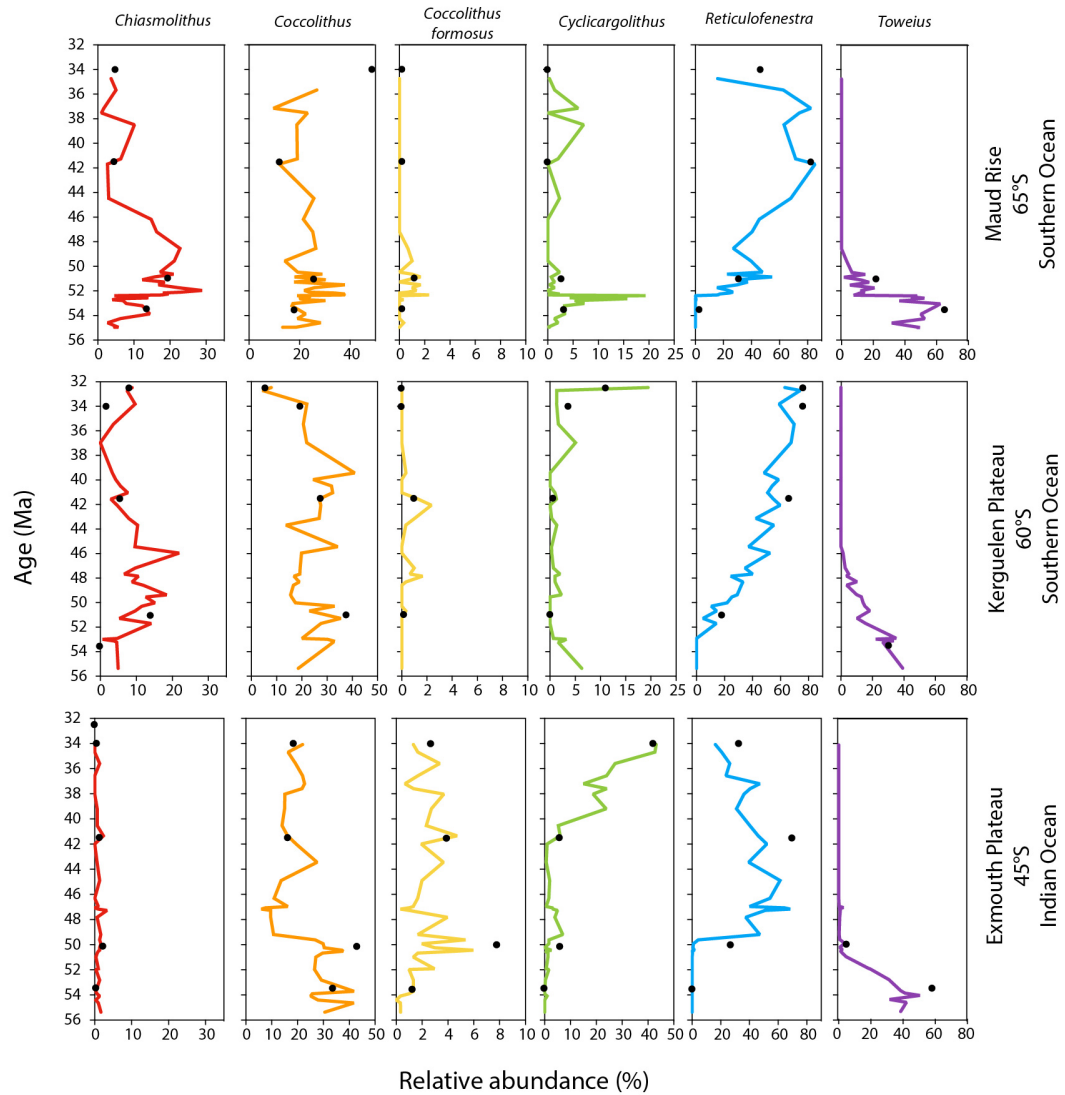
Figure A4.3: Relative abundance of the six genera used for community size reconstructions at Goban Spur, Walvis Ridge and Shatsky Rise by sample age (lines) with the relative cellular abundance of the genus during each interval shown as black dots. The relative coccolith abundance is a selective reproduction of Figure 3 in Schneider et al. (2011) and cellular relative abundance was calculated from this by dividing by the typical number of coccoliths per cell of that genus specific to each time interval reconstruction. Note the different x-axis scale for each genus.
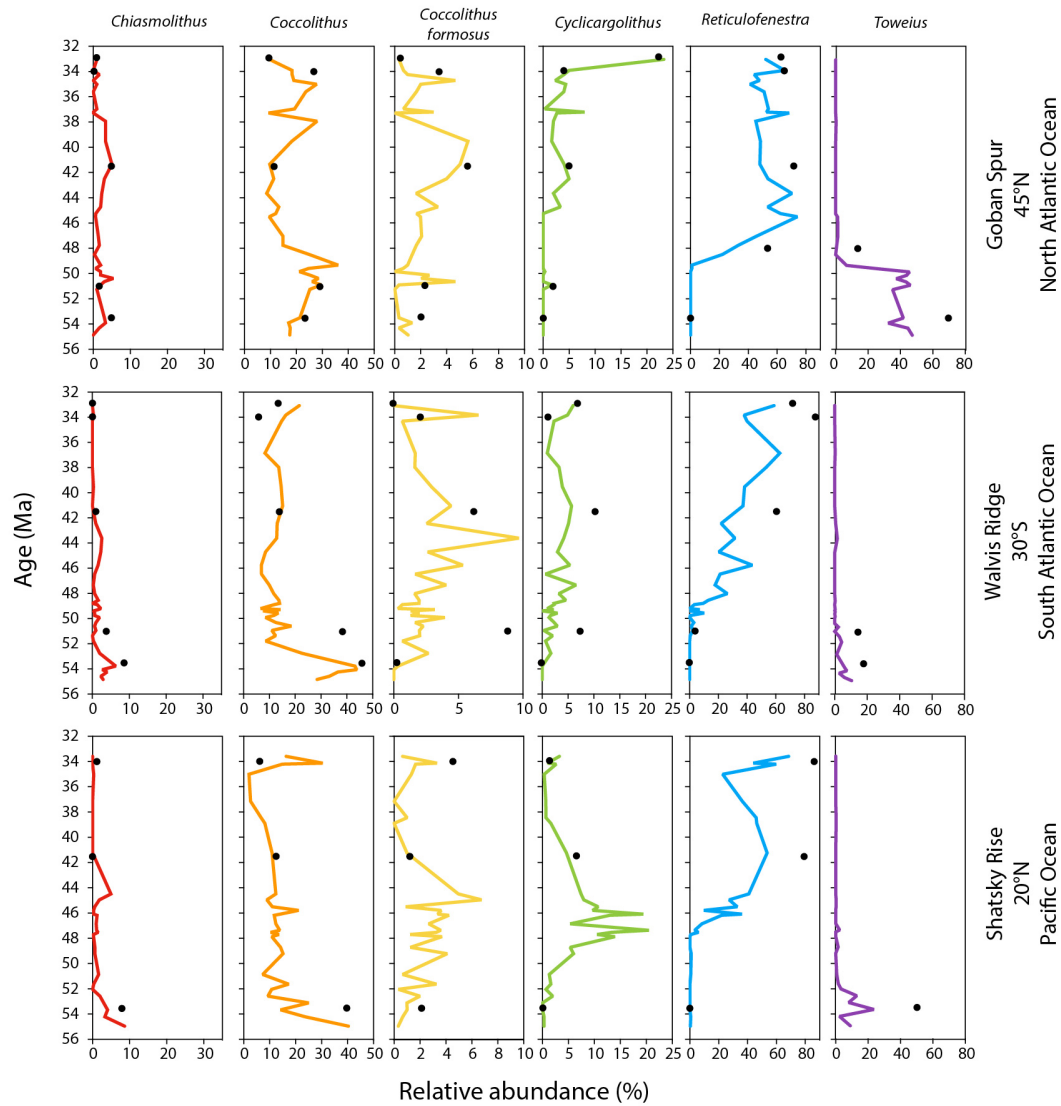
Table A4.3: Statistical summary of community cell size distributions at each site during each time interval (EE - Early Eocene; EME – Early-Mid Eocene; ME – Mid Eocene; LE – Late Eocene; EO – Earliest Oligocene) corresponding to Figures 4.3 to 4.5. Min/Max is the minimum/maximum cell size bin midpoint; 5th, 25th, 75th and 95th refer to the relevant percentile bin mid-points and GMean is the geometric mean cell size of the community, which better reflects the mean than the arithmetic mean due to the strongly skewed nature of the size profiles. All sizes are in μm.

	Interval	Min	5th	25th	GMean	75th	95th	Max
Maud Rise	EE	1.5	2.5	3.5	**5.6**	7.5	17.5	36.5
65 °S	EME	0.5	2.5	4.5	**7.1**	11.5	17.5	38.5
	ME	2.5	3.5	4.5	**7.4**	9.5	26.5	38.5
	LE	1.5	4.5	7.5	**10.2**	13.5	31.5	38.5
	EO	-	-	-	**-**	-	-	-
Kerguelen Plateau	EE	-	-	-	**-**	-	-	-
60 °S	EME	1.5	2.5	4.5	**7.2**	10.5	16.5	38.5
	ME	2.5	3.5	5.5	**8.0**	10.5	23.5	38.5
	LE	0.5	3.5	6.5	**9.1**	12.5	31.5	38.5
	EO	0.5	3.5	5.5	**8.0**	11.5	20.5	38.5
Exmouth Plateau	EE	1.5	2.5	3.5	**5.5**	7.5	11.5	25.5
45 °S	EME	0.5	3.5	5.5	**7.9**	10.5	15.5	38.5
	ME	2.5	3.5	5.5	**7.3**	9.5	17.5	38.5
	LE	1.5	3.5	6.5	**9.0**	12.5	33.5	38.5
	EO	-	-	-	**-**	-	-	-
Goban Spur	EE	1.5	2.5	3.5	**5.3**	7.5	13.5	35.5
45 °N	EME	0.5	3.5	4.5	**6.7**	9.5	15.5	38.5
	ME	0.5	3.5	5.5	**7.2**	9.5	17.5	38.5
	LE	0.5	3.5	6.5	**9.7**	13.5	33.5	38.5
	EO	2.5	3.5	5.5	**7.5**	10.5	16.5	38.5
Walvis Ridge	EE	1.5	3.5	5.5	**7.3**	9.5	16.5	36.5
30 °S	EME	1.5	3.5	6.5	**8.2**	11.5	15.5	35.5
	ME	2.5	3.5	5.5	**7.6**	10.5	18.5	38.5
	LE	1.5	3.5	5.5	**8.2**	11.5	22.5	38.5
	EO	2.5	3.5	5.5	**7.9**	10.5	16.5	38.5
Shatsky Rise	EE	1.5	2.5	4.5	**6.0**	8.5	15.5	36.5
20 °N	EME	-	-	-	**-**	-	-	-
	ME	2.5	3.5	4.5	**6.9**	9.5	15.5	38.5
	LE	1.5	3.5	6.5	**11.5**	25.5	37.5	38.5
	EO	-	-	-	**-**	-	-	-

References

Arrigo, K.R., 2005, Marine microorganisms and global nutrient cycles. *Nature*, 437, 349–355, doi: 10.1038/nature04158.

Bach, L.T., Riebesell, U., and Schulz, K.G., 2011, Distinguishing between the effects of ocean acidification and ocean carbonation in the coccolithophore *Emiliania huxleyi*. *Limnology and Oceanography*, 56, 6, 2040–2050, doi: 10.4319/lo.2011.56.6.2040.

Bach, L.T., Riebesell, U., Gutowska, M.A., Federwisch, L., and Schulz, K.G., 2015, A unifying concept of coccolithophore sensitivity to changing carbonate chemistry embedded in an ecological framework. *Progress in Oceanography*, 135, 125–138, doi: 10.1016/j.pocean.2015.04.012.

Badger, M.P.S., Schmidt, D.N., Mackensen, A., and Pancost, R.D., 2013, High-resolution alkenone palaeobarometry indicates relatively stable pCO$_2$ during the Pliocene (3.3-2.8 Ma). *Philosophical transactions of the Royal Society A*, 371, 20130094, doi: 10.1098/rsta.2013.0094.

Balch, W.M., Fritz, J., and Fernandez, E., 1996, Decoupling of calcification and photosynthesis in the coccolithophore *Emiliania huxleyi* under steady-state light -limited growth. *Marine Ecology Progress Series*, 142, 87–97, doi: 10.3354/meps142087.

Balch, W.M., Kilpatrick, K.A., Holligan, P.M., and Cucci, T., 1993, Coccolith production and detachment by *Emiliania huxleyi* (Prymnesiophyceae). *Journal of Phycology*, 29, 5, 566–575, doi: 10.1111/j.0022-3646.1993.00566.x.

Banavar, J.R., Damuth, J., Maritan, A., and Rinaldo, A., 2002, Supply-demand balance and metabolic scaling. *Proceedings of the National Academy of Sciences*, 99, 16, 10506–10509, doi: 10.1073/pnas.162216899.

Beardall, J., Allen, D., Bragg, J., Finkel, Z.V., Flynn, K.J., Quigg, A., Rees, T.A.V, Richardson, A., and Raven, J.A., 2009, Allometry and stoichiometry of unicellular, colonial and multicellular phytoplankton. *New Phytologist*, 181, 295–309, doi: 10.1111/j.1469-8137.2008.02660.x.

Beaufort, L., and Heussner, S. 2001, Seasonal dynamics of calcareous nannoplankton on a West European continental margin: the Bay of Biscay. *Marine Micropaleontology*, 43, 27–55, doi: 10.1016/S0377-8398(01)00020-2.

Beaufort, L., Probert, I., de Garidel-Thoron, T., Bendif, E.M., Ruiz-Pino, D., Metzl, N., Goyet, C., Buchet, N., Coupel, P., Grelaud, M., Rost, B., Rickaby, R.E.M., and de Vargas, C., 2011, Sensitivity of coccolithophores to carbonate chemistry and ocean acidification. *Nature*, 476,

80–83, doi: 10.1038/nature10295.

Beerling, D.J., and Royer, D.L., 2011, Convergent Cenozoic CO_2 history. *Nature Geoscience*, 4, 418–420, doi: 10.1038/ngeo1186.

Berelson, W.M., Balch, W.M., Najjar, R., Feely, R.A., Sabine, C., and Lee, K., 2007, Relating estimates of $CaCO_3$ production, export, and dissolution in the water column to measurements of $CaCO_3$ rain into sediment traps and dissolution on the sea floor: A revised global carbonate budget. *Global Biogeochemical Cycles*, 21, 1, GB1024, doi: 10.1029/2006GB002803.

Berglund, J., Müren, U., Båmstedt, U., and Andersson, A., 2007, Efficiency of a phytoplankton-based and a bacterial-based food web in a pelagic marine system. *Limnology and Oceanography*, 52, 1, 121–131, doi: 10.4319/lo.2007.52.1.0121.

Bergquist, A.M., Carpenter, S.R., and Latino, J.C., 1985, Shifts in phytoplankton size structure and community composition during grazing by contrasting zooplankton assemblages. *Limonology and Oceanography*, 30, 5, 1037–1045, doi: 10.4319/lo.1985.30.5.1037.

Bidigare, R.R., Fluegge, A., Freeman, K.H., Hanson, K.L., Hayes, J.M., Hollander, D., Jasper, J.P., King, L.L., Laws, E.A., Milder, J., Millero, F.J., Pancost, R., Popp, B.N., Steinberg, P.A., and Wakeham, S.G., 1997, Consistent fractionation of ^{13}C in nature and in the laboratory: growth rate effects in some haptophyte algae. *Global Biogeochemical Cycles*, 11, 2, 279–292, doi: 10.1029/96GB03939.

Bijl, P.K., Bendle, J.A.P., Bohaty, S.M., Pross, J., Schouten, S., Tauxe, L., Stickley, C.E., McKay, R.M., Röhl, U., Olney, M., Sluijs, A., Escutia, C., Brinkhuis, H., and Expedition 318 Scientists, 2013, Eocene cooling linked to early flow across the Tasmanian Gateway. *Proceedings of the National Academy of Sciences*, 110, 24, 9645–9650, doi: 10.1073/pnas.1220872110.

Billard, C., and Inouye, I., 2004, What is new in coccolithophore biology?, *in* Thierstein, H.R. and Young, J.R. eds., *Coccolithophores: From Molecular Processes to Global Impact*, Springer-Verlag, Heidelberg, Germany, p. 1–29, doi: 10.1007/978-3-662-06278-4.

Boeckel, B., and Baumann, K-H., 2008, Vertical and lateral variations in coccolithophore community structure across the subtropical frontal zone in the South Atlantic Ocean. *Marine Micropaleontology*, 67, 255-273, doi: 10.1016/j.marmicro.2008.01.014.

Bollmann, J., 1997, Morphology and biogeography of *Gephyrocapsa* coccoliths in Holocene sediments. *Marine Micropaleontology*, 29, 3-4, 319–350, doi: 10.1016/S0377-8398(96)00028-X.

Bolton, C.T., and Stoll, H.M., 2013, Late Miocene threshold response of marine algae to carbon

dioxide limitation. *Nature*, 500, 558–562, doi: 10.1038/nature12448.

Bolton, C.T., Stoll, H.M., and Mendez-Vicente, A., 2012, Vital effects in coccolith calcite: Cenozoic climate- pCO$_2$ drove the diversity of carbon acquisition strategies in coccolithophores? *Paleoceanography*, 27, PA4204, doi: 10.1029/2012PA002339.

Bordiga, M., Henderiks, J., Tori, F., Monechi, S., Fenero, R., Legarda-Lisarri, A., and Thomas, E., 2015, Microfossil evidence for trophic changes during the Eocene–Oligocene transition in the South Atlantic (ODP Site 1263, Walvis Ridge). *Climate of the Past*, 11, 1249–1270, doi: 10.5194/cp-11-1249-2015.

Bown, P.R., 2005a, Paleogene calcareous nannofossils from the Kilwa and Lindi areas of coastal Tanzania (Tanzania Drilling Project 2003-2004). *Journal of Nannoplankton Research*, 27, 1, 21–95.

Bown, P., 2005b, Selective calcareous nannoplankton survivorship at the Cretaceous-Tertiary boundary. *Geology*, 33, 8, 653-656, doi: 10.1130/G21566.1.

Bown, P.R., Dunkley Jones, T., Young, J.R., and Randell, R., 2009, A Paleogene record of extant lower photic zone calcareous nannoplankton. *Palaeontology*, 52, 2, 457–469, doi: 10.1111/j.1475-4983.2009.00853.x.

Bown, P.R., Gibbs, S.J., Sheward, R., and O'Dea, S.A., 2014, Searching for cells: the potential of fossil coccospheres in coccolithophore research. *Journal of Nannoplankton Research*, 34, 5–21.

Bown, P.R., and Dunkley Jones, T., 2006, New Paleogene calcareous nannofossil taxa from coastal Tanzania: Tanzania Drilling Project Sites 11 to 14. *Journal of Nannoplankton Research*, 28, 17–34.

Bown, P.R., Jones, T.D., Lees, J. A., Randell, R.D., Mizzi, J.A., Pearson, P.N., Coxall, H.K., Young, J.R., Nicholas, C.J., Karega, A., Singano, J., and Wade, B.S., 2008, A Paleogene calcareous microfossil Konservat-Lagerstätte from the Kilwa Group of coastal Tanzania. *Geological Society of America Bulletin*, 120, 3–12, doi: 10.1130/B26261.1.

Bown, P.R., Jones, T.D., and Young, J.R., 2007, *Umbilicosphaera jordanii* Bown, 2005 from the Paleogene of Tanzania: confirmation of generic assignment and a Paleocene origination for the Family Calcidiscaceae. *Journal of Nannoplankton Research*, 29, 25–30.

Bown, P.R., Lees, J.A., and Young, J.R., 2004, Calcareous nannoplankton evolution and diversity through time, *in* Thierstein, H.R. and Young, J.R. eds., *Coccolithophores: From Molecular Processeses to Global Impact*, Springer Verlag, Heidelberg, Germany, p. 481–508, doi: 10.1007/978-3-662-06278-4.

Bown, P., and Pearson, P., 2009, Calcareous plankton evolution and the Paleocene/Eocene thermal

maximum event: New evidence from Tanzania. *Marine Micropaleontology*, 71, 1-2, 60–70, doi: 10.1016/j.marmicro.2009.01.005.

Bown, P.R., and Young, J.R., 1998, Techniques, *in* Bown, P.R. ed., *Calcareous Nannofossil Biostratigraphy*, Chapman & Hall, London, UK, p. 16–28, ISBN: 978-0412789700.

Boyd, P.W., Dillingham, P.W., McGraw, C.M., Armstrong, E.A., Cornwall, C.E., Feng, Y. -y., Hurd, C.L., Gault-Ringold, M., Roleda, M.Y., Timmins-Schiffman, E., and Nunn, B.L., 2015, Physiological responses of a Southern Ocean diatom to complex future ocean conditions. *Nature Climate Change*, 6, 207-213, doi: 10.1038/nclimate2811.

Boyd, P.W., Strzepek, R., Fu, F., and Hutchins, D.A., 2010, Environmental control of open-ocean phytoplankton groups: Now and in the future. *Limnology and Oceanography*, 55, 3, 1353–1376, doi: 10.4319/lo.2010.55.3.1353.

Bralower, T.J., 2002, Evidence of surface water oligotrophy during the Paleocene-Eocene thermal maximum: Nannofossil assemblage data from Ocean Drilling Program Site 690, Maud Rise, Weddell Sea. *Paleoceanography*, 17, 1-12, doi: 10.1029/2001PA000662.

Bralower, T.J. and Parrow, M., 1996, Morphometrics of Paleocene coccolith genera *Cruciplacolithus*, *Chiasmolithus*, and *Sullivania*: A complex evolutionary history. *Paleobiology*, 22, 3, 352-385.

Brassell, S.C., 2014, Climatic influences on the Paleogene evolution of alkenones. *Paleoceanography*, 29, 1–18, doi: 10.1002/2013PA002576.

Brierley, A.S., and Kingsford, M.J., 2009, Impacts of climate change on marine organisms and ecosystems. *Current biology*, 19, R602–14, doi: 10.1016/j.cub.2009.05.046.

Broecker, W., and Clark, E., 2009, Ratio of coccolith $CaCO_3$ to foraminifera $CaCO_3$ in late Holocene deep sea sediments. *Paleoceanography*, 24, PA3205, doi: 10.1029/2009PA001731.

Brown, J.H., Gillooly, J.F., Allen, A.P., Savage, V.M., and West, G.B., 2004, Toward a metabolic theory of ecology. *Ecology*, 85, 7, 1771-1789, doi: 10.1890/03-9000.

Buitenhuis, E.T., Pangerc, T., Franklin, D.J., Le Quéré, C., and Malin, G., 2008, Growth rates of six coccolithophorid strains as a function of temperature. *Limnology and Oceanography*, 53, 3, 1181–1185, doi: 10.4319/lo.2008.53.3.1181.

Burgess, C.E., Pearson, P.N., Lear, C.H., Morgans, H.E.G., Handley, L., Pancost, R.D., and Schouten, S., 2008, Middle Eocene climate cyclicity in the southern Pacific: Implications for global ice volume. *Geology*, 36, 651-654, doi: 10.1130/G24762A.1.

Caballero, R., and Huber, M., 2013, State-dependent climate sensitivity in past warm climates and its implications for future climate projections. *Proceedings of the National Academy of Sciences*, 110, 35, 14162–14167, doi: 10.1073/pnas.1303365110.

Candelier, Y., Minoletti, F., Probert, I., and Hermoso, M., 2013, Temperature dependence of oxygen isotope fractionation in coccolith calcite: A culture and core top calibration of the genus *Calcidiscus. Geochimica et Cosmochimica Acta*, 100, 264–281, doi: 10.1016/j.gca.2012.09.040.

Cermeño, P., de Vargas, C., Abrantes, F., and Falkowski, P.G., 2010, Phytoplankton biogeography and community stability in the ocean. *PLOS ONE*, 5, 4, e10037, doi: 10.1371/journal.pone.0010037.

Chisholm, S.W., 1992, Phytoplankton size, *in* Falkowski, P.G. and Woodhead, A.D. eds., *Primary Productivity and Biogeochemical Cycles in the Sea*, Springer, New York, p. 213–237, doi: 10.1007/978-1-4899-0762-2.

Conte, M.H., Thompson, A., Eglinton, G., and Green, J.C., 1995, Lipid biomarker diversity in the coccolithophorid *Emiliania huxleyi* (Prymnesiophyceae) and the related species *Gephyrocapsa oceanica. Journal of Phycology*, 31, 2, 272–282.

Covington, M., 1985, New morphologic information on Cretaceous nannofossils from the Niobrara Formation (Upper Cretaceous) of Kansas. *Geology*, 13, 683–686, doi: 10.1130/0091-7613(1985)13<683:NMIOCN>2.0.CO.

Daniels, C.J., Sheward, R.M., and Poulton, A.J., 2014, Biogeochemical implications of comparative growth rates of *Emiliania huxleyi* and *Coccolithus* species. *Biogeosciences*, 11, 6915–6925, doi: 10.5194/bg-11-6915-2014.

Davis, C.V., Badger, M.P.S., Bown, P.R., and Schmidt, D.N., 2013, The response of calcifying plankton to climate change in the Pliocene. *Biogeosciences*, 10, 6131–6139, doi: 10.5194/bg-10-6131-2013.

Diner, R.E., Benner, I., Passow, U., Komada, T., Carpenter, E.J., and Stillman, J.H., 2015, Negative effects of ocean acidification on calcification vary within the coccolithophore genus *Calcidiscus. Marine Biology*, 162, 1287–1305, doi: 10.1007/s00227-015-2669-x.

Doney, S., Ruckelshaus, M., Duffy, E., Barry, J., Chan, F., English, C., Galindo, H., Grebmeier, J., Hollowed, A., Knowlton, N., Polovina, J., Rabalais, N., Sydeman, W., and Talley, L., 2012, Climate change impacts on marine ecosystems. *Annual Review of Marine Science*, 4, 11–37, doi: 10.1146/annurev-marine-041911-111611.

Dunkley Jones, T., Bown, P.R., and Pearson, P.N., 2009, Exceptionally well preserved upper Eocene to lower Oligocene calcareous nannofossils (Prymnesiophyceae) from the Pande Formation (Kilwa Group), Tanzania. *Journal of Systematic Palaeontology*, 7, 4, 359–411, doi: 10.1017/S1477201909990010.

Dunkley Jones, T., Bown, P.R., Pearson, P.N., Wade, B.S., Coxall, H.K., and Lear, C.H., 2008, Major shifts in calcareous phytoplankton assemblages through the Eocene-Oligocene transition of Tanzania and their implications for low-latitude primary production. *Paleoceanography*, 23, PA4204, doi: 10.1029/2008PA001640.

Edwards, M., and Richardson, A.J., 2004, Impact of climate change on marine pelagic phenology and trophic mismatch, *Nature*, 430, 881-884, doi: 10.1038/nature02808.

Epstein, B.L., D'Hondt, S., and Hargraves, P.E., 2001, The possible metabolic role of C_{37} alkenones in *Emiliania huxleyi*. *Organic Geochemistry*, 32, 867–875, doi: 10.1016/S0146-6380(01)00026-2.

Falkowski, P.G., Barber, R. T., and Smetacek, V., 1998, Biogeochemical controls and feedbacks on ocean primary production. *Science*, 281, 200–206, doi: 10.1126/science.281.5374.200.

Finkel, Z.V., 2007, Does Phytoplankton Cell Size Matter? The evolution of modern marine food webs, *in* Falkowski, P.G. and Knoll, A.H. eds., *Evolution of Primary Producers in the Sea*, Elsevier Academic Press, London, UK, p. 333–350, doi: 10.1016/B978-012370518-1/50001.

Finkel, Z.V, 2001, Light absorption and size scaling of light-limited metabolism in marine diatoms. *Limnology and Oceanography*, 46, 1, 86–94, doi: 10.4319/lo.2001.46.1.0086.

Finkel, Z.V., Beardall, J., Flynn, K.J., Quigg, A., Rees, T.A.V., and Raven, J.A., 2010, Phytoplankton in a changing world: cell size and elemental stoichiometry. *Journal of Plankton Research*, 32, 1, 119–137, doi: 10.1093/plankt/fbp098.

Finkel, Z.V., and Irwin, A.J., 2000, Modeling size-dependent photosynthesis: Light absorption and the allometric rule. *Journal of Theoretical Biology*, 204, 361-369, doi: 10.1006/jtbi.2000.2020.

Finkel, Z.V, Katz, M.E., Wright, J.D., Schofield, O.M.E., and Falkowski, P.G., 2005, Climatically driven macroevolutionary patterns in the size of marine diatoms over the Cenozoic. *Proceedings of the National Academy of Sciences*, 102, 25, 8927–32, doi: 10.1073/pnas.0409907102.

Finkel, Z.V, Sebbo, J., Feist-Burkhardt, S., Irwin, A.J., Katz, M.E., Schofield, O.M.E., Young, J.R., and Falkowski, P.G., 2007, A universal driver of macroevolutionary change in the size of marine phytoplankton over the Cenozoic. *Proceedings of the National Academy of Sciences*, 104, 51, 20416–20, doi: 10.1073/pnas.0709381104.

Fiorini, S., Gattuso, J.P., van Rijswijk, P., and Middelburg, J., 2010, Coccolithophores lipid and carbon isotope composition and their variability related to changes in seawater carbonate chemistry. *Journal of Experimental Marine Biology and Ecology*, 394, 74–85, doi: 10.1016/j.jembe.2010.07.020.

Fiorini, S., Middelburg, J.J., and Gattuso, J.-P., 2011, Testing the effects of elevated pCO$_2$ on Coccolithophores (Prymnesiophyceae): Comparison between haploid and diploid life stages. *Journal of Phycology*, 47, 1281–1291, doi: 10.1111/j.1529-8817.2011.01080.x.

Firth, J.V., and Wise Jr, S.W., 1992, A preliminary study of the evolution of *Chiasmolithus* in the middle Eocene to Oligocene of Sites 647 and 748. *Proceedings of the Ocean Drilling Program, Scientific Results* v. 120, Texas A&M University, College Station TX, United States, p. 493–508, ISSN: 0884-5891.

Franklin, D.J., Steinke, M., Young, J., Probert, I., and Malin, G., 2010, Dimethylsulphoniopropionate (DMSP), DMSPlyase activity (DLA) and dimethylsulphide (DMS) in 10 species of coccolithophore. *Marine Ecology Progress Series*, 410, 13–23, doi: 10.3354/meps08596.

Fresnel, J., and Probert, I., 2005, The ultrastructure and life cycle of the coastal coccolithophorid *Ochrosphaera neapolitana* (Prymnesiophyceae). *European Journal of Phycology*, 40, 1, 105–122, doi: 10.1080/09670260400024659.

Geider, R., and La Roche, J., 2002, Redfield revisited: variability of C:N:P in marine microalgae and its biochemical basis. *European Journal of Phycology*, 37, 1, 1–17, doi: 10.1017/S0967026201003456.

Geisen, M., Billard, C., Broerse, A.T.C., Cros, L., Probert, I., and Young, J.R., 2002, Life-cycle associations involving pairs of holococcolithophorid species: intraspecific variation or cryptic speciation? *European Journal of Phycology*, 37, 531–550, doi: 10.1017/S0967026202003852.

Geisen, M., Young, J.R., Probert, I., Saez, A.G., Baumann, K.H., Sprengel, C., Bollmann, J., Cros, L., De Vargas, C., and Medlin, L.K., 2004, Species level variation in coccolithophores, *in* Thierstein, H.R. and Young, J.R. eds., *Coccolithophores: From Molecular Processeses to Global Impact*, Springer Verlag, Heidelberg, Germany, p. 327-366, doi: 10.1007/978-3-662-06278-4.

Gerecht, A.C., Šupraha, L., Edvardsen, B., Langer, G., and Henderiks, J., 2015, Phosphorus availability modifies carbon production in *Coccolithus pelagicus* (Haptophyta). *Journal of Experimental Marine Biology and Ecology*, 472, 24–31, doi: 10.1016/j.jembe.2015.06.019.

Gerecht, A.C., Šupraha, L., Edvardsen, B., Probert, I., and Henderiks, J., 2014, High temperature

decreases the PIC/POC ratio and increases phosphorus requirements in *Coccolithus pelagicus* (Haptophyta). *Biogeosciences*, 11, 3531–3545, doi: 10.5194/bg-11-3531-2014.

Gibbs, S.J., Bown, P.R., Sessa, J.A, Bralower, T.J., and Wilson, P.A, 2006a, Nannoplankton extinction and origination across the Paleocene-Eocene Thermal Maximum. *Science*, 314, 1770–1773, doi: 10.1126/science.1133902.

Gibbs, S.J., Bralower, T.J., Bown, P.R., Zachos, J.C., and Bybell, L.M., 2006b, Shelf and open-ocean calcareous phytoplankton assemblages across the Paleocene-Eocene Thermal Maximum: Implications for global productivity gradients. *Geology*, 34, 233-236, doi: 10.1130/G22381.1.

Gibbs, S.J., Poulton, A.J., Bown, P.R., Daniels, C.J., Hopkins, J., Young, J.R., Jones, H.L., Thiemann, G.J., O'Dea, S.A., and Newsam, C., 2013, Species-specific growth response of coccolithophores to Palaeocene–Eocene environmental change. *Nature Geoscience*, 6, 3, 218–222, doi: 10.1038/ngeo1719.

Gibbs, S.J., Stoll, H.M., Bown, P.R., and Bralower, T.J., 2010, Ocean acidification and surface water carbonate production across the Paleocene-Eocene thermal maximum. *Earth and Planetary Science Letters*, 295, 583–592, doi: 10.1016/j.epsl.2010.04.044.

Gould, S.J., 1966, Allometry and size in ontogeny and phylogeny. *Biological Reviews*, 41, 4, 587-638, doi: 10.1111/j.1469-185X.1966.tb01624.x.

Guidi, L., Jackson, G.A., Stemmann, L., Miquel, J.C., Picheral, M., and Gorsky, G., 2008, Relationship between particle size distribution and flux in the mesopelagic zone. *Deep Sea Research Part I*, 55, 1364–1374, doi: 10.1016/j.dsr.2008.05.014.

Gussone, N., Langer, G., Geisen, M., Steel, B.A., and Riebesell, U., 2007, Calcium isotope fractionation in coccoliths of cultured *Calcidiscus leptoporus*, *Helicosphaera carteri*, *Syracosphaera pulchra* and *Umbilicosphaera foliosa*. *Earth and Planetary Science Letters*, 260, 505–515, doi: 10.1016/j.epsl.2007.06.001.

Hannisdal, B., Henderiks, J., and Liow, L.H., 2012, Long-term evolutionary and ecological responses of calcifying phytoplankton to changes in atmospheric CO_2. *Global Change Biology*, 18, 3504–3516, doi: 10.1111/gcb.12007.

Hansen, B., Bjørnsen, P.K., and Hansen, P.J., 1994, The size ratio between planktonic predators and their prey. *Limnology and Oceanography*, 39, 2, 395–403, doi: 10.4319/lo.1994.39.2.0395.

Haq, B.U., and Lohmann, G.P., 1976, Early Cenozoic calcareous nannoplankton biogeography of the Atlantic Ocean. *Marine Micropaleontology*, 1, 119–194, doi:10.1016/0377-8398(76)90008-6.

Harris, R.P., 1994, Zooplankton grazing on the coccolithophore *Emiliania huxleyi* and its role in inorganic carbon flux. *Marine Biology*, 119, 431–439, doi: 10.1007/BF00347540.

Hays, G.C., Richardson, A.J., and Robinson, C., 2005, Climate change and marine plankton. *Trends in Ecology and Evolution*, 20, 6, 337–344, doi: 10.1016/j.tree.2005.03.004.

Henderiks, J., 2008, Coccolithophore size rules — Reconstructing ancient cell geometry and cellular calcite quota from fossil coccoliths. *Marine Micropaleontology*, 67, 143–154, doi: 10.1016/j.marmicro.2008.01.005.

Henderiks, J., and Pagani, M., 2008, Coccolithophore cell size and the Paleogene decline in atmospheric CO_2. *Earth and Planetary Science Letters*, 269, 576–584, doi: 10.1016/j.epsl.2008.03.016.

Henderiks, J., and Pagani, M., 2007, Refining ancient carbon dioxide estimates: Significance of coccolithophore cell size for alkenone-based pCO_2 records. *Paleoceanography*, 22, PA32303, doi: 10.1029/2006PA001399.

Herrmann, S., and Thierstein, H.R., 2012, Cenozoic coccolith size changes—Evolutionary and/or ecological controls? *Palaeogeography, Palaeoclimatology, Palaeoecology*, 333-334, 92–106, doi: 10.1016/j.palaeo.2012.03.011.

Ho, T-Y., Quigg, A., Finkel, Z.V., Milligan, A.J., Wyman, K., Falkowski, P.G., and Morel, F.M.M., 2003, The elemental composition of some marine phytoplankton. *Journal of Phycology*, 39, 1145-1159, doi: 10.1111/j.0022-3646.2003.03-090.x.

Hoegh-Guldberg, O., and Bruno, J.F., 2010, The impact of climate change on the world's marine ecosystems. *Science*, 328, 1523–1528, doi: 10.1126/science.1189930.

Honjo, S., 1976, Coccoliths: Production, transportation and sedimentation. *Marine Micropaleontology*, 1, 65–79, doi: 10.1016/0377-8398(76)90005-0.

Horigome, M.T., Ziveri, P., Grelaud, M., Baumann, K.-H., Marino, G., and Mortyn, P.G., 2014, Environmental controls on the *Emiliania huxleyi* calcite mass. *Biogeosciences*, 11, 2295–2308, doi: 10.5194/bg-11-2295-2014.

Huber, M., and Sloan, L.C., 2001, Heat transport, deep waters, and thermal gradients: Coupled simulation of an Eocene greenhouse climate. *Geophysical Research Letters*, 28, 18, 3481–3484, doi: 10.1029/2001GL012943.

Huete-Ortega, M., Cermeño, P., Calvo-Díaz, A., and Marañón, E., 2012, Isometric size-scaling of metabolic rate and the size abundance distribution of phytoplankton. *Proceedings of the Royal*

Society B, 279, 1815–1823, doi: 10.1098/rspb.2011.2257.

Hutchinson, G.E., 1957, Concluding remarks. *Cold Spring Harbor Symposia on Quantitative Biology*, 22, 415–427.

Inglis, G.N., Farnsworth, A., Lunt, D., Foster, G.L., Hollis, C.J., Pagani, M., Jardine, P.E., Pearson, P.N., Markwick, P., Galsworthy, A.M.J., Raynham, L., Taylor, K.W.R., and Pancost, R.D., 2015, Descent toward the Icehouse: Eocene sea surface cooling inferred from GDGT distributions. *Paleoceanography*, 30, 1000–1020, doi: 10.1002/2014PA002723.

Jimènez Berrocoso, À., Huber, B.T., MacLeod, K.G., Petrizzo, M.R., Lees, J.A., Wendler, I., Coxall, H., Mweneinda, A.K., Falzoni, F., Birch, H., Singano, J.M., Haynes, S., Cotton, L., Wendler, J., Bown, P.R., Robinson, S.A., and Gould, J., 2012, Lithostratigraphy, biostratigraphy and chemostratigraphy of Upper Cretaceous and Paleogene sediments from southern Tanzania: Tanzania Drilling Project Sites 27–35. *Journal of African Earth Sciences*, 70, 36–57, doi: 10.1016/j.jafrearsci.2012.05.006.

Jin, P., Gao, K., and Beardall, J., 2013, Evolutionary responses of a Coccolithophorid *Gephyrocapsa oceanica* to ocean acidification. *Evolution*, 67, 7, 1869-1878, doi: 10.1111/evo.12112.

John, C.M., Bohaty, S.M., Zachos, J.C., Sluijs, A., Gibbs, S., Brinkhuis, H., and Bralower, T.J., 2008, North American continental margin records of the Paleocene-Eocene thermal maximum: Implications for global carbon and hydrological cycling. *Paleoceanography*, 23, PA2217, doi: 10.1029/2007PA001465.

John, E.H., Wilson, J.D., Pearson, P.N., and Ridgwell, A., 2014, Temperature-dependent remineralization and carbon cycling in the warm Eocene oceans. *Palaeogeography, Palaeoclimatology, Palaeoecology*, 413, 158–166, doi: 10.1016/j.palaeo.2014.05.019.

Jones, B.M., Iglesias-Rodriguez, M.D., Skipp, P.J., Edwards, R.J., Greaves, M.J., Young, J.R., Elderfield, H., and O'Connor, C.D., 2013, Response of the *Emiliania huxleyi* proteome to ocean acidification. *PLOS ONE*, 8, 4, e61868, doi: 10.1371/journal.pone.0061868.

Kaffes, A., Thoms, S., Trimborn, S., Rost, B., Langer, G., Richter, K-U., Köhler, A., Norici, A., and Giordano, M., 2010, Carbon and nitrogen fluxes in the marine coccolithophore *Emiliania huxleyi* grown under different nitrate conditions. *Journal of Experimental Marine Biology and Ecology*, 393, 1-8, doi:10.1016/j.jembe.2010.06.004.

Kalb, A.L., and Bralower, T.J., 2012, Nannoplankton origination events and environmental changes in the late Paleocene and early Eocene. *Marine Micropaleontology*, 92-93, 1–15, doi: 10.1016/j.marmicro.2012.03.003.

Kamp, P.J.J., Waghorn, D.B., and Nelson, C.S., 1990, Late Eocene-Early Oligocene integrated isotope stratigraphy and biostratigraphy for paleoshelf sequences in southern Australia: paleoceanographic implications. *Palaeogeography, Palaeoclimatology, Palaeoecology*, 80, 311–323, doi: 10.1016/0031-0182(90)90140-3.

Keller, M.D., Selvin, R.C., Claus, W., and Guillard, R.R.L., 1987, Media for the culture of oceanic ultraphytoplankton. *Journal of Phycology*, 23, 633–638, doi: 10.1111/j.1529-8817.1987.tb04217.x.

Key, T., McCarthy, A., Campbell, D.A., Six, C., Roy, S., and Finkel, Z.V., 2010, Cell size trade-offs govern light exploitation strategies in marine phytoplankton. *Environmental Microbiology*, 12, 1, 95–104, doi: 10.1111/j.1462-2920.2009.02046.x.

Knappertsbusch, M., 2000, Morphologic evolution of the coccolithophorid *Calcidiscus leptoporus* from the Early Miocene to Recent. *Journal of Paleontology*, 74, 4, 712–730, doi: 10.1017/S0022336000032820.

Knappertsbusch, M., Cortes, M.Y., and Thierstein, H.R., 1997, Morphologic variability of the coccolithophorid *Calcidiscus leptoporous* in the plankton, surface sediments and from the early Pleistocene. *Marine Micropaleontology*, 30, 4, 293–317, doi: 10.1016/S0377-8398(96)00053-9.

Krug, S.A., Schulz, K.G., and Riebesell, U., 2011, Effects of changes in carbonate chemistry speciation on *Coccolithus braarudii*: A discussion of coccolithophorid sensitivities. *Biogeosciences*, 8, 771–777, doi: 10.5194/bg-8-771-2011.

Langer, G., and Bode, M., 2011, CO_2 mediation of adverse effects of seawater acidification in *Calcidiscus leptoporus*. *Geochemistry, Geophysics, Geosystems*, 12, 5, Q05001, doi: 10.1029/2010GC003393.

Langer, G., Geisen, M., Baumann, K.-H., Kläs, J., Riebesell, U., Thoms, S., and Young, J.R., 2006, Species-specific responses of calcifying algae to changing seawater carbonate chemistry. *Geochemistry, Geophysics, Geosystems*, 7, 9, Q09006, doi: 10.1029/2005GC001227.

Langer, G., Nehrke, G., and Jansen, S., 2007, Dissolution of *Calcidiscus leptoporus* coccoliths in copepod guts? A morphological study. *Marine Ecology Progress Series*, 331, 139–146, doi: 10.3354/meps331139.

Langer, G., Nehrke, G., Probert, I., Ly, J., and Ziveri, P., 2009, Strain-specific responses of *Emiliania huxleyi* to changing seawater carbonate chemistry. *Biogeosciences*, 6, 2637–2646, doi: 10.5194/bg-6-2637-2009.

Langer, G., Oetjen, K., and Brenneis, T., 2012, Calcification of *Calcidiscus leptoporus* under nitrogen

and phosphorus limitation. *Journal of Experimental Marine Biology and Ecology*, 413, 131–137, doi: 10.1016/j.jembe.2011.11.028.

Langer, G., Oetjen, K., and Brenneis, T., 2013, Coccolithophores do not increase particulate carbon production under nutrient limitation: A case study using *Emiliania huxleyi* (PML B92/11). *Journal of Experimental Marine Biology and Ecology*, 443, 155–161, doi: 10.1016/j.jembe.2013.02.040.

Laws, E.A., Popp, B.N., Cassar, N., and Tanimoto, J., 2002, ^{13}C discrimination patterns in oceanic phytoplankton: likely influence of CO_2 concentrating mechanisms, and implications for palaeoreconstructions. *Functional Plant Biology*, 29, 3, 323–333, doi: 10.1071/PP01183.

Lear, C.H., Elderfield, H., and Wilson, P.A., 2000, Cenozoic deep-sea temperatures and global ice volumes from Mg/Ca in benthic foraminiferal calcite. *Science*, 287, 269–272, doi: 10.1126/science.287.5451.269.

Li, W.K.W., McLaughlin, F.A, Lovejoy, C., and Carmack, E.C., 2009, Smallest algae thrive as the Arctic Ocean freshens. *Science*, 326, 539, doi: 10.1126/science.1179798.

Liu, Z., Pagani, M., Zinniker, D., DeConto, R., Huber, M., Brinkhuis, H., Shah, S.R., Leckie, R.M., and Pearson, A., 2009, Global cooling during the Eocene-Oligocene climate transition. *Science*, 323, 1187–1190, doi: 10.1126/science.1166368.

Lohbeck, K.T., Riebesell, U., and Reusch, T.B.H., 2012, Adaptive evolution of a key phytoplankton species to ocean acidification. *Nature Geoscience*, 5, 346–351, doi: 10.1038/ngeo1441.

Lohbeck, K.T., Riebesell, U., and Reusch, T.B.H., 2014, Gene expression changes in the coccolithophore *Emiliania huxleyi* after 500 generations of selection to ocean acidification. *Proceedings of the Royal Society B,* 281, 2014003, doi: 10.1098/rspb.2014.0003.

Mai, H., 1999, Paleocene coccoliths and coccospheres in deposits of the Maastrichtian stage at the 'type locality' and type area in SE Limburg, The Netherlands. *Marine Micropaleontology*, 36, 1, 1–12, doi: 10.1016/S0377-8398(98)00023-1.

Marañón, E., Cermeño, P., López-Sandoval, D.C., Rodríguez-Ramos, T., Sobrino, C., Huete-Ortega, M., Blanco, J.M., and Rodríguez, J., 2013, Unimodal size scaling of phytoplankton growth and the size dependence of nutrient uptake and use. *Ecology Letters*, 16, 371–379, doi: 10.1111/ele.12052.

Margalef, R., 1978, Life-forms of phytoplankton as survival alternatives in an unstable environment. *Oceanologica Acta*, 1, 4, 493–509.

Marlowe, I., Brassell, S., Eglinton, G., and Green, J., 1990, Long-chain alkenones and alkyl alkenoates and the fossil coccolith record of marine sediments. *Chemical Geology*, 88, 349–375, doi: 10.1016/0009-2541(90)90098-R.

Marlowe, I.T., Green, J.C., Neal, A.C., Brassell, S.C., Eglinton, G., and Course, P.A., 1984, Long chain (n-C_{37}-C_{39}) alkenones in the Prymnesiophyceae. Distribution of alkenones and other lipids and their taxonomic significance. *British Phycological Journal*, 19, 3, 203–216, doi: 10.1080/00071618400650221.

Martini, E., 1971, Standard Tertiary and Quaternary calcareous nannoplankton zonation, *in* Farinacci, A. ed., *Proceedings of the II Planktonic Conference, Roma, 1969*. Tecnoscienza, Rome, p. 739–785.

Mei, Z-P., Finkel, Z.V., and Irwin, A.J., 2011, Phytoplankton growth allometry and size-dependent C:N stoichiometry revealed by a variable quota model. *Marine Ecology Progress Series*, 434, 29-43, doi: 10.3354/meps09149.

Menden-Deuer, S., and Lessard, E.J., 2000, Carbon to volume relationships for dinoflagellates, diatoms, and other protist plankton. *Limnology and Oceanography*, 45, 3, 569–579, doi: 10.4319/lo.2000.45.3.0569.

Meyer, J., and Riebesell, U., 2015, Reviews and Syntheses: Responses of coccolithophores to ocean acidification: a meta-analysis. *Biogeosciences*, 12, 1671–1682, doi: 10.5194/bg-12-1671-2015.

Michaels, A.F., and Silver, M.W., 1988, Primary production, sinking fluxes and the microbial food web. *Deep-Sea Research*, 35, 4, 473–490.

Miller, K.G., Sugarman, P.J., Browning, J. V., Olsson, R.K., Pekar, S.F., Reilly, T.J., Cramer, B.S., Aubry, M., Lawrence, R.P., Curran, J., Stewart, M., Metzger, J.M., Uptegrove, J., Bukry, D., et al., 1998, Bass River Site, *in* Miller, K.G., Sugarman, P.J., Browning, J.V., et al., *Proceedings of the Ocean Drilling Program, Initial Reports* v. 174AX, Texas A&M University, College Station TX, United States, p. 5–43, doi:10.2973/odp.proc.ir.174ax.101.1998.

Montadert, L., Roberts, D.G., Auffret, G.A., Bock, W.D., Dupeuble, P.A., Hailwood, E.A., Harrison, W.E., et al., 1979, Site 401, *in* Montadert, L., Roberts, D.G., Auffret, G.A., et al., *Initial Reports of the Deep Sea Drilling Project* v. 48, Washington, U.S. Government Printing Office, p. 73-123, doi: 10.2973/dsdp.proc.48.104.1979.

Moore, C.M., Mills, M.M., Arrigo, K.K., Berman-Frank, I., Bopp, L., Boyd, P.W., Galbraith, E.D., Geider, R.J., Guieu, C., Jaccard, S.L., Jickells, T.D., La Roche, J., Lenton, T.M., Mahowald, N.M., Marañón, E., Marinov, I., Moore, J.K., Nakatsuka, T., Oschlies, M., Saito, M.A.,

Thingstad, T.F., Tsuda, A., and Ulloa, O., 2013, Processes and patterns of nutrient limitation. *Nature Geoscience*, 6, 701–710, doi: 10.1038/NGEO1765.

Morgans, H.E.G., 2009, Late Paleocene to middle Eocene foraminiferal biostratigraphy of the Hampden Beach section, eastern South Island, New Zealand. *New Zealand Journal of Geology and Geophysics*, 52, 4, 273–320, doi: 10.1080/00288306.2009.9518460.

Müller, M.N., Antia, A.N., and LaRoche, J., 2008, Influence of cell cycle phase on calcification in the coccolithophore *Emiliania huxleyi*. *Limnology and Oceanography*, 53, 2, 506–512, doi: 10.4319/lo.2008.53.2.0506.

Müller, M.N., Lebrato, M., Riebesell, U., Barcelos e Ramos, J., Schulz, K.G., Blanco-Ameijeiras, S., Sett, S., Eisenhauer, A., and Stoll, H.M., 2014, Influence of temperature and CO_2 on the strontium and magnesium composition of coccolithophore calcite. *Biogeosciences*, 11, 1065–1075, doi: 10.5194/bg-11-1065-2014.

Müller, M.N., Schulz, K.G., and Riebesell, U., 2010, Effects of long-term high CO_2 exposure on two species of coccolithophores. *Biogeosciences*, 7, 1109–1116, doi: 10.5194/bg-7-1109-2010.

Nicholas, C.J., Pearson, P.N., Bown, P.R., Jones, T.D., Huber, B.T., Karega, A., Lees, J. A., McMillan, I.K., O'Halloran, A., Singano, J.M., and Wade, B.S., 2006, Stratigraphy and sedimentology of the Upper Cretaceous to Paleogene Kilwa Group, southern coastal Tanzania. *Journal of African Earth Sciences*, 45, 431–466, doi: 10.1016/j.jafrearsci.2006.04.003.

Norris, R.D., 1991, Parallel evolution in the keel structure of planktonic foraminifera. *Journal of Foraminiferal Research*, 21, 319–331, doi:10.2113/gsjfr.21.4.319.

Norris, R.D., Turner, S.K., Hull, P.M., Ridgwell, A., and Kirtland Turner, S., 2013, Marine ecosystem responses to Cenozoic global change. *Science*, 492, 492–498, doi: 10.1126/science.1240543.

O'Dea, S.A., Gibbs, S.J., Bown, P.R., Young, J.R., Poulton, A.J., Newsam, C., and Wilson, P.A., 2014, Coccolithophore calcification response to past ocean acidification and climate change. *Nature Communications*, 5, 5363, doi: 10.1038/ncomms6363.

Paasche, E., 2001, A review of the coccolithophorid *Emiliania huxleyi* (Prymnesiophyceae), with particular reference to growth, coccolith formation, and calcification-photosynthesis interactions. *Phycologia*, 40, 6, 503–529, doi: 10.2216/i0031-8884-40-6-503.1.

Paasche, E., 1998, Roles of nitrogen and phosphorus in coccolith formation in *Emiliania huxleyi* (Prymnesiophyceae). *European Journal of Phycology*, 33, 33–42, doi:

10.1017/S0967026297001480.

Pagani, M., 2002, The alkenone–CO_2 proxy and ancient atmospheric carbon dioxide. *Philosophical transactions of the Royal Society A*, 360, 609–632, doi: 10.1098/rsta.2001.0959.

Pagani, M., Huber, M., Liu, Z., Bohaty, S.M., Henderiks, J., Sijp, W., Krishnan, S., and DeConto, R.M., 2011, The role of carbon dioxide during the onset of Antarctic glaciation. *Science*, 334, 1261–4, doi: 10.1126/science.1203909.

Pagani, M., Zachos, J.C., Freeman, K.H., Tipple, B., and Bohaty, S., 2005, Marked decline in atmospheric carbon dioxide concentrations during the Paleogene. *Science*, 309, 600–603, doi: 10.1126/science.1110063.

Pearson, P.N., and Burgess, C.E., 2008, Foraminifer test preservation and diagenesis: comparison of high latitude Eocene sites, *in* Austin, W.E.N. and James, R.H. eds., *Biogeochemical Controls on Palaeoceanographic Environmental Proxies*, Geological Society Special Publications, London, 303, 59–72, doi: 10.1144/SP303.5.

Pearson, P.N., van Dongen, B.E., Nicholas, C.J., Pancost, R.D., Schouten, S., Singano, J.M., and Wade, B.S., 2007, Stable warm tropical climate through the Eocene Epoch. *Geology*, 35, 211-214, doi: 10.1130/G23175A.1.

Pearson, P.N., Nicholas, C.J., Singano, J.M., Bown, P.R., Coxall, H.K., van Dongen, B.E., Huber, B.T., Karega, A., Lees, J.A., MacLoed, K., McMillan, I.K., Pancost, R.D., Pearson, M., and Msaky, E., 2006, Further Paleogene and Cretaceous sediment cores from the Kilwa area of coastal Tanzania: Tanzania Drilling Project Sites 6-10. *Journal of African Earth Sciences*, 45, 279–317, doi: doi:10.1016/j.jafrearsci.2006.02.005.

Pearson, P.N., Nicholas, C.J., Singano, J.M., Bown, P.R., Coxall, H.K., van Dongen, B.E., Huber, B.T., Karega, A., Lees, J. A., Msaky, E., Pancost, R.D., Pearson, M., and Roberts, A.P., 2004, Paleogene and Cretaceous sediment cores from the Kilwa and Lindi areas of coastal Tanzania: Tanzania Drilling Project Sites 1–5. *Journal of African Earth Sciences*, 39, 25–62, doi: 10.1016/j.jafrearsci.2004.05.001.

Pearson, P.N., and Wade, B.S., 2009, Taxonomy and stable isotope paleoecology of well-preserved planktonic foraminifera from the uppermost Oligocene of Trinidad. *Journal of Foraminiferal Research*, 39, 3, 191–217, doi: 10.2113/gsjfr.39.3.191.

Perch-Nielsen, K., 1985, Cenozoic calcareous nannofossils, *in* Bolli, H.M., Saunders, J.B., and Perch-Nielsen, K. eds., *Plankton Stratigraphy*, Cambridge University Press, Cambridge, p. 427–555, ISBN: 9780521367196.

Persico, D., and Villa, G., 2008, A new Eocene *Chiasmolithus* species: hypothetical reconstruction of its phyletic lineage. *Journal of Nannoplankton Research*, 30, 1, 23–33.

Persico, D., and Villa, G., 2004, Eocene–Oligocene calcareous nannofossils from Maud Rise and Kerguelen Plateau (Antarctica): paleoecological and paleoceanographic implications. *Marine Micropaleontology*, 52, 153–179, doi: 10.1016/j.marmicro.2004.05.002.

Popp, B.N., Laws, E.A., Bidigare, R.R.R., Dore, J.E., Hanson, K.L., Wakeman, S.G., and Wakeham, S.G., 1998, Effect of phytoplankton cell geometry on carbon isotopic fractionation. *Geochimica et Cosmochimica Acta*, 62, 1, 69–77, doi: 10.1016/S0016-7037(97)00333-5.

Poulton, A.J., Charalampopoulou, A., Young, J.R., Tarran, G.A., Lucas, M.I., and Quartly, G.D., 2010, Coccolithophore dynamics in non-bloom conditions during late summer in the central Iceland Basin (July-August 2007). *Limnology and Oceanography*, 55, 4, 1601–1613, doi: 10.4319/lo.2010.55.4.1601.

Poulton, A.J., Stinchcombe, M.C., Achterberg, E.P., Bakker, D.C.E., Dumousseaud, C., Lawson, H.E., Lee, G.A., Richier, S., Suggett, D.J., and Young, J.R., 2014, Coccolithophores on the north-west European shelf: Calcification rates and environmental controls. *Biogeosciences*, 11, 3919–3940, doi: 10.5194/bg-11-3919-2014.

Probert, I., Fresnel, J., Billard, C., Geisen, M., and Young, J.R., 2007, Light and electron microscope observations of *Algirosphaera robusta* (Prymnesiophyceae). *Journal of Phycology*, 43, 319–332, doi: 10.1111/j.1529-8817.2007.00324.x.

Probert, I., Fresnel, J., and Young, J., 2014, The life cycle and taxonomic affinity of the coccolithophore *Jomonlithus littoralis* (Prymnesiophyceae). *Cryptogamie Algologie*, 35, 4, 389–405, doi: 10.7872/crya.v35.iss4.2014.389.

Raffi, I., Backman, J., Fornaciari, E., Pälike, H., Rio, D., Lourens, L., and Hilgen, F.J., 2006, A review of calcareous nannofossil astrobiochronology encompassing the past 25 million years. *Quaternary Science Reviews*, 25, 23-24, 3113–3137, doi: 10.1016/j.quascirev.2006.07.007.

Read, B.A., Kegel, J., Klute, M.J., Kuo, A., Lefebvre, S.C., Maumus, F., Mayer, C., Miller, J., Monier, A., Salamov, A., Young, J., Aguilar, M., Claverie, J.-M., Frickenhaus, S., et al., 2013, Pan genome of the phytoplankton *Emiliania* underpins its global distribution. *Nature*, 499,209-213, doi: 10.1038/nature12221.

Redfield, A.C., 1934, On the proportions of organic derivatives in the sea water and their relation to the composition of plankton, *in* Daniel, R.J. ed., *James Johnstone Memorial Volume*, Univeristy Press of Liverpool, Liverpool, p. 176-192.

Rickaby, R.E.M., Bard, E., Sonzogni, C., Rostek, F., Beaufort, L., Barker, S., Rees, G., and Schrag, D.P., 2007, Coccolith chemistry reveals secular variations in the global ocean carbon cycle? *Earth and Planetary Science Letters*, 253, 83–95, doi: 10.1016/j.epsl.2006.10.016.

Rickaby, R.E.M., Henderiks, J., and Young, J.N., 2010, Perturbing phytoplankton: response and isotopic fractionation with changing carbonate chemistry in two coccolithophore species. *Climate of the Past*, 6, 771-785, doi:10.5194/cp-6-771-2010.

Rickaby, R.E.M., Schrag, D.P., Zondervan, I., and Riebesell, U., 2002, Growth rate dependence of Sr incorporation during calcification of *Emiliania huxleyi. Global Biogeochemical Cycles*, 16, 1, 1–8, doi: 10.1029/2001GB001408.

Ridgwell, A., Schmidt, D.N., Turley, C., Brownlee, C., Maldonado, M.T., Tortell, P., and Young, J.R., 2009, From laboratory manipulations to Earth system models: scaling calcification impacts of ocean acidification. *Biogeosciences*, 6, 2611–2623, doi: 10.5194/bg-6-2611-2009.

Riebesell, U., and Tortell, P.D., 2011, Effects of ocean acidification on pelagic organisms and ecosystems, *in* Gattuso, J.-P. and Hansson, L. eds., *Ocean Acidification*, Oxford University Press, Oxford, p. 99–121, ISBN: 9780199591091.

Riebesell, U., Zondervan, I., Rost, B., Tortell, P.D., Zeebe, R.E., and Morel, F.M.M., 2000, Reduced calcification of marine plankton in response to increased atmospheric CO_2. *Nature*, 407, 364-367, doi:10.1038/35030078.

Sáez, A.G., Probert, I., Geisen, M., Quinn, P., Young, J.R., and Medlin, L.K., 2003, Pseudo-cryptic speciation in coccolithophores. *Proceedings of the National Academy of Sciences*, 100, 12, 7163–8, doi: 10.1073/pnas.1132069100.

Schlüter, L., Lohbeck, K.T., Gutowska, M. A., Gröger, J.P., Riebesell, U., and Reusch, T.B.H., 2014, Adaptation of a globally important coccolithophore to ocean warming and acidification. *Nature Climate Change*, 4, 1024-1030, doi: 10.1038/nclimate2379.

Schmidt, D.N., Thierstein, H.R., and Bollmann, J., 2004a, The evolutionary history of size variation of planktic foraminiferal assemblages in the Cenozoic. *Palaeogeography, Palaeoclimatology, Palaeoecology*, 212, 159–180, doi: 10.1016/j.palaeo.2004.06.002.

Schmidt, D.N., Thierstein, H.R., Bollmann, J., and Schiebel, R., 2004b, Abiotic forcing of plankton evolution in the Cenozoic. *Science*, 303, 207–210, doi: 10.1126/science.1090592.

Schneider, L.J., Bralower, T.J., and Kump, L.R., 2011, Response of nannoplankton to early Eocene ocean destratification. *Palaeogeography, Palaeoclimatology, Palaeoecology*, 310, 152–162, doi:

10.1016/j.palaeo.2011.06.018.

Seki, O., Foster, G.L., Schmidt, D.N., Mackensen, A., Kawamura, K., and Pancost, R.D., 2010, Alkenone and boron-based Pliocene pCO$_2$ records. *Earth and Planetary Science Letters*, 292, 201–211, doi: 10.1016/j.epsl.2010.01.037.

Sheward, R.M., Daniels, C.J., and Gibbs, S.J., 2014, Growth rates and biometric measurements of coccolithophores (*Coccolithus pelagicus*, *Coccolithus braarudii*, *Emiliania huxleyi*) during experiments. doi: 10.1594/PANGAEA.836841.

Sijp, W.P., and England, M.H., 2016, The effect of low ancient greenhouse climate temperature gradients on the ocean's overturning circulation. *Climate of the Past*, 12, 543-552, doi: 10.5194/cpd-12-543-2016.

Sijp, W.P., von der Heydt, A.S., Dijkstra, H.A., Flögel, S., Douglas, P.M.J., and Bijl, P.K., 2014, The role of ocean gateways on cooling climate on long time scales. *Global and Planetary Change*, 119, 1–22, doi: 10.1016/j.gloplacha.2014.04.004.

Smith, H.E.K., 2014, The contribution of mineralising phytoplankton to the biological carbon pump in high latitudes. PhD Thesis, University of Southampton, 232 pp.

Srivastava, S.P., Arthur, M.A., Clement, B., Aksu, A., Baldauf, J., Bohrmann, G., Busch, W., Cederberg, T., Cremer, M., Dadey, K., De Vernal, A., Firth, J., Hall, F., Head, M., Hiscott, R., Jarrad, R., Kaminski, M., Lazarus, D., Monjanel, A-L., Nielsen, O.B., Stein, R., Thiebault, F., Zachos, J., and Zimmerman, H., 1987, *Proceedings of the Ocean Drilling Program, Initial Reports* v. 105, Texas A&M University, College Station TX, United States, doi: 10.2973/odp.proc.ir.105.1987.

Stanley, S.M., 1973, An explanation for Cope's Rule. *Evolution*, 27, 1, 1–26, doi: 10.2307/2407115.

Stoll, H.M., Klaas, C.M., Probert, I., Encinar, J.R., and Alonso, J.I.G., 2002a, Calcification rate and temperature effects on Sr partitioning in coccoliths of multiple species of coccolithophorids in culture. *Global and Planetary Change*, 34, 153–171, doi: 10.1016/S0921-8181(02)00112-1.

Stoll, H.M., Ruiz Encinar, J., Ignacio Garcia Alonso, J., Rosenthal, Y., Probert, I., and Klaas, C., 2001, A first look at paleotemperature prospects from Mg in coccolith carbonate: Cleaning techniques and culture measurements. *Geochemistry Geophysics Geosystems*, 2, 5, 2000GC000144, doi: 10.1029/2000GC000144.

Stoll, H.M., and Schrag, D.P., 2000, Coccolith Sr/Ca as a new indicator of coccolithophorid calcification and growth rate. *Geochemistry Geophysics Geosystems*, 1, 5, 1006, doi:

10.1029/1999GC000015.

Stoll, H.M., Shimizu, N., Archer, D., and Ziveri, P., 2007, Coccolithophore productivity response to greenhouse event of the Paleocene–Eocene Thermal Maximum. *Earth and Planetary Science Letters*, 258, 192–206, doi: 10.1016/j.epsl.2007.03.037.

Stoll, H.M., Ziveri, P., Geisen, M., Probert, I., and Young, J.R., 2002b, Potential and limitations of Sr/Ca ratios in coccolith carbonate: new perspectives from cultures and monospecific samples from sediments. *Philosophical transactions of the Royal Society A*, 360, 719–747, doi: 10.1098/rsta.2001.0966.

Sun, J., and Liu, D., 2003, Geometric models for calculating cell biovolume and surface area for phytoplankton. *Journal of Plankton Research*, 25, 11, 1331–1346, doi: 10.1093/plankt/fbg096.

Šupraha, L., Gerecht, A.C., Probert, I., and Henderiks, J., 2015, Eco-physiological adaptation shapes the response of calcifying algae to nutrient limitation. *Scientific Report*, 5, 16499, doi: 10.1038/srep16499.

Tang, E.P.Y., 1995, The allometry of algal growth rates. *Journal of Plankton Research*, 17, 6, 1325-1335, doi: 10.1093/plankt/17.6.1325.

Taylor, A.R., Russell, M.A., Harper, G.M., Collins, T.F.T., and Brownlee, C., 2007, Dynamics of formation and secretion of heterococcoliths by *Coccolithus pelagicus* ssp. *braarudii*. *European Journal of Phycology*, 42, 2, 125–136, doi: 10.1080/09670260601159346.

Thierstein, H.R., Geitzenauer, K.R., Molfino, B., and Shackleton, N.J., 1977, Global synchroneity of quaternary coccolith datum levels: validations by oxygen isotopes. *Geology*, 5, p. 400–404, doi: 10.1130/0091-7613(1977)5<400:GSOLQC>2.0.CO;2.

Tilman, D., 1982, *Resource competition and community structure*, Princeton University Press, Princeton, NJ, 296 pp., ISBN: 9780691083025.

Tremolada, F., and Bralower, T.J., 2004, Nannofossil assemblage fluctuations during the Paleocene–Eocene Thermal Maximum at Sites 213 (Indian Ocean) and 401 (North Atlantic Ocean): palaeoceanographic implications. *Marine Micropaleontology*, 52, 107–116, doi: 10.1016/j.marmicro.2004.04.002.

de Vargas, C., Aubry, M.-P., Probert, I., and Young, J., 2007, Origin and evolution of coccolithophores: From coastal hunters to oceanic farmers, *in* Falkowski, P.G. and Knoll, A.H. eds., *Evolution of Primary Producers in the Sea*, Elsevier Academic Press, London, UK, p. 251-286, doi: 10.1016/B978-012370518-1/50001.

de Vargas, C., Sáez, A.G., Medlin, L.K., and Thierstein, H.R., 2004, Super-species in the calcareous plankton, *in*: Thierstein, H.R., and Young, J.R. (eds) *Coccolithophores: From Molecular Processes to Global Impact*, Springer-Verlag, Heidelberg, Germany, p. 271-298, doi: 10.1007/978-3-662-06278-4.

Villa, G., Fioroni, C., Pea, L., Bohaty, S., and Persico, D., 2008, Middle Eocene–late Oligocene climate variability: Calcareous nannofossil response at Kerguelen Plateau, Site 748. *Marine Micropaleontology*, 69, 2, 173–192, doi: 10.1016/j.marmicro.2008.07.006.

Villa, G., and Persico, D., 2006, Late Oligocene climatic changes: Evidence from calcareous nannofossils at Kerguelen Plateau Site 748 (Southern Ocean). *Palaeogeography, Palaeoclimatology, Palaeoecology*, 231, 110–119, doi: 10.1016/j.palaeo.2005.07.028.

Volkman, J.K., Barrett, S.M., Blackburn, S.I., and Sikes, E.L., 1995, Alkenones in *Gephyrocapsa oceanica*: Implications for studies of paleoclimate. *Geochimica et Cosmochimica Acta*, 59, 3, 513–520, doi: 10.1016/0016-7037(95)00325-T.

Wade, B.S., 2007, Investigation of pristine planktonic foraminifera from Puerto Rico: taxonomic and geochemical analysis. *Palaeontological Association Newsletter*, 65, 108–111.

Wade, B.S., and Twitchett, R.J., 2009, Extinction, dwarfing and the Lilliput effect. *Palaeogeography, Palaeoclimatology, Palaeoecology*, 284, 1–3, doi: 10.1016/j.palaeo.2009.08.019.

Wei, W., and Wise, S.W., 1990, Biogeographic gradients of middle Eocene-Oligocene calcareous nannoplankton in the South Atlantic Ocean. *Palaeogeography, Palaeoclimatology, Palaeoecology,* 79, 1-2, 29–61, doi: 10.1016/0031-0182(90)90104-F.

Wilson, W.H., Tarran, G.A., Schroeder, D., Cox, M.J., Oke, J., and Malin, G., 2002, Isolation of viruses responsible for the demise of an *Emiliania huxleyi* bloom in the English Channel. *Journal of the Marine Biological Association of the United Kingdom*, 82, 369–377, doi: 10.1017/S002531540200560X.

Winter, A., Jordan, R.W., and Roth, P.H., 1994, Biogeography of living coccolithophore in ocean waters, *in* Winter, A. and Siesser, W.G. eds., *Coccolithophores*, Cambridge University Press, Cambridge, UK, p. 161–177, ISBN: 9780521031691.

Young, J.R., 1994, Functions of coccoliths, *in* Winter, A. and Siesser, W.G. eds., *Coccolithophores*, Cambridge University Press, Cambridge, UK, p. 63-82, ISBN: 9780521031691.

Young, J.R., Bown, P.R., and Lees, J.A., 2014, Nannotax3 website. International Nannoplankton Association. URL: http://ina.tmsoc.org/Nannotax3.

Young, J., Davis, S., Bown, P., and Mann, S., 1999, Coccolith ultrastructure and biomineralisation. *Journal of Structural Biology*, 126, 195–215, doi: 10.1006/jsbi.1999.4132.

Young, J., Geisen, M., Cros, L., Kleijne, A., Sprengel, C., Probert, I., and Ostergaard, J., 2003, A guide to extant coccolithophore taxonomy. *Journal of Nannoplankton Research*, Special Issue.

Young, J.R., Geisen, M., and Probert, I., 2005, A review of selected aspects of coccolithophore biology with implications for paleobiodiversity estimation. *Micropaleontology*, 51, 4, 267–288, doi: 10.2113/gsmicropal.51.4.267.

Young, J.R., and Ziveri, P., 2000, Calculation of coccolith volume and it use in calibration of carbonate flux estimates. *Deep Sea Research Part II: Topical Studies in Oceanography*, 47, 1679–1700, doi: 10.1016/S0967-0645(00)00003-5.

Zachos, J.C., Dickens, G.R., and Zeebe, R.E., 2008, An early Cenozoic perspective on greenhouse warming and carbon-cycle dynamics. *Nature*, 451, 279–83, doi: 10.1038/nature06588.

Zachos, J., Pagani, M., Sloan, L., Thomas, E., and Billups, K., 2001, Trends, rhythms, and aberrations in global climate 65 Ma to present. *Science*, 292, 686–93, doi: 10.1126/science.1059412.

Zhang, Y.G., Pagani, M., Liu, Z., Bohaty, S.M., and DeConto, R., 2013, A 40-million-year history of atmospheric CO_2. *Philosophical transactions of the Royal Society A*, 371, 20130096, doi: 10.1098/rsta.2013.0096.

Zhao, Y., Wang, Y., and Quigg, A., 2015, Comparison of population growth and photosynthetic apparatus changes in response to different nutrient status in a diatom and a coccolithophore. *Journal of Phycology*, 51, 5, 872–884, doi: 10.1111/jpy.12327.

Ziveri, P., Baumann, K.H., Böckel, B., Bollmann, J., and Young, J.R., 2004, Biogeography of selected Holocene coccoliths in the Atlantic Ocean, *in* Thierstein, H.R. and Young, J.R. eds., *Coccolithophores: From Molecular Processes to Global Impact*, Springer-Verlag, Heidelberg, Germany, p. 403-428, doi: 10.1007/978-3-662-06278-4.

Ziveri, P., de Bernardi, B., Baumann, K.H., Stoll, H.M., and Mortyn, P.G., 2007, Sinking of coccolith carbonate and potential contribution to organic carbon ballasting in the deep ocean. *Deep-Sea Research Part II: Topical Studies in Oceanography*, 54, 659–675, doi: 10.1016/j.dsr2.2007.01.006.

Ziveri, P., Rutten, A., De Lange, G.J., Thomson, J., and Corselli, C., 2000, Present-day coccolith fluxes recorded in central eastern Mediterranean sediment traps and surface sediments.

Palaeogeography, Palaeoclimatology, Palaeoecology, 158, 175–195, doi: 10.1016/S0031-0182(00)00049-3.

Ziveri, P., Stoll, H., Probert, I., Klaas, C., Geisen, M., Ganssen, G., and Young, J., 2003, Stable isotope "vital effects" in coccolith calcite. *Earth and Planetary Science Letters*, 210, 137–149, doi: 10.1016/S0012-821X(03)00101-8